HYDRODYNAMIC NOTE AG-18

FLAP CONTROL OF INCIDENCE HINGE MOMENT AND FOIL CAVITATION

H. R. WRIGHT, JR.

APRIL 30, 1973

INDEX

INDEX (Continued)

INDEX (Continued)

SUMMARY

The use of flaps to control the incidence hinge moment and cavitation characteristics for incidence lift control foils is examined in the light of the measured prototype lift and moment characteristics of Reference 3. The flap management considered here is a function of speed and is critical only at minimum flight speed, to avoid crossover, and at maximum speed, to avoid exceeding design hinge moment. The numerical summary is for the AG(EH) fwd. foils but is typical for foils of any size and of any speed less then 50 - 60 knots.

Trailing edge flaps would reduce the existing incidence lift control hinge moment about 40%. The existing hinge moment could be reduced about 60% by also changing the hinge position but that moment would be bidirectional and is considered to present an intolerable crossover problem. Hinging for positive hinge moment rather than negative, would double the moment. Abnormal flap chords do not aid moment or cavitation control. and flaps do not relieve the requirement to design the basic section for the design speed.

The flaps can be employed to increase the incipient cavitation foil loading by some 400 psf or to increase the cavitation [illegible] speed by up to about 10 knots, This cavitation control can be extended by incorporating the section geometry into the control procedure. Flap control of cavitation is not state of the art, being dependent upon the effective cavitation boundaries which are unknown for the flapped foil.

h-ailing edge flaps do not provide control over the flying foil.

The Interim Report conclusion that an appropriately selected fixed incidence angle would provide the flap lift control system with the optimum incipient cavitation bucket was a coincidental result of the numerical value assigned ζ 'in that report. A confident evaluation of this parameter will probably compromise the optimum bucket for the fixed incidence, flap lift control system.

INTRODUCTION

Incidence lift control provides three qualitative advantages over flap lift control:

1. Superior cavitation characteristics,
2. Lower (profile) drag,
3. More confident performance predictability.

None of these advantages can be evaluated quantitatively yet, even to establish whether the differences are significant or not, because no confidence level has yet been established for the performance of the flap lift control system.

The only disadvantage associated wit;! incidence lift control is the high hinge moment relative to the flap lift control system but this is a real disadvantage which has already produced design and operational difficulties. Reference 1 demonstrates that unflapped incidence lift control hinge moments are generally proportional to craft displacement and that the PGH-1 and AG(EH) hinge moments are characteristic.

This note is intended to employ the results of Reference 2 to examine the feasibility for adjustable flap control of the hinge moments for an incidence lift control system including the case for the "flying" flap controlled foil. A closely related problem, employment of flaps for the control of the incipient cavitation bucket, is included for completeness.

The general equations developed in this note are illustrated by application to the AG(EH) fwd. foil geometry but are, of course, applicable to any foil configuration.

CONCLUSIONS

1. The maximum incidence lift hinge moment is increased by:
   - A. Spreading the minimum and maximum foil loading,
   - B. Increasing the normal acceleration margin requirement,
   - C. Spreading the minimum and maximum flight speed,
   - D. Reducing the nominal minimum submergence,
   - E. Allowance for prediction precision for:
     - a. aerodynamic center,
     - b. residual moment,
     - c. flap load distribution, ζ
2. Flaps will reduce th maximum hinge moment by about 40% and will compensate for the prediction errors of 1 E, above.
3. Hinging for bi-directional moment reduces the hinge moment about 35% more but not to a tolerable level for crossover. Hinging for positive moment doubles the moment.
4. Moments for the various hinge and flap schedule options are compared numerically in Table VII.
5. Flaps can increase the incipient cavitation foil loading by 400 psf or increase the incipient cavitation speed by up to 10 knots (See Figure 17).
6. Intelligent flap scheduling will always improve the hinge moment and the incipient cavitation bucket but the optimum flap schedules are not the same for the two objectives.
7. Optimum hinge positions are summarized in Table V and the corresponding maximum moments are summarized in Table VI.

8. A more concise derivation of the cavitation equations of the Interim Report including accountability for buoyancy and extending the results to the case for the flapped incidence lift control foil, is presented in this note. Eq. (24) presents the incipient cavitation foil loading for flap lift control and Eq. (29) presents this foil loading for the flapped incidence lift control system. Eq. (29) includes the case for the unflapped foil.

9. The hinge moment equation of this note, Eq. (10), includes the unflapped hinge moments of Reference 1 as a special case.

10. All of the moment and cavitation results of this note are subject to inadequate confidence levels for the hydrodynamic characteristics of flaps; specifically for the parameter, ζ, and for the flapped effective cavitation boundaries.

11. The trailing edge flap will not control the "flying" foil because the flap angles required are intolerable for cavitation.

12. The Interim Report conclusion that an appropriately selected fixed incidence angle would provide the flap lift control system with the optimum incipient cavitation bucket was a coincidental result of the numerical value assigned ζ in that report. A confident evaluation of this parameter will probably compromise the optimum bucket for the fixed incidence, flap lift control system.

13. Existing flap lift control prototypes are not, necessarily, models of future designs, If future prototypes are to be designed with confidence, the <u>general</u> theory for flapped hydrofoils must be experimentally validated.

RECOMMENDATIONS

1. An adequate map of' the effective cavitation houndaries for some, any, flapped hydrofoil. is urgently required. The AG(EH) foil would be an ideal model. for this map because of' the theoretical and experimental background already available for this configuration. The AG(EH) configuration is also ideally suited to Be Grumman whirling tank in span and aspect ratio and will provide this map more'economically and more reliably than any existing facility. It is therefore recommended that Grumman's "Proposal for Extension To AG(EH) Lift Control Study For Cavitation Sealed Model Testing", 31 October 1972, be undertaken without further delay. No general theory for flapped foil performance, incidence or flap lift control, can be formulated in the absence of this map. Any prototype built without this map is an experimental prototype.

2. A general theoretical and experimental attack upon tie hydrodynamic characteristics of the flapped foil is required though no such program is formulated here.

3. Theoretical and experimental examination of the possibility for extending the conventionalfoil speed range by the use of flaps is recommended though no such program is formulated here.

4. Theoretical and experimental examination of the characteristics of a flying foil controlled by a boom mounted foil is recommended though no such program is formulated here,.

5. Recommendations with regard to the "Plainview", specifically, as a result of the studies of this note are reserved for completion of studies of flap hinge moment and control power.

DISCUSSION

BASIC EQUATIONS

Alternative forms of the total lift equation for the foil with flap are:

(1)
$$\frac{C_{L\alpha\infty}}{C_{L\alpha}} C_L = \frac{C_{L\alpha\infty}}{C_{L\alpha}} \frac{(W/S)_H}{q} = C_{L\alpha\infty}\alpha + C_{Li'\infty} i' + C_{L\delta\infty}\delta + C_{L0\infty}$$
$$= C_{L\alpha\infty}\alpha + \frac{C_{Li'}}{C_{L\alpha}} C_{L\alpha\infty} i' + \frac{d\alpha}{d\delta}\frac{C_{Li'}}{C_{L\alpha}} C_{L\alpha\infty}\delta + C_{L0\infty}$$

The corresponding foil loading equation is particularly useful to this note:

(2)
$$\frac{C_{L\alpha\infty}}{C_{L\alpha}}\left(\frac{W}{S}\right)_H = \left(\frac{W}{S}\right)_{\alpha\infty} + \left(\frac{W}{S}\right)_{i'\infty} + \left(\frac{W}{S}\right)_{\delta\infty} + \left(\frac{W}{S}\right)_{0\infty} .$$
$$= \left(\frac{W}{S}\right)_{\alpha\infty} + \left(\frac{W}{S}\right)_{\delta\infty} + \left(\frac{W}{S}\right)_{ref.\infty} .$$

where $\left(\frac{W}{S}\right)_\alpha$ accounts for orbital angle of attach or for craft pitch+, $\left(\frac{W}{S}\right)_\theta$.

The hinge moment analyses of this note assume, as in References 1 and 2, that $C_{Hc_L} = C_{H_{L\alpha}} = C_{Hc_{L_i}}$ so that the total hinge moment is given by:

(3)
$$H = C_{Hc_L} C_{L\alpha}\alpha q\, SMAC + C_{Hc_L} C_{Li} i q\, SMAC + C_{Hc_{L\delta}} C_{L\delta}\delta q\, SMAC + C_{H0} q\, SMAC + H_B$$

$$\frac{H}{SMAC} = C_{Hc_L}\left(C_{L\alpha}\alpha + C_{Li} i\right) q + C_{Hc_{L\delta}} C_{L\delta}\delta q + C_{H0} q + \frac{H_B}{SMAC}$$

(3) (Continued)

It is convenient for the purpose of this note to consider the buoyant hinge moment in the form:

(4) $$H_B = \left(\frac{H}{c} - b.c.\right) MAC \times \left(\frac{W}{S}\right)_B S$$

$$\frac{H_B}{S\,MAC} = \left(\frac{H}{c} - a.c. + a.c. - b.c.\right)\left(\frac{W}{S}\right)_B$$

$$= \left(C_{H_{C_L}} + a.c. - b.c.\right)\left(\frac{W}{S}\right)_B$$

In Reference 2 the $C_{H_{C_{L\delta}}}$ has been defined as:

(5) $$C_{H_{C_{L\delta}}} = C_{H_{C_L}} - \frac{1}{4}\left(1 + \frac{T_4/\pi}{T_{10}/\pi}\right)$$

$$= C_{H_{C_L}} - \Delta$$

where the symbol Δ is employed for brevity.

The zero lift hinge moment is not well defined for the flapped, incidence lift control foil because there are many combinations of pitch, incidence, and flap angle which will produce a zero lift, all with different zero lift hinge moments. For the particular case where the pitch and incidence lift aerodynamic center are the same however, $C_{H_{C_{L\alpha}}} = C_{H_{C_{L_i}}}$, the residual hinge moment can be related to the zero-flap, zero lift hinge moment by:

(6) $$C_{H_0} = C'_{H_{C_L=0}} + C_{H_{C_L}} C_{L_0}$$

(6) (Continued)

where the prime is a reminder that the relationship must be evaluated for common pitch and incidence lift aerodynamic centers and for zero flap.

Subsitiuting Eqs. (4) - (6) in Eq. (3):

(7)
$$\frac{H}{S/MAC} = C_{H_{C_L}}\left(C_{L_\alpha}\alpha + C_{L_i} i\right)q + \left(C_{H_{C_L}} - \Delta\right)C_{L_\delta}\delta q$$

$$+ C'_{H_{C_L=0}} q + C_{H_{C_L}} C_{L_0} q + \left(C_{H_{C_L}} + a.c. - b.c.\right)\left(\frac{W}{S}\right)_B$$

$$= C_{H_{C_L}}\left[\left(C_{L_\alpha}\alpha + C_{L_i} i + C_{L_\delta}\delta + C_{L_0}\right)q + \left(\frac{W}{S}\right)_B\right]$$

$$+ (a.c. - b.c.)\left(\frac{W}{S}\right)_B - \Delta C_{L_\delta}\delta q + C'_{H_{C_L=0}} q$$

$$= C_{H_{C_L}}\left[\left(\frac{W}{S}\right)_H + \left(\frac{W}{S}\right)_B\right] + (a.c. - b.c.)\left(\frac{W}{S}\right)_B - \Delta\left(\frac{W}{S}\right)_\delta + C'_{H_{C_L=0}} q$$

$$= C_{H_{C_L}} \frac{W}{S} + (a.c. - b.c.)\left(\frac{W}{S}\right)_B - \Delta\left(\frac{W}{S}\right)_\delta + C'_{H_{C_L=0}} q$$

For brevity, β is defined to be

(8)
$$\beta = (a.c. - b.c.)\left(\frac{W}{S}\right)_B$$

Only one term of Eq. (7) is depth sensitive and that term is more conveniently written:

$$C'_{H_{C_L=0}} = \frac{C_{L\alpha}}{C_{L\alpha\infty}} C'_{H\infty_{C_L=0}} \tag{9}$$

Then Eq. (7) may be written

$$\frac{H}{S_f A C} = C_{H_{C_L}} \frac{W}{S} + \beta - \Delta\left(\frac{W}{S}\right)_\delta + \frac{C_{L\alpha}}{C_{L\alpha\infty}} C'_{H\infty_{C_L=0}} \; q \tag{10}$$

which is the farm employed for the moment analyses in following sections.

From References 2 - 4 the following coefficients are practical for the AG(EH) foils with 20% chord flaps at infinite depth:

(11) $C_{L_i}/C_{L_\alpha} = .838$

$d\alpha/d\delta = .467$

$C_{L_{\alpha_\infty}} = 2.97 = .0519/\text{deg.}$

$C_{L_{i_\infty}} = .838 \times 2.97 = 2.49 = .0435/\text{deg.}$

$C_{L_{\delta_\infty}} = .467 \times 2.49 = 1.164 = .0203/\text{deg.}$

$C_{L_{0_\infty}} = .111$

$C_{H_{C_L}} = C_{H_{C_{L_\alpha}}} = C_{H_{C_{L_i}}} = .07$ (existing)

$\Delta = \frac{1}{4}\left(1 + \frac{T_8/\pi}{T_{10}/\pi}\right) = .1852$

$C_{H_{C_{L_\delta}}} = C_{H_{C_L}} - \Delta = .07 - .1852 = -.1152$ (existing)

$C_{H_{0_\infty}} = -.0608$

$C'_{H_{0_\infty C_L = 0}} = C_{H_{0_\infty}} - C_{H_{C_L}} C_{L_{0_\infty}} = -.0686$ (prototype)

$C_{H_{\alpha_\infty}} = C_{H_{C_L}} C_{L_{\alpha_\infty}} = 2.97 \times .07 = .208 = .00363/\text{deg.}$ (existing)

$C_{H_{i_\infty}} = C_{H_{C_L}} C_{L_{i_\infty}} = 2.49 \times .07 = .1744 = .00304/\text{deg.}$ (existing)

$C_{H_{\delta_\infty}} = C_{H_{C_{L_\delta}}} C_{L_{\delta_\infty}} = 1.164(-.1152) = -.1342 = -.002345/\text{deg.}$ (existing)

(11) (Continued)

$S\,MAC = 2100$

$(W/S)_B \approx 90$

$H_B = -7580$

$H_B/S\,MAC = -3.61$

$a.c. = a.c._\alpha = a.c._i = .315$

$b.c. = .486$

$\beta = (a.c. - b.c.)\left(\frac{W}{S}\right)_B = (.315 - .486) \times 90 = -15.4$

$d_{min.} = 1\ MAC = 9.33\ ft.$

$C_{L\alpha_{1c}}/C_{L\alpha_\infty} = .923$

It is to be noted that the mominal minimum foil depth is quite arbitrary. Grumman prefers to employ that depth for which the nominal maximum foil loading will not ventilate the foil. That depth is an experimental characteristic which has not been established for the AG (EH) foil system and the 1 MAC depth is assumed.

CAVITATION REVIEW

A proper appreciation for the potentialities of Eq. (10) requires a better instuitive appreciation for the effect of flaps on cavitation than is provided by Reference 4 and the subject is therefore reviewed here. This review will also provide on opportunity to incorporate the revised evaluation for the parameter ζ of Reference 2 and to provide accountability for buoyant lift, which was not mentioned in Reference 4.

The following derivation for the cavitation foil loading is more concise than that of Reference 4 and therefore, perhaps, more satisfying intuitively.

The pressure coefficient, S , on the section perpendicular to the quarter-chord line is given by:

$$(12) \quad \sqrt{1-S} = \frac{v}{V} \pm \frac{\Delta v}{V} \pm \frac{\Delta v_a}{V}\left[\left(c'_{l_H} - c'_{l_b}\right) - c_{l_{i\,eff}}\right] \pm \left(\frac{\Delta v}{V}\right)_F c'_{l_b}$$

basic flap load distribution

additional load distribution (angle of attack)

camber (distribution for $c_{l_{i\,eff}}$)

distribution for thickness distribution

where primes indicate plane perpendicular to quarter-chord

The parameters ψ and ζ are d&-fined in Reference 4.

$$(13) \quad \psi = \frac{v}{V} \pm \frac{\Delta v}{V} \mp \frac{\Delta v_a}{V} c_{l_{i\,eff.}}$$

(14) $$\zeta = C_{l_b} / C_{l_F}$$

Then Eq. (12) nay be written:

(15) $$\sqrt{S} = \frac{\nu}{V} \pm \frac{\Delta \nu}{V} \mp \frac{\Delta \nu_a}{V} C_{l_{i\,eff}} \pm \left(C'_{l_H} - C'_{l_b}\right)\frac{\Delta \nu_a}{V} \pm \left(\frac{\Delta \nu}{V}\right)_F C'_{l_b}$$

$$= \gamma \pm \left(C'_{l_H} - C'_{l_b}\right)\frac{\Delta \nu_a}{V} \pm \left(\frac{\Delta \nu}{V}\right)_F C'_{l_b}$$

$$= \gamma \pm \left(C'_{l_H} - \zeta C'_{l_F}\right)\frac{\Delta \nu_a}{V} \pm \zeta \left(\frac{\Delta \nu}{V}\right)_F C'_{l_F}$$

The total hydrodynamic lift coefficient, C_{l_H}, includes the effective design lift corfficient (camber) plus pitch, incidence, and flap components:

(16)

$$\sqrt{S} = \gamma \pm \left[(C'_l)_\alpha + (C'_l)_i + (C'_l)_\delta + C'_{l_{i\,eff}} - \zeta (C'_l)_\delta\right]\frac{\Delta \nu_a}{V} \pm \zeta \left(\frac{\Delta \nu}{V}\right)_F (C'_l)_\delta$$

$$\sqrt{S} - \gamma = \pm\left[(C'_l)_\alpha + (C'_l)_i + (C'_l)_\delta + C'_{l_{i\,eff}} - \zeta (C'_l)_\delta\right]\frac{\Delta \nu_a}{V} \pm \zeta \left(\frac{\Delta \nu}{V}\right)_F (C'_l)_\delta$$

Each of these components of the section lift coefficient is related to the corresponding foil average lift coefficient'component by the appropriate spanwise lift distribution where it is to be noted that the spanwise distribution for camber lift is identical with that for incidence lift:

(17)

$$\sqrt{5}-\psi$$

$$= \pm\left[\left(\frac{c_l}{c_L}\right)_d (c_l')_d + \left(\frac{c_l}{c_L}\right)_i (c_l')_i + \left(\frac{c_l}{c_L}\right)_\delta (c_l')_\delta + \left(\frac{c_l}{c_L}\right)_i c'_{l_{i\,eff}} - \zeta\left(\frac{c_l}{c_L}\right)_\delta (c_l')_\delta\right]\frac{\Delta v_a}{V}$$
$$\pm\, \zeta\left(\frac{c_l}{c_L}\right)_\delta \left(\frac{\Delta v}{V}\right)_F (c_l')_\delta$$

Multiplying this equation through by q' we obtain foil loading components which are independent of the flow orientation. Note that the product, $q'\ c'_{l_{i\,eff}}$ is a theoretical $\left(\frac{W}{S}\right)_o$ which is identified with the experimental value at this point. (for $\alpha_i = 0$ only)

(18)

$$(\sqrt{5}-\psi)q'$$

$$= \pm\left[\left(\frac{c_l}{c_L}\right)_d \left(\frac{W}{S}\right)_d + \left(\frac{c_l}{c_L}\right)_i \left(\frac{W}{S}\right)_i + \left(\frac{c_l}{c_L}\right)_\delta \left(\frac{W}{S}\right)_\delta + \left(\frac{c_l}{c_L}\right)_i \left(\frac{W}{S}\right)_o - \zeta\left(\frac{c_l}{c_L}\right)_\delta \left(\frac{W}{S}\right)_\delta\right]\frac{\Delta v_a}{V}$$
$$\pm\, \zeta\left(\frac{\Delta v}{V}\right)_F \left(\frac{c_l}{c_L}\right)_\delta \left(\frac{W}{S}\right)_\delta$$

$$\pm(\sqrt{5}-\psi)q' = \left[\left(\frac{c_l}{c_L}\right)_d \left(\frac{W}{S}\right)_d + \left(\frac{c_l}{c_L}\right)_i \left(\frac{W}{S}\right)_i + \left(\frac{c_l}{c_L}\right)_i \left(\frac{W}{S}\right)_o\right]\frac{\Delta v_a}{V}$$
$$+ (1-\zeta)\left(\frac{c_l}{c_L}\right)_\delta \left(\frac{W}{S}\right)_\delta \frac{\Delta v_a}{V} + \zeta\left(\frac{c_l}{c_L}\right)_\delta \left(\frac{W}{S}\right)_\delta \left(\frac{\Delta v}{V}\right)_F$$

$$= \left[\left(\frac{c_l}{c_L}\right)_d \left(\frac{W}{S}\right)_d + \left(\frac{c_l}{c_L}\right)_i \left(\frac{W}{S}\right)_i + \left(\frac{c_l}{c_L}\right)_i \left(\frac{W}{S}\right)_o\right]\frac{\Delta v_a}{V}$$
$$+ \zeta\left[\left(\frac{\Delta v}{V}\right)_F - \frac{\Delta v_a}{V}\right]\left(\frac{c_l}{c_L}\right)_\delta \left(\frac{W}{S}\right)_\delta + \frac{\Delta v_a}{V}\left(\frac{c_l}{c_L}\right)_\delta \left(\frac{W}{S}\right)_\delta$$

The parameter, ω, was defined in Reference 4 for convenience:

$$\omega = \delta\left[\left(\frac{\Delta V}{V}\right)_F - \frac{\Delta V_a}{V}\right] \tag{19}$$

and Eq, (18) may be written

(20)

$$\pm(\sqrt{S} - \gamma)q' = \left[\left(\frac{C_\ell}{C_L}\right)_\alpha\left(\frac{W}{S}\right)_\alpha + \left(\frac{C_\ell}{C_L}\right)_i\left(\frac{W}{S}\right)_i + \left(\frac{C_\ell}{C_L}\right)_i\left(\frac{W}{S}\right)_o\right]\frac{\Delta V_a}{V} - \omega\left(\frac{C_\ell}{C_L}\right)_\delta\left(\frac{W}{S}\right)_\delta + \frac{\Delta V_a}{V}\left(\frac{C_\ell}{C_L}\right)_\delta\left(\frac{W}{S}\right)_\delta$$

$$= \left[\left(\frac{C_\ell}{C_L}\right)_\alpha\left(\frac{W}{S}\right)_\alpha + \left(\frac{C_\ell}{C_L}\right)_i\left(\frac{W}{S}\right)_i + \left(\frac{C_\ell}{C_L}\right)_i\left(\frac{W}{S}\right)_o\right]\frac{\Delta V_a}{V} + \left(\frac{\Delta V_a}{V} - \omega\right)\left(\frac{C_\ell}{C_L}\right)_\delta\left(\frac{W}{S}\right)_\delta$$

where:

$$S = 1 + \frac{P_a - P_v + \rho g h}{q'} = 1 + \sigma'$$

$$\frac{W}{S} = \left(\frac{W}{S}\right)_\alpha + \left(\frac{W}{S}\right)_i + \left(\frac{W}{S}\right)_\delta + \left(\frac{W}{S}\right)_o + \left(\frac{W}{S}\right)_B$$

$$= \left(\frac{W}{S}\right)_{ref.} + \left(\frac{W}{S}\right)_\alpha + \left(\frac{W}{S}\right)_\delta + \left(\frac{W}{S}\right)_B$$

$$= \left(\frac{W}{S}\right)_H + \left(\frac{W}{S}\right)_B$$

W/S is the incipient cavitation foil loading for any given $\sqrt{S}$ and q' (or q) and Eq. (20) is the most general form of the relationship.

For a flap lift control system Eq (20) is more conveniently handled by:

(21) $$\text{Let } \left(\frac{W}{S}\right)_\delta = \frac{W}{S} - \left(\frac{W}{S}\right)_\alpha - \left(\frac{W}{S}\right)_i - \left(\frac{W}{S}\right)_o - \left(\frac{W}{S}\right)_B$$
$$= \frac{W}{S} - \left(\frac{W}{S}\right)_{ref} - \left(\frac{W}{S}\right)_\alpha - \left(\frac{W}{S}\right)_B$$

Subsitiuting in Eq. (20):

(22)

$$\pm\left(\sqrt{5}-\gamma\right)q' = \left[\left(\frac{C_D}{C_L}\right)_\alpha \left(\frac{W}{S}\right)_\alpha + \left(\frac{C_D}{C_L}\right)_i \left(\frac{W}{S}\right)_{ref}\right]\frac{\Delta V_a}{V}$$
$$+\left[\frac{W}{S} - \left(\frac{W}{S}\right)_{ref} - \left(\frac{W}{S}\right)_\alpha - \left(\frac{W}{S}\right)_B\right]\left(\frac{C_D}{C_L}\right)_\delta\left(\frac{\Delta V_a}{V}-\omega\right)$$
$$=\left(\frac{C_D}{C_L}\right)_\delta\left(\frac{\Delta V_a}{V}-\omega\right)\frac{W}{S} + \left[\left(\frac{C_D}{C_L}\right)_i\frac{\Delta V_a}{V} - \left(\frac{C_D}{C_L}\right)_\delta\left(\frac{\Delta V_a}{V}-\omega\right)\right]\left(\frac{W}{S}\right)_{ref}$$
$$+\left[\left(\frac{C_D}{C_L}\right)_\alpha\frac{\Delta V_a}{V} - \left(\frac{C_D}{C_L}\right)_\delta\left(\frac{\Delta V_a}{V}-\omega\right)\right]\left(\frac{W}{S}\right)_\alpha - \left(\frac{C_D}{C_L}\right)_\delta\left(\frac{\Delta V_a}{V}-\omega\right)\left(\frac{W}{S}\right)_B$$
$$\pm\frac{\left(\sqrt{5}-\gamma\right)q'}{(C_D/C_L)_\delta} = \left(\frac{\Delta V_a}{V}-\omega\right)\frac{W}{S} + \left[\frac{(C_D/C_L)_i}{(C_D/C_L)_\delta}\frac{\Delta V_a}{V} - \frac{\Delta V_a}{V} + \omega\right]\left(\frac{W}{S}\right)_{ref}$$
$$+\left[\frac{(C_D/C_L)_\alpha}{(C_D/C_L)_\delta}\frac{\Delta V_a}{V} - \frac{\Delta V_a}{V} + \omega\right]\left(\frac{W}{S}\right)_\alpha - \left(\frac{\Delta V_a}{V}-\omega\right)\left(\frac{W}{S}\right)_B$$

The parameter, ξ , is defined for convenience in Reference 4:

(23)
$$\xi_i = \frac{(C_D/C_L)_i}{(C_D/C_L)_\delta} - 1$$
$$\xi_\alpha = \frac{(C_D/C_L)_\alpha}{(C_D/C_L)_\delta} - 1$$

and Eq. (22) may be written:

(24)

$$\pm \frac{(\sqrt{S} - \psi)\, q'}{(C_\ell/C_L)_\delta} = \left(\frac{\Delta v_a}{V} - \omega\right)\left[\frac{W}{S} - \left(\frac{W}{S}\right)_B\right] + \left(\zeta_i \frac{\Delta v_a}{V} + \omega\right)\left(\frac{W}{S}\right)_{ref} + \left(\zeta_\alpha \frac{\Delta v_a}{V} + \omega\right)\left(\frac{W}{S}\right)_\alpha$$

$$\left(\frac{\Delta v_a}{V} - \omega\right)\left(\frac{W}{S}\right)_H = \pm \frac{(\sqrt{S} - \psi)\, q'}{(C_\ell/C_L)_\delta} - \left(\omega + \zeta_i \frac{\Delta v_a}{V}\right)\left(\frac{W}{S}\right)_{ref} - \left(\omega + \zeta_\alpha \frac{\Delta v_a}{V}\right)\left(\frac{W}{S}\right)_\alpha$$

which is identical with Eq. (6.2.19) of Reference 4 except for the obvious refinement that the total W/S is now identified as the hydrodynamic foil loading.

For the case where the full exposed span is flapped Eq. (24) reduces to

(25)

$$\left(\frac{\Delta v_a}{V} - \omega\right)\left(\frac{W}{S}\right)_H = \pm \frac{(\sqrt{S} - \psi)\, q'}{(C_\ell/C_L)_\delta} - \omega\left(\frac{W}{S}\right)_{ref} - \left(\omega + \zeta_\alpha \frac{\Delta v_a}{V}\right)\left(\frac{W}{S}\right)_\alpha$$

$$\left[\text{For } \left(\frac{C_\ell}{C_L}\right)_\delta = \left(\frac{C_\ell}{C_L}\right)_i\right]$$

which is Eq. (6.2.21) of Reference 4.

For the incidence lift control case for a flapped foil,

(26) $$\text{Let: } \left(\frac{W}{S}\right)_i = \frac{W}{S} - \left(\frac{W}{S}\right)_B - \left(\frac{W}{S}\right)_0 - \left(\frac{W}{S}\right)_\delta - \left(\frac{W}{S}\right)_\alpha$$

and substitute in Eq. (~~23~~ 20):

(27)

$$\pm\left(\sqrt{S}-\mathcal{V}\right)\zeta'$$

$$=\left[\left(\frac{c_l}{c_L}\right)_\alpha\left(\frac{W}{S}\right)_\alpha+\left(\frac{c_l}{c_L}\right)_i\left(\frac{W}{S}\right)_0+\left(\frac{c_l}{c_L}\right)_i\frac{W}{S}-\left(\frac{c_l}{c_L}\right)_i\left(\frac{W}{S}\right)_H-\left(\frac{c_l}{c_L}\right)_i\left(\frac{W}{S}\right)_0-\left(\frac{c_l}{c_L}\right)_i\left(\frac{W}{S}\right)_\delta-\left(\frac{c_l}{c_L}\right)_i\left(\frac{W}{S}\right)_\alpha\right]\frac{\Delta v_a}{V}$$

$$+\left(\frac{\Delta v_a}{V}-\omega\right)\left(\frac{c_l}{c_L}\right)_\delta\left(\frac{W}{S}\right)_\delta$$

$$=\left\{\left(\frac{W}{S}\right)_H\left(\frac{c_l}{c_L}\right)_i-\left(\frac{c_l}{c_L}\right)_i\left(\frac{W}{S}\right)_\delta+\left[\left(\frac{c_l}{c_L}\right)_\alpha-\left(\frac{c_l}{c_L}\right)_i\right]\left(\frac{W}{S}\right)_\alpha\right\}\frac{\Delta v_a}{V}$$

$$+\left(\frac{\Delta v_a}{V}-\omega\right)\left(\frac{c_l}{c_L}\right)_\delta\left(\frac{W}{S}\right)_\delta$$

$$=\left(\frac{c_l}{c_L}\right)_i\frac{\Delta v_a}{V}\left(\frac{W}{S}\right)_H+\left[\left(\frac{c_l}{c_L}\right)_\delta\left(\frac{\Delta v_a}{V}-\omega\right)-\left(\frac{c_l}{c_L}\right)_i\frac{\Delta v_a}{V}\right]\left(\frac{W}{S}\right)_\delta$$

$$+\left[\left(\frac{c_l}{c_L}\right)_\alpha-\left(\frac{c_l}{c_L}\right)_i\right]\frac{\Delta v_a}{V}\left(\frac{W}{S}\right)_\alpha$$

For the special case where the full exposed span is flapped, a very convenient reduction results by dividing through by $(c_l/c_L)_\delta$:

(28)

$$\pm\frac{\left(\sqrt{S}-\mathcal{V}\right)\zeta'}{(c_l/c_L)_\delta}=\frac{(c_l/c_L)_i}{(c_l/c_L)_\delta}\frac{\Delta v_a}{V}\left(\frac{W}{S}\right)_H+\left[\frac{\Delta v_a}{V}-\omega-\frac{(c_l/c_L)_i}{(c_l/c_L)_\delta}\frac{\Delta v_a}{V}\right]\left(\frac{W}{S}\right)_\delta$$

$$+\left[\frac{(c_l/c_L)_\alpha}{(c_l/c_L)_\delta}-\frac{(c_l/c_L)_i}{(c_l/c_L)_\delta}\right]\frac{\Delta v_a}{V}\left(\frac{W}{S}\right)_\alpha$$

$$=\frac{\Delta v_a}{V}\left(\frac{W}{S}\right)_H-\omega\left(\frac{W}{S}\right)_\delta+\xi_\alpha\frac{\Delta v_a}{V}\left(\frac{W}{S}\right)_\alpha$$

$$\frac{\Delta v_a}{V}\left(\frac{W}{S}\right)_H=\pm\frac{\left(\sqrt{S}-\mathcal{V}\right)\zeta'}{(c_l/c_L)_\delta}+\omega\left(\frac{W}{S}\right)_\delta-\xi_\alpha\frac{\Delta v_a}{V}\left(\frac{W}{S}\right)_\alpha$$

$$\left[\text{For } (c_l/c_L)_\delta=(c_l/c_L)_i\right]$$

(28) (Continued)

For the more general case, however, it is more convenient to divide Eq. (27) through by $\left(C_l / C_L\right)_i$:

(29)

$$\pm \frac{(\sqrt{S}-V)\rho'}{(C_l/C_L)_i} = \frac{\Delta v_a}{V}\left(\frac{W}{S}\right)_H + \left[\frac{(C_l/C_L)_\delta}{(C_l/C_L)_i}\left(\frac{\Delta v_a}{V}-\omega\right) - \frac{\Delta v_a}{V}\right]\left(\frac{W}{S}\right)_\delta$$

$$+\left[\frac{(C_l/C_L)_\alpha}{(C_l/C_L)_i} - 1\right]\frac{\Delta v_a}{V}\left(\frac{W}{S}\right)_\alpha$$

$$\frac{\Delta v_a}{V}\left(\frac{W}{S}\right)_H = \pm \frac{(\sqrt{S}-V)\rho'}{(C_l/C_L)_i} - \left[\frac{(C_l/C_L)_\delta}{(C_l/C_L)_i}\left(\frac{\Delta v_a}{V}-\omega\right) - \frac{\Delta v_a}{V}\right]\left(\frac{W}{S}\right)_\delta$$

$$+\left[1-\frac{(C_l/C_L)_\alpha}{(C_l/C_L)_i}\right]\frac{\Delta v_a}{V}\left(\frac{W}{S}\right)_\alpha$$

which, of course, reduces immediately to Eq. (28) for

$\left(C_l/C_L\right)_\delta = \left(C_l/C_L\right)_i$.

Note that for the unflapped foil EQ. (29) reduce's to

(30)

$$\frac{\Delta v_a}{V}\left(\frac{W}{S}\right)_H = \pm \frac{(\sqrt{S}-V)\rho'}{(C_l/C_L)_i} + \left[1-\frac{(C_l/C_L)_\alpha}{(C_l/C_L)_i}\right]\frac{\Delta v_a}{V}\left(\frac{W}{S}\right)_\alpha$$

(for incidence lift control with unflapped foil)

an5 if the foil is rigidly attached to the pod, $\left(C_l/C_L\right)_i = \left(C_l/C_L\right)_\alpha$, there is a further reduction to:

$$(31)\quad \frac{\Delta V_{a.c.}}{V}\left(\frac{W}{S}\right)_H = \pm \frac{(\sqrt{5} - 7K)\beta'}{C_D/C_L} \qquad \left(\begin{array}{l}\text{for pitch lift control}\\ \text{with unflapped foil}\end{array}\right)$$

which is Eq. (6.1.4) of Reference 4.

Some inconsistencies have entered the AG(EH) study by way of interpolating the section characteristics and Figures 1 and 2 present graphical interpolations from the velocity distributions of Reference 6 to avoid this problem in the future.

(31) (Continued)

Figure 4 presents three of Allen's basic flap load distributions, Reference 5, for ready reference for this study.

For any given lift coefficient, whatever its components, the cavitation speed is proportional to the depth function:

(32) $$V_C \approx \sqrt{P_A - P_V + \rho g h}$$

Thus a cavitation bucket derived for any particular depth can be transformed to another depth by use of the functions:

$$\frac{V_C}{V_{C_0}} = \sqrt{1 + \frac{\rho g h}{P_A - P_V}}$$

(33) $$\frac{W/S}{(W/S)_0} = \left(\frac{V_C}{V_{C_0}}\right)^2 = 1 + \frac{\rho g h}{P_A - P_V}$$

The function Vc/Vc_0 is presented on Figure 3 for convenience in transforming the cavitation buckets of this note to other depths. Figure 3 was not employed in the derivation of the cavitation buckets of this note which were all derived directly from the equations of this section.

Figure 3 is valid only for the theoretical incipient cavitation bucket of course; there is no theoretical accountability at present for the cavitation inhibiting effect of the free surface.

UPDATING THE INTERIM REPORT

CAVITATION BUCKET .

The AG(EH) fwd. foil incidence lift cavitation buckets of Reference 4 are inappropriate to this study for five reasons:

1. Foil buoyancy was not accounted for,
2. The model camber was presented rather than the prototype camber (for evaluation of the towing tank test results),
3. The depth was model depth (8.5 ft) rather than the 1 MAC depth (9.33 ft) preferred for this study,
4. Zero pitch was assumed to simplify the calculations while a more realistic pitch (1°) is preferred for this study,
5. The cavitation parameter, ζ, was reevaluated in Reference 2.

The first four modifications to the cavitation buckets of Reference 4 are discussed in this section and the effect of reevaluating ζ is considered in a later section. The necessary section and cavitation characteristics are presented in Tables I and II.

Typical buoyant and depth effects are shown on Figure 5. The 8.5 ft. depth, zero buoyancy bucket of Figure 5 is almost identical with the incidence lift buckets of Reference 4 though that of Figure 5 was derived from Eq. (28). The top of the bucket of Figure 5 is almost a knot higher than that of Reference 4 for some reason not explored here though it was noted that the section bucket of Figure 6.2 of Reference 4 is slightly in error for the mid-chord stations.

Buoyancy is a scale effect, as discussed elsewhere in these notes, having a negligible'value in model scale, The buoyancy effect of Figure 5, then, actually exists in the comparison of model and prototype data. Note that buoyancy shifts the bucket on the foil loading scale, by the value of the buoyant foil loading, while increasing depths expand the bucket at all three boundaries, Again it is to be noted that this depth effect is theoretical, 'Near the surface there is a significant and unpredictable cavitation inhibiting effect, most familiar on yawed struts.

The effects of pitch and camber are illustrated on Figure 6. The effect of pitch is slight because it represents a redistribution of the total lift between pitch and incidence lift. Increasing pitch expands all three boundaries because the spanwise lift distribution for pitch lift is more favorable than that for incidence lift.

Increasing camber lowers the top of the bucket and rotates the bucket about the axis to the right. The AG(EH) bucket top is much higher than necessary and substantially more camber could be added or, alternatively, a new section of inferior cavitation characteristics but more favorabie $c_{m_{a.c.}}$ could be employed.

The prototype bucket of Figure 6 is employed as the basic, or reference, cavitation bucket throughout the rest of this note.

FLAP CONTROL OF CAVITATION

The principle employed here was introduced in Reference 4. In essence, the simultaneous solution of Eq. (28) evaluated for the leading edge and the flap hinge station on the upper surface is the flap foil loading, $C_{L_\delta}q$, which provides simultaneous incipient cavitation at those two stations and the corresponding total foil loading. This flap angle redistributes the unflapped incidence lift contol chordwise load distribution in an approximation for the ideal distribution for cavitation. An identical solution is provided by Eq. (25), which was the equation employed in Reference 4, except that the solutions are total foil loading and reference foil loading where reference foil loading and flap foil loading are related by the foil loading relationships in Eq. (20).

For the purpose of deriving this optimum cavitation bucket it is convenient to rearrange Eq. (28) in the form.

$$(34)\qquad \frac{\Delta v_a}{V}\left(\frac{W}{S}\right)_H = \pm\frac{(\sqrt{S}-\gamma)q'}{(c_\ell/C_L)_\delta} + \omega\left(\frac{W}{S}\right)_\delta - \xi_\alpha\frac{\Delta v_a}{V}\left(\frac{W}{S}\right)_\alpha$$

$$\frac{\Delta v_a}{V}\left(\frac{W}{S}\right)_H - \omega\left(\frac{W}{S}\right)_\delta = \pm\frac{(\sqrt{S}-\gamma)q'}{(c_\ell/C_L)_\delta} - \xi_\alpha\frac{\Delta v_a}{V}\left(\frac{W}{S}\right)_\alpha$$

$$\left(\frac{W}{S}\right)_H - \frac{\omega}{\Delta v_a/V}\left(\frac{W}{S}\right)_\delta = \pm\frac{(\sqrt{S}-\gamma)q'}{\frac{\Delta v_a}{V}\left(\frac{c_\ell}{C_L}\right)_\delta} - \xi_\alpha\left(\frac{W}{S}\right)_\alpha$$

$$\left(\frac{W}{S}\right)_H - \frac{\delta\left[\frac{\Delta v_a}{V}-\left(\frac{\Delta v}{V}\right)_F\right]}{\Delta v_a/V}\left(\frac{W}{S}\right)_\delta = \pm\frac{(\sqrt{S}-\gamma)q'}{\frac{\Delta v_a}{V}\left(\frac{c_\ell}{C_L}\right)_\delta} - C_{L_\alpha}\alpha\,\xi_\alpha\,q$$

$$\left(\frac{W}{S}\right)_H - \delta\left[1-\frac{(\Delta v/V)_F}{\Delta v_a/V}\right]\left(\frac{W}{S}\right)_\delta = \pm\frac{(\sqrt{S}-\gamma)q'}{\frac{\Delta v_a}{V}\left(\frac{c_\ell}{C_L}\right)_\delta} - C_{L_\alpha}\alpha\,\xi_\alpha\frac{q}{q'}q'$$

$$= \left[\pm\frac{\sqrt{S}-\gamma}{\frac{\Delta v_a}{V}\left(\frac{c_\ell}{C_L}\right)_\delta} - \frac{C_{L_\alpha}\alpha}{q'/q}\right]q'$$

(34) (Continued)

This is still in its most general form, appropriate for any station on any foil. Restricted to the upper surface of the AG(EH) foil, Eq. (34) becomes:

$$(35) \quad \left(\frac{W}{S}\right)_{\mu} - \zeta\left[1 - \frac{(\Delta v/V)_F}{\Delta v_a/V}\right]\left(\frac{W}{S}\right)_{\delta} = \left[\frac{\sqrt{\sigma} - \gamma}{\frac{\Delta v_a}{V}\left(\frac{C_L}{C_{L\delta}}\right)_{\delta}} - \frac{C_{L\alpha}\, \alpha}{\rho'/\rho}\,\zeta_{\alpha}\right]\rho'$$

$$= \left[\frac{\sqrt{\sigma} - \gamma}{1.31\,\frac{\Delta v_a}{V}} - \frac{.048}{.668}(-.109)\right]\rho' \qquad [\theta = 1^{\circ}]$$

$$= \left[\frac{\sqrt{\sigma} - \gamma}{1.31\,\frac{\Delta v_a}{V}} + .00784\right]\rho'$$

The incipient cavitation foil loadings, flap schedules, and incidence angles provided by Eq. (35) for several section and operating parameters are shown on Figures 7 — 9. These figures relate the reference cavitation buckets of the Interim Report to the updated reference buckets of this note. The first curve of Figure 7 is the reference curve of the Interim Report and is for the model section. The difference between curves #1 and #2 is the advantage afforded by the increase& camber of the prototype. The difference between curves #2 and #3 presents some advantage in depth and pitch angle but mostly due to accountability for buoyancy. The flap load distribution parameter, ζ , has no effect on the boundary of Figure 7.

figure 8 presents the flap schedules which produce the boundaries of Figure 7 and here the parameter ζ does make a difference. Throughout this note the revised definition of Reference 2 for ζ was employed to evaluate this parameter

Figure 9 presents the incidence angles associated with the boundaries of Figure 7. These angles have no particular significance to the incidence control foil but the ζ comparison of Figure 9 is very significant to one conclusion of the Interim Report and is discussed in some detail in the next section.

The use of flaps as a cavitation control device suggests the use of a symmetric section with a 50% chord flap to approximate an a = 1.0 camber distribution of adjustable design lift coefficient. Figure 10 presents an evaluation of this possibility. The results indicate that the basic section must be designed for the design speed conditions, though flaps can be employed to unload the leading edge at low speed and improve the boundary there.

Figure 10 indicates that larger flaps improve the cavitation bucket slightly but the structural disadvantage is considered too great for further consideration. The flap schedules and incidence angles for the boundaries of Figure 10 are presented on Figures 11 and 12 for information but only the prototype section of 20% chord flap is considered further in this note.

Figure 10 presents a relatively confident incipient cavitation advantage for the flaps but no conclusions can be drawn about the effects of flaps on the effective cavitation boundaries in the absence of an adequate experimental cavitation map for some, any, flapped foil.

CORRECTING AN INTERIM REPORT CONCLUSION

The boundary incidence angles of Figure 9 are the optimum (cavitation) incidence angles for the flap left control foil. The Interim Report concludes, on the basis of curve #1 of Figure 9, that the incidence for the flap lift control foil could be permanently fixed at an angle which would produce the optimum cavitation bucket at any speed. Figure 9 indicates that the near-zero slope of curve 1 is a coincidental result of the evaluation adopted for ζ in the Interim Report. That indication has been confirmed by a calculation, not shown, for curve 1 with a ζ of .65 which has a substantial negative slope for the curve throughout.

****

Neither ζ value of Figure 9 is adequately supported and no confident consideration can be given to the incidence angle for the flap lift control foil until such experimental support is provided.

REFERENCE FLAP SCHEDULES

The *three* flap schedules of Figure 13 are investigated in detail in this note. The first schedule is the degenerate case of the unflapped foil, $(W/S)_\delta = 0$. The second case is the "optimum cavitation" schedule of Figure 11 for the AG(EH) prototype with a 20% chord flap and with the revised (.466) value for ζ. The third case will be developed more fully in a 'later section but has a slope of:

$$(36) \qquad \frac{d(\frac{W}{S})_\delta}{dq} = C'_{H\infty_{C_L=0}} / \Delta$$

$$= -.0686/.1852$$

$$= -.37$$

This slope is passed through the aerodynamic 30° flap foil loading at a minimum flight speed of 30 knots:

$$(37) \qquad \left(\frac{W}{S}\right)_{\delta_{30K}} = C_{L\delta_\infty} \times 30^\circ \times q_{30K}$$

$$= .0203 \times 30 \times 2550$$

$$= 1552$$

The flap schedule of Eqs. (36) and (37) is referred to as the "optimum moment" OR "MINIMUM MOMENT" schedule for reasons to be developed later.

REFERENCE CAVITATION BUCKETS

The cavitation buckets for the three flap schedules of Figure 13 are presented on Figures 14 - 17. Figures 14 - 16 present the construction of the cavitation buckets because it is instructive to view the relationship between the incipient cavitation speeds for all of the chord stations; i.e., the variation of chordwise pressure distribution with speed.

Only the stations bracketing the cavitation bucket (see Tables III & IV) have been considered in this note to conserve time. Where movement of the chord station for initial cavitation is indicated, as on the upper surface, leading edge boundary of Figure 14, it is abvious that intermediate stations would provide a more detailed boundary though the difference would be insignificant.

The spacing of the individual station boundaries of Figure 14 is a qualitative indication of the chordwise spread of cavitation as the incipient boundary is more deeply penetrated; the spanwise load distribution of Figure 6.1 of Reference 4 provides the same qualitative indication of the spanwise spread of cavitation.

Close station boundary spacing, for unit chordwise stations, indicates rapid cavity growth and a relatively "hard" boundary, The upper right corner of the bucket, then, is the "hardest" region of the bucket because the boundaries for every station pivot about ~~station pivot about~~ a point near this corner; this is perhaps seen more clearly on Figure 6.2 of Reference 4. The effective cavitation boundaries (peak lift, cavitation drag, etc.) all spring from the incipient bucket at this corner. The upper surface leading edge boundary is so "soft" that it carries no significance.

The upper surface, mid-chord and lower surface, leading edge boundaries have never been mapped. The upper surface is expected to be a hard boundary since at least 20% of the chord is on the verge of cavitation here. The lower surface boundary is expected to be soft except that propeller experience indicates that the erosion boundary may coincide with the incipient boundary for the lower (pressure) surface.

These intuitive and poorly understood characteristics of the cavitation bucket must be borne in mind in evaluating the bucket. On Figure 15, for example, it is evident that the flap has shifted the bucket to higher foil loadings without affecting its general characteristics, Figure 16 presents a qualitatively different and very interesting flap effect. Here the bucket has been straightened up and 10 knots added to the top of the bucket. The "corner" of the bucket has been softened very substantially, The hinge line boundary is not significant because foils typically operate cavitated at low speed, because it is a very local condition which might not develop in practice, and because a alight adjustment in the flap schedule would eliminate this boundary.

Remembering that Figure 16 results from the addition of a flap to an existing foil, with no consideration for cavitation, a very real potential for a high speed (~ 80 knot), cavitation free, conventional section foil is suggested here, Pursuit of this possibility, however, lies outside the scope of the AG(EH) lift study.

The three reference buckets are compared on Figure 17. The adequacy of the optimum moment bucket depends entirely upon its effective boundary and upon the normal acceleration requirement. The maximum foil loading indicated provides a 1/4 g margin over the 1435 psf design foil loading and is probably extreme. Note that even with the hinge line boundary, the optimum moment bucket provides a lower cavitation-free speed at 1435 psf than does the unflapped bucket.

Note that the optimum moment bucket intersects the optimum cavitation bucket at the speed for which they have a common flap angle on Figure 13. Similarly the optimum moment bucket intersects the unflapped bucket at the speed at which the flap schedule passes through zero on Figure 13. There is no comparable intersection between the optimum cavitation and unflapped buckets because the zero flap angle for optimum cavitation occurs at a speed above both buckets.

CLASSES OF MOMENT CONTROL (An Intuitive Review)

Symmetric Section

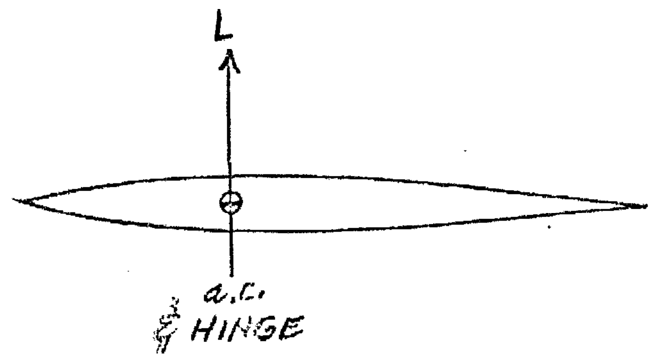

The symmetric section has no $C_{m_{a.c.}}$, hence always presents a zero hinge moment when hinged at the aerodynamic center, Such a section does not present a useful incipient cavitation bucket at high speed, though its effective cavitation 'bucket has never been established, and has never been employed for hydrofoils. The symmetric section should be considered for low speed ad/or lightly loaded application however; e.g. this would appear to be the logical section ~~from~~ for SWATH trim control. The hinge might be set off of the a.c. by a nominal amount to insure undirectional hinge moments.

Cambered Section

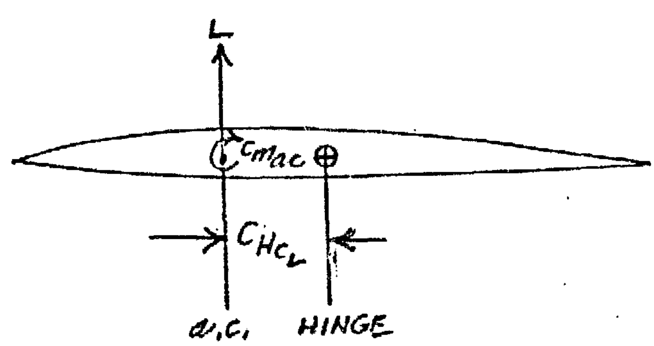

The cambered section is discussed in some detail in Reference 1. It presents hinge moments defined by

(38) $$C_H = C_{Hc_L} C_L + C_{Mac}$$

(38) (Continued)

where the C_{Mac} is always negative for hydrofoils. Dimensionally the hinge moment is:

(39) $$\frac{H}{SMAC} = C_H\, q = C_{Hc_L}\frac{W}{S} + C_{Mac}\, q$$

Because the moment is a function of q, no single hinge location $\left(C_{Hc_L}\right)$ will produce a zero hinge moment over the speed range. This type foil must be hinged to produce a vanishing hinge moment at one flight speed extreme, accepting whatever results at the other flight speed extreme. The extreme moment is always less if the foil is hinged to produce a 'zero moment at minimum flight speed, which is why hydrofoil hinge moments are always negative.

Flapped (Incidence Lift Control) Section

In terms of the concept of lift-at-a.c./moment-about-a.c., Eq. (10) may be presented as:

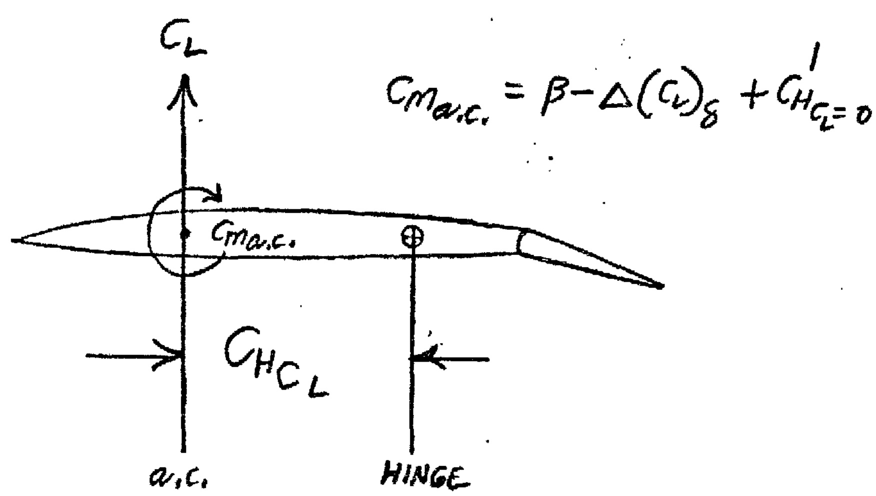

The alternative center-of-pressure concept is awkward for analysis and is not employed in the analysis of this note. It does have intuitive value however in identifying the significance of the coefficients of the moment equation. Presented in terms of centers of pressure, Eq. (10) may be presented as:

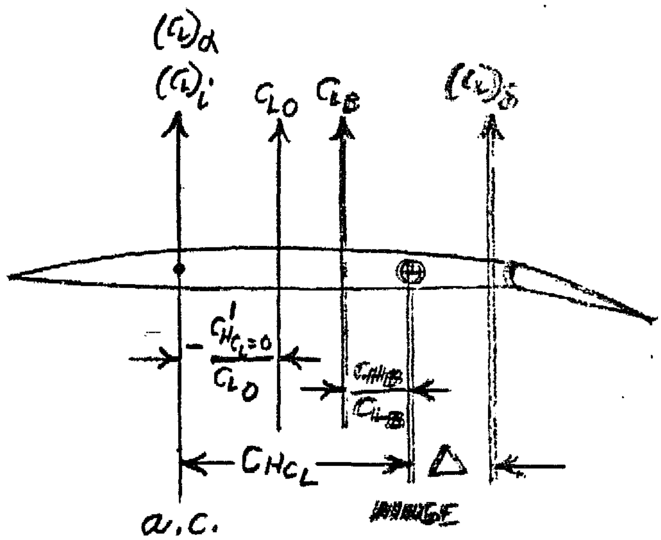

The chordwise pressure distributions present an even more fundamental view of the hinge moment equation and one which is particularly useful to an intuitive appreciation for this note. The buoyant lift and moment are omitted from this intuitive review for clarity.

The camber lift distribution is a function of the camber and for hydrofoils the a = 1.0 camber line is employed for cavitation reasons. Theoretically, then, the chordwise distribution of the camber lift with which we are concerned has the shape:

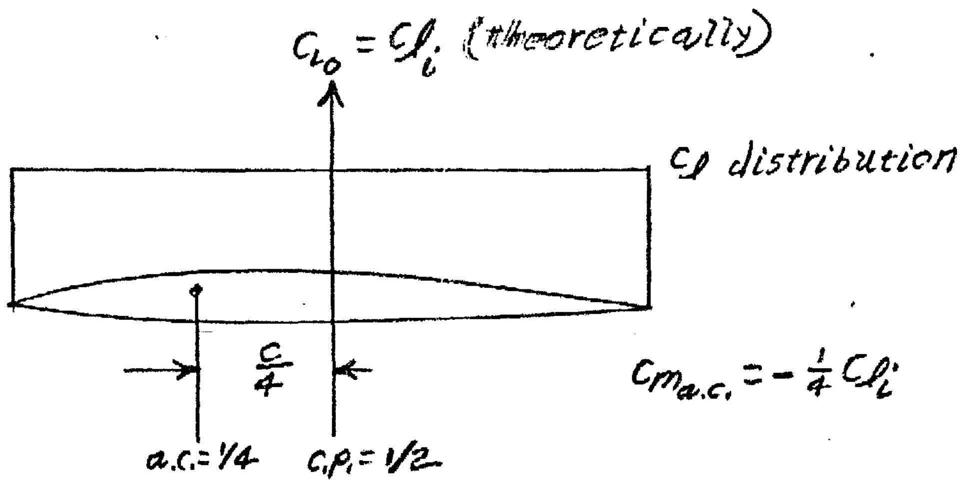

The chordwise lift distribution due to pitch or incidence is the classic "additional" lift distribution, which is a function of section thickness distribution though the C.P. is about at the quarter-chord for any section:

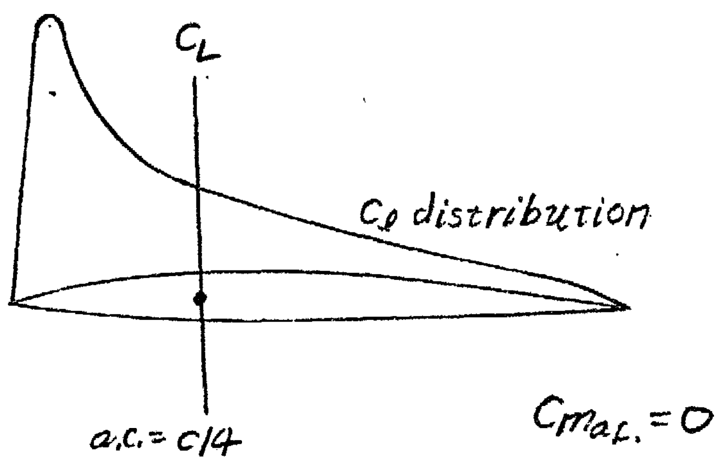

The chordwise flap load distribution, in Allen's view, has two components, one identical with the "additional" lift distribution and one which is a function of flap chord:

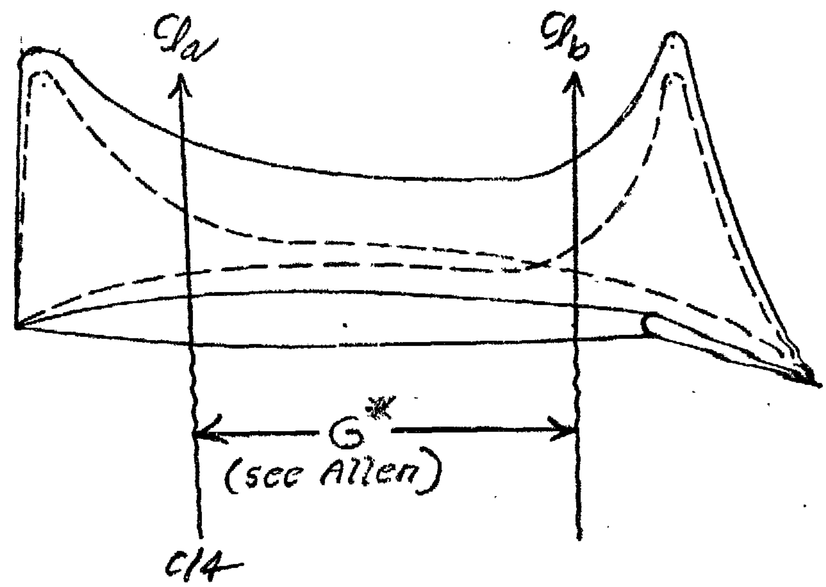

The optimum flap schedule for cavitation of Reference 4 makes the leading edge and hinge line pressure identical throughout the flight speed range thereby achieving almost a flat chordwise lift distribution throughout that range:

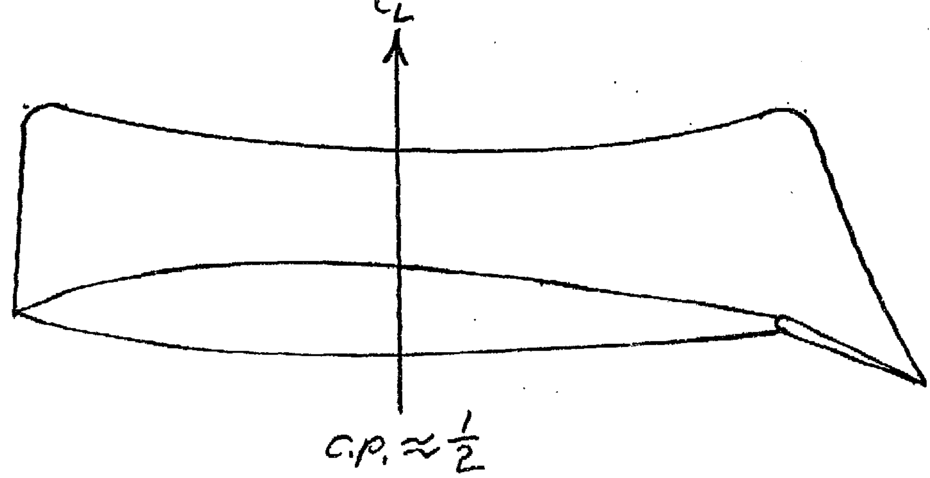

As a consequence, the center of pressure remains at about half-chord throughout the flight speed range, This means that the cavitation control and mean hinge moment control objectives for the flap schedule are virtually identical since the foil could be hinged at the fixed c.p. position to provide a zero mean hinge moment across the speed range. The difficulty is that this is only the mean hinge moment, the lift for acceleration margin must still be supplied in the form of additional load distribution having its c.p. at the 1/4 chord point - 1/4 chord away from the zero mean moment hinge:

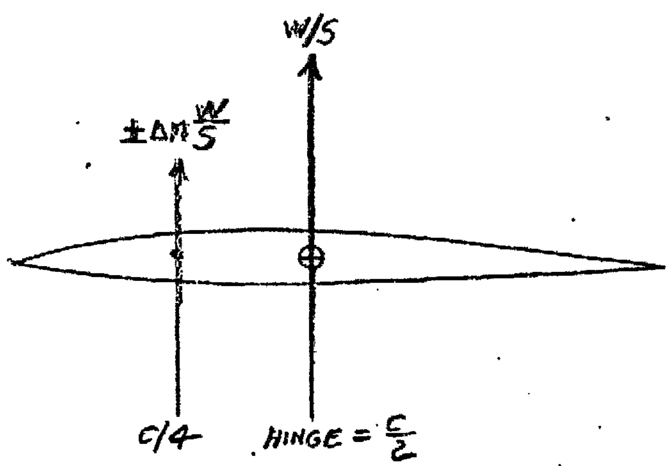

Therefore the zero mean moment foil still presents a maximum hinge moment of

$$\frac{H_{max}}{SMAC} = \frac{1}{4} \times \left(\pm \Delta n \frac{W}{S}\right)$$

For example the AG(EH) fwd foil, hinged and operated for a zero mean moment with ± 1/4 g acceleration margins, would present a maximum moment of:

$$\frac{H_{max}}{S_{MAC}} = \pm \frac{1}{4} \times \frac{1}{4} \times 1435 = 89.7 \text{ psf}$$

$$H_{max} \times 10^{-6} = \pm .0897 \times 2.1 = .1885 \text{ ft. lbs.} = 2.26 \text{ in. lbs.}$$

compared with the existing 10 X PO^6 in. lbs. The feasibility for the zero mean moment system, however, depends upon the feasibility for designing a control systemiohandle this moment with no significant angular discontinuity at crossover.

For the AG(EH) example the extreme c.p.'s are:

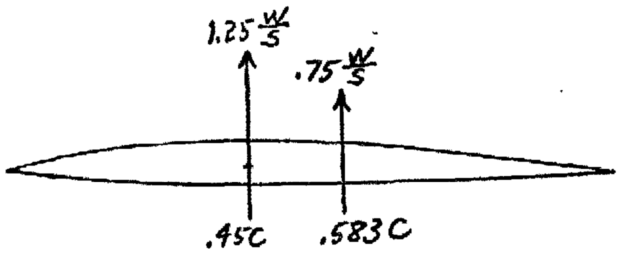

To make the moments undirectional there are the options for hinging at .583C where the maximum moment is:

$$\frac{H_{max}}{S_{MAC}} = +1.25 \frac{W}{S} (.583 - .45) = .1663 \frac{W}{S} = 239 \text{ psf for } \frac{W}{S} = 1435$$

or at .45C where

$$\frac{H_{max}}{S_{MAC}} = -.75 \frac{W}{S} (.583 - .45) = -.1 \frac{W}{S} = -143.5 \text{ psf for } \frac{W}{S} = 1435$$

and, in general, the maximum hinge moment will be reduced by the factor $(1-\Delta n)/(1+\Delta n)$ if the foil is hinged to produce negative undirectional moments rather than positive.

What has been reviewed intuitively here with respect to flap control of incidence hinge moment will be validated rationally in a later section but two limitation upon that analysis are noted here:

(1) It is evident that the thickness distribution, camber distribution and flap chord ratio could al.1 be tailored for still further optimization of the cavitation and/or moment characteristics. Such efforts would over-extend the existing accuracy state-of-the-art for flap cavitation and moment characteristics however and'this analysis assumes the existing foil configuration with the anticipated 20% chord flaps.

(2) The optimum cavitation flap schedule is defined on the basis of the incipient cavitation bucket while it is the effective cavitation bucket, still totally unknown for flapped hydrofoils, which is significant. The same limitation, incidently, applies to the universal use of 16-series sections and the a = 1.0 mean line for incidence lift control hydrofoils though no demonstrations are available that these sections arceffectively superior-to: older or newer sections.

THE REFLEXED SECTION

Eq. (10) is repeated here for convenience:

$$\frac{H}{S\,MAC} = \left[C_{H_{C_L}} \frac{W}{S} + \beta\right] - \left[\Delta (C_L)_\delta - C'_{H_{C_L=0}}\right] q \qquad (10)$$

One way to produce a zero hinge moment throughout the speed range is to make both bracketed terms vanish; i.e.

1. Set $\Delta (C_L)_\delta = C'_{H_{C_L=0}}$

2. Offset the hinge off of the a.c. only far enough to cancel the buoyant moment.

A trivial solution to the two requirements is provided by the unflapped, symmetric section but this solution is known to be inadequate for cavitation for a lifting foil. Thus the solution, if it exists, presents a cambered section with the flap deflected in oppostion to the camber and by a fixed amount; i.e., the section is essentially a reflexed, unflapped section.

The general subject of reflexed sections lies far beyond the scope of this note but *an* evaluation of flap supplied reflex for one particular case will demonstrate a negligible probability of feasibility for reflexed sections generally for lifting foils.

For the AG(EH) fwd foils with 20% chord flaps, the requirement for a vanishing q term in Eq. (10) implies:

$$(C_L)_\delta = \frac{C'_{H_{C_L=0}}}{\Delta}$$

$$C_{L_\delta}\delta = -.0686/.1852$$

$$.0203\ \delta^\circ = -.37$$

$$\delta^\circ = -18.23$$

Obviously such a flap deflection defeats the purpose of the camber provided for high speed and would have a disastrous effect upon the low speed cavitation performance. Minimization of this adverse effect would' require impractically large flap chord ratios and/or ineffectively small cambers.

In summary, the employment of flaps to eliminate the q term of the hinge moment requires a fixed flap angle and therefore a reflexed section would be employed rather than a flap. Evaluation of one particular flap case, as an approximation for the reflexed section, indicates that the cavitation effect is so negative as not to justify further investigation in the time available.

RATIONAL CONSIDERATION OF HINGE MOMENT CONTROL

Where flaps are employed for moment control, it is the hinge position of the first term of Eq. (10) and the flap schedule of the third term which are juggled to produce the optimum result. The second term is a fixed (by craft geometry) component of the zero speed hinge moment intercept. The last term is the basic slope term and is considered fixed by craft geometry in these analyses though in the distant future, when these terms are known with much better precision, the section camber may also be employed as an optimization variable. Only the infinite and one chord depth slopes, $C_{L\alpha}/C_{L\alpha_{\infty}}$, are considered here for the fourth term.

In general, the moment curve has the appearance:

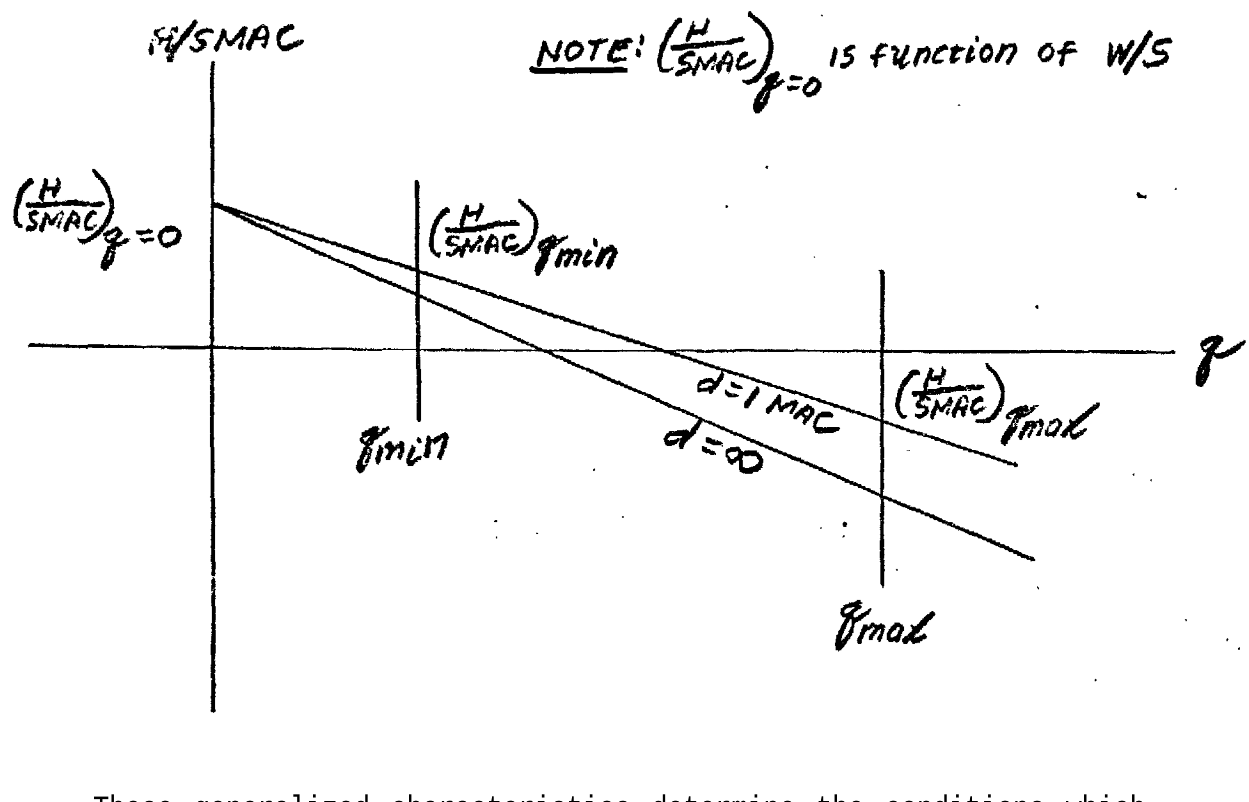

These generalized characteristics determine the conditions which govern optimization for the three cases considered.

The craft weight will vary between extremes presented by the minimum flight weight at the maximum negative normal acceleration margin and the maximum flight weight at the maximum positive acceleration margin. To represent these extreme foil loadings it is convenient to define the parameter, K:

$$K = \frac{\left(\frac{W}{S}\right)_{max} - \left(\frac{W}{S}\right)_{min}}{2\left(\frac{W}{S}\right)_{m}} = \frac{\left(\frac{W}{S}\right)_{max} - \left(\frac{W}{S}\right)_{min}}{\left(\frac{W}{S}\right)_{max} + \left(\frac{W}{S}\right)_{min}} \tag{40}$$

$$\text{where: } \left(\frac{W}{S}\right)_{max} = (1+\Delta n)\left(\frac{W}{S}\right)_{nom.\ max}$$

$$\left(\frac{W}{S}\right)_{min} = (1-\Delta n)\left(\frac{W}{S}\right)_{nom.\ min.}$$

$$\left(\frac{W}{S}\right)_{m} = \frac{1}{2}\left[\left(\frac{W}{S}\right)_{max} + \left(\frac{W}{S}\right)_{min}\right]$$

For example, this note employs for the AG(EH) fwd foils:

$$\left(\frac{W}{S}\right)_{max} = 1\tfrac{1}{4} \times 1435 = 1795 \tag{41}$$

$$\left(\frac{W}{S}\right)_{min.} = \frac{3}{4} \times 1220 = 915$$

$$\left(\frac{W}{S}\right)_{m} = \frac{1795+915}{2} = \frac{2710}{2} = 1355$$

$$K = \frac{1795-915}{2710} = \frac{880}{2710} = .325$$

(41) (Continued)

K serves the same purpose as Δm but imcorporates the flight weight range:

$$\left(\frac{W}{S}\right)_{max/min} = \left(1 \pm K\right)\left(\frac{W}{S}\right)_M \tag{42}$$

MINIMUM HINGE MOMENT

Referring to Eq. (10) the incidence hinge moments are minimized by setting:

$$\left(\frac{H}{S\,MAC}\right)_{q_{min},\ +K,\ d/c=1} + \left(\frac{H}{S\,MAC}\right)_{q_{max},\ -K,\ d/c=\infty} = 0$$

(43)

$$C_{H_{C_L}}(1+K)\left(\frac{W}{S}\right)_m + \beta - \Delta\left(\frac{W}{S}\right)_S q_{min} + \frac{C_{L_{\alpha_{1c}}}}{C_{L_{\alpha_\infty}}} C'_{H_{\alpha_{C_L=0}}} q_{min}$$
$$+ C_{H_{C_L}}(1-K)\left(\frac{W}{S}\right)_m + \beta - \Delta\left(\frac{W}{S}\right)_S q_{max} + C'_{H_{\alpha_{C_L=0}}} q_{max} = 0$$

$$2C_{H_{C_L}}\left(\frac{W}{S}\right)_m + 2\beta - \Delta\left[\left(\frac{W}{S}\right)_S q_{min} + \left(\frac{W}{S}\right)_S q_{max}\right] + C'_{H_{\alpha_{C_L=0}}}\left(\frac{C_{L_{\alpha_{1c}}}}{C_{L_{\alpha_\infty}}} q_{min} + q_{max}\right) =$$

$$C_{H_{C_L}}\left(\frac{W}{S}\right)_m = -\beta + \frac{1}{2}\left[\left(\frac{W}{S}\right)_S q_{min} + \left(\frac{W}{S}\right)_S q_{max}\right]\Delta - \frac{1}{2}\left(\frac{C_{L_{\alpha_{1c}}}}{C_{L_{\alpha_\infty}}} q_{min} + q_{max}\right) C'_{H_{\alpha_{C_L=0}}}$$

which locates the optimum hinge position when the flap schedule has been established.

The corresponding maximum hinge moment may be established either at q_{min} or q_{max} by substituting Eq. (43) into the appropriate form of Eq. (10). For the optimum hinge position and flap schedule the maximum hinge moment occurs at q min, where it is positive, and identically at q max, where it is negative. The absolute value of the maximum hinge moment is therefore given at q min.

$$\frac{|H_{max}|}{SMAC} = \left(\frac{H}{SMAC}\right)_{q_{min}, +K,\ d/c=1} \tag{44}$$

$$= \frac{(1+K)\left(\frac{W}{S}\right)_m}{(W/S)_m}\left\{-\beta + \frac{1}{2}\left[\left(\frac{W}{S}\right)_\delta q_{min} + \left(\frac{W}{S}\right)_\delta q_{max}\right]\Delta\right.$$

$$\left.\frac{1}{2}\left(\frac{C_{L\alpha_{1c}}}{C_{L\alpha_\infty}} q_{min} + q_{max}\right)C'_{H\alpha_{C_L=0}}\right\}$$

$$+\beta - \Delta\left(\frac{W}{S}\right)_\delta q_{min} + \frac{C_{L\alpha_{1c}}}{C_{L\alpha_\infty}} C'_{H\alpha_{C_L=0}} q_{min}$$

$$= (1-1-K)\beta - \left\{\left(\frac{W}{S}\right)_\delta q_{min} - \frac{1}{2}(1+K)\left[\left(\frac{W}{S}\right)_\delta q_{min} + \left(\frac{W}{S}\right)_\delta q_{max}\right]\right\}\Delta$$

$$+\left[\frac{C_{L\alpha_{1c}}}{C_{L\alpha_\infty}} q_{min} - \frac{1}{2}(1+K)\left(\frac{C_{L\alpha_{1c}}}{C_{L\alpha_\infty}} q_{min} + q_{max}\right)\right]C'_{H\alpha_{C_L=0}}$$

$$= -K\beta - \left[\frac{1}{2}(1-K)\left(\frac{W}{S}\right)_\delta q_{min} - \frac{1}{2}(1+K)\left(\frac{W}{S}\right)_\delta q_{max}\right]\Delta$$

$$+\left[\frac{1}{2}(1-K)\frac{C_{L\alpha_{1c}}}{C_{L\alpha_\infty}} q_{min} - \frac{1}{2}(1+K)q_{max}\right]C'_{H\alpha_{C_L=0}}$$

$$= -K\beta - \frac{1}{2}\left[(1-K)\left(\frac{W}{S}\right)_\delta q_{min} - (1+K)\left(\frac{W}{S}\right)_\delta q_{max}\right]\Delta$$

$$-\frac{1}{2}\left[(1+K)q_{max} - (1-K)\frac{C_{L\alpha_{1c}}}{C_{L\alpha_\infty}} q_{min}\right]C'_{H\alpha_{C_L=0}}$$

The first term is a minor adjustment for buoyancy. The zero lift hinge moment coefficient of the third term is negative so the third term is positive. Thus the maximum hinge moment is reduced by increasing the minimum speed flap angle and by reducing the maximum speed flap angle, No limit upon these foil loadings is presented by Eq. (44) except as to their relative value, or slope, as discussed below. There are practical limitations upon the flap angles however. Large flap angles present practical design problems and linearity effects which are not considered in this note. A $+30^{\circ}$ flap angle limit is assumed in this note. The high speed flap angle, which can be negative, is limited by the compromises one cares to take on the cavitation bucket.

Eq. (44) can be written in a form which emphasizes the effect of K upon the maximum hinge moment and the fact that the unflapped foil is a degenerate special case of the equation:

$$(45)\quad \frac{|H_{max}|}{SMAC} = -K\beta - \frac{1}{2}C'_{H_{\alpha_{C_L=0}}}\left[\left(q_{max} - \frac{C_{L_{\alpha_{\infty}}}}{C_{L_{\alpha_0}}} q_{min}\right) + K\left(q_{max} + \frac{C_{L_{\alpha_{\infty}}}}{C_{L_{\alpha_0}}} q_{min}\right)\right] - \frac{1}{2}\Delta\left\{\left[\left(\frac{W}{S}\right)_{\delta_{q_{min}}} - \left(\frac{W}{S}\right)_{\delta_{q_{max}}}\right] - K\left[\left(\frac{W}{S}\right)_{\delta_{q_{min}}} + \left(\frac{W}{S}\right)_{\delta_{q_{max}}}\right]\right\}$$

$$= \frac{|H_{max}|_{unflapped}}{SMAC} - \frac{1}{2}\Delta\left\{\left[\left(\frac{W}{S}\right)_{\delta_{q_{min}}} - \left(\frac{W}{S}\right)_{\delta_{q_{max}}}\right] - K\left[\left(\frac{W}{S}\right)_{\delta_{q_{min}}} + \left(\frac{W}{S}\right)_{\delta_{q_{max}}}\right]\right\}$$

Note that the speed range and the weight range both contribute to the maximum hinge moment for the unflapped foil. Provision of flaps can eliminate the effect of the speed range but not the effect of the weight range; nearly all of the maximum hinge moment for tha flapped foil which has been optimized for moments is due to the weight range with the remainder being due to provision for limited depth, Thus a craft designed for platforming operation at a fixed weight could be provided with a zero moment system. On the other hand, the *very* long ranges now being considered would present relatively high hinge moments for an incidence lift control system. Note, too, that the final term means that flaps do not necessarily reduce the maximum hinge moment.

Increasing the minimum speed flap angle and reducing the maximum speed flap angle reduces the moment slope. When the one chord depth slope vanishes, Eq. (43) becomes invalid and must be redefined. Further changes in the flap schedule produce a positive 1 chord depth moment elope and a zero infinite depth slope; then further changes make both slopes positive. It is in this region that the flap schedule begins to compromise the cavitation bucket and the optimum flap schedule is ultimately a subjective judgement of that compromise.

In order to provide a well defined "optimum" flap schedule for moments for this note, the optimum flap schedule is defined to have a slope which makes the infinite depth hinge moment slope vanish; i.e.,

$$\frac{d\frac{H}{SMAC}}{dq} = -\Delta\frac{d\left(\frac{W}{S}\right)_\delta}{dq} + \frac{C_{L_\alpha}}{C_{L_{\alpha\infty}}} C'_{H_{\infty C_L=0}} = 0 \tag{46}$$

$$\frac{d\left(\frac{W}{S}\right)_\delta}{dq} = C'_{H_{\infty C_L=0}} / \Delta$$

and this slope is passed through a 30° flap angle at q min. This in the "optimum moment" flap schedule of Eqs. (36) and (37) and of Pigure 13. It will be recognized that the 1 chord depth slope could have been made to vanish or that the 1 chord and infinite depth slopes could have been assigned equal values of apposite sign, which would have produced a still lower H max. The definition adopted here is entirely arbitrary.

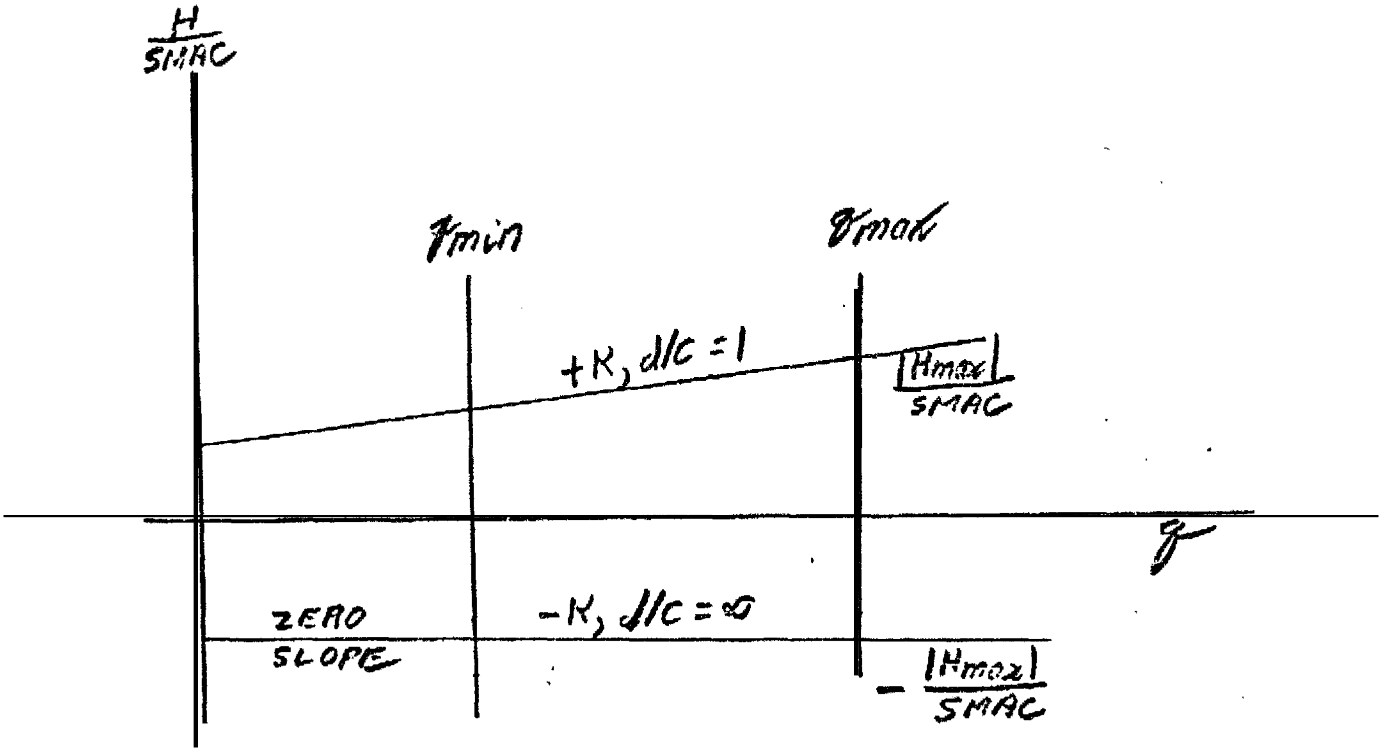

For this case Eq. (10) may be modified to (employing primes to indicate a restricted case):

(47)

$$\frac{H'}{SMAC} = C_{H_{C_L}}\frac{W}{S} + \beta - \Delta\left[\left(\frac{W}{S}\right)_{S\,q_{max}} + \frac{d\left(\frac{W}{S}\right)_S}{dq}\left(q - q_{max}\right)\right] + \frac{C_{L\alpha}}{C_{L\alpha_0}} C'_{H\alpha_{C_L=0}}\, q$$

$$= C_{H_{C_L}}\frac{W}{S} + \beta - \Delta\left[\left(\frac{W}{S}\right)_{S\,q_{max}} + \frac{C'_{H\alpha_{C_L=0}}}{\Delta}\left(q - q_{max}\right)\right] + \frac{C_{L\alpha}}{C_{L\alpha_0}} C'_{H\alpha_{C_L=0}}\, q$$

$$= C_{H_{C_L}}\frac{W}{S} + \beta - \Delta\left(\frac{W}{S}\right)_{S\,q_{max}} + C'_{H\alpha_{C_L=0}}\, q_{max} - C'_{H\alpha_{C_L=0}}\, q + \frac{C_{L\alpha}}{C_{L\alpha_0}} C'_{H\alpha_{C_L=0}}\, q$$

$$= C_{H_{C_L}}\frac{W}{S} + \beta - \Delta\left(\frac{W}{S}\right)_{S\,q_{max}} + C'_{H\alpha_{C_L=0}}\, q_{max} - \left(1 - \frac{C_{L\alpha}}{C_{L\alpha_0}}\right) C'_{H\alpha_{C_L=0}}\, q$$

The corresponding maximum hinge moment is minimized by setting:

(48)

$$\left(\frac{H'}{S_{MAC}}\right)_{q_{max},\,+K,\,d/c=1} + \left(\frac{H'}{S_{MAC}}\right)_{q_{max},\,-K,\,d/c=\infty} = 0$$

$$C_{H_{C_L}}(1+K)\left(\frac{W}{S}\right)_m + \beta - \Delta\left(\frac{W}{S}\right)_S q_{max} + C'_{H_{\alpha_{C_L=0}}}\gamma_{max} - \left(1-\frac{C_{L\alpha_{1c}}}{C_{L\alpha_\infty}}\right)C'_{H_{\alpha_{C_L=0}}}\gamma_{max}$$

$$+ C_{H_{C_L}}(1-K)\left(\frac{W}{S}\right)_m + \beta - \Delta\left(\frac{W}{S}\right)_S q_{max} + C'_{H_{\alpha_{C_L=0}}}\gamma_{max} = 0$$

$$2C_{H_{C_L}}\left(\frac{W}{S}\right)_m + 2\beta - 2\Delta\left(\frac{W}{S}\right)_S q_{max} + \left(1+\frac{C_{L\alpha_{1c}}}{C_{L\alpha_\infty}}\right)C'_{H_{\alpha_{C_L=0}}}\gamma_{max} = 0$$

$$C'_{H_{C_L}}\left(\frac{W}{S}\right)_m = -\beta + \Delta\left(\frac{W}{S}\right)_S q_{max} - \frac{1}{2}\left(1+\frac{C_{L\alpha_{1c}}}{C_{L\alpha_\infty}}\right)C'_{H_{\alpha_{C_L=0}}}\gamma_{max}$$

For this hinge position in Eq. (47):

(49)

$$\frac{|H'_{max}|}{S_{MAC}} = \left(\frac{H'}{S_{MAC}}\right)_{q_{max},\, +K,\ d/c=1}$$

$$= \frac{(1+K)(W/S)_m}{(W/S)_m}\left\{-\beta + \Delta\left(\frac{W}{S}\right)_{\delta q_{max}} - \frac{1}{2}\left(1+\frac{C_{L\alpha_{IC}}}{C_{L\alpha_\infty}}\right)C'_{H\alpha_{C_L=0}}\, q_{max}\right\}$$

$$+\beta - \Delta\left(\frac{W}{S}\right)_{\delta q_{max}} + C'_{H\alpha_{C_L=0}}\, q_{max} - \left(1-\frac{C_{L\alpha_{IC}}}{C_{L\alpha_\infty}}\right)C'_{H\alpha_{C_L=0}}\, q_{max}$$

$$= -K\beta + K\Delta\left(\frac{W}{S}\right)_{\delta q_{max}} + \left[-\frac{1}{2}(1+K)\left(1+\frac{C_{L\alpha_{IC}}}{C_{L\alpha_\infty}}\right) + \frac{C_{L\alpha_{IC}}}{C_{L\alpha_\infty}}\right]C'_{H\alpha_{C_L=0}}\, q_{max}$$

$$= K\left[-\beta + \Delta\left(\frac{W}{S}\right)_{\delta q_{max}}\right] + \left[-\frac{1}{2}\left(1+\frac{C_{L\alpha_{IC}}}{C_{L\alpha_\infty}}\right) - \frac{1}{2}K\left(1+\frac{C_{L\alpha_{IC}}}{C_{L\alpha_\infty}}\right) + \frac{C_{L\alpha_{IC}}}{C_{L\alpha_\infty}}\right]C'_{H\alpha_{C_L=0}}\, q_{max}$$

$$= K\left[-\beta + \Delta\left(\frac{W}{S}\right)_{\delta q_{max}}\right] + \left[-\frac{1}{2}\left(1-\frac{C_{L\alpha_{IC}}}{C_{L\alpha_\infty}}\right) - \frac{1}{2}K\left(1+\frac{C_{L\alpha_{IC}}}{C_{L\alpha_\infty}}\right)\right]C'_{H\alpha_{C_L=0}}\, q_{max}$$

$$= K\left[-\beta + \Delta\left(\frac{W}{S}\right)_{\delta q_{max}} - \frac{1}{2}\left(1+\frac{C_{L\alpha_{IC}}}{C_{L\alpha_\infty}}\right)C'_{H\alpha_{C_L=0}}\, q_{max}\right] - \frac{1}{2}\left(1-\frac{C_{L\alpha_{IC}}}{C_{L\alpha_\infty}}\right)C'_{H\alpha_{C_L=0}}\, q_{max}$$

The bracketed term vanishes for a zero weight spread and the second term vanishes for deep depth operation; i.e. this result presents analytically the condition for which a zero moment can be designed.

Eq. (49) can be made to vanish for the general case with a sufficiently low top speed flap foil loading (~ - 2300 psf for the AG(EH)) but this approach is back to the reflexed foil case and presents an intolerable compromise of the cavitation bucket. Therefore Eq. (~~26~~ 49) only says that the maximum speed flap foil loading should be as low as one's judgement of the cavitation effect trill allow.

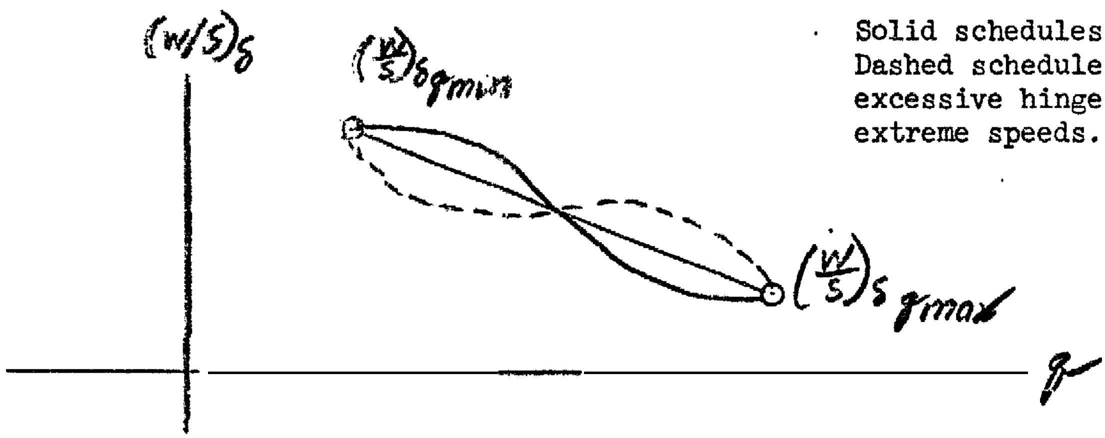

Solid schedules are safe. Dashed schedule invites excessive hinge moment at extreme speeds.

Just as there is no well defined optimum flap foil loading for minimum or maximum speed, there is no optimum flap schedule connecting those points. Some care must be exercised at the two speed extremes to avoid producing hinge moments in excess of the moments at those extremes, which are presumably design values, but the flap schedule at intermediate speeds is completely arbitrary.

The three flap schedules of Figure 13 are evaluated for moments in this note. It is evident on Figure 13 that the optimum moment schedule compromises the unflapped cavitation bucket for q's above 6750 psf (48.7 knots) and that it compromises the optimum cavitation bucket for q's below 4130 psf (38 knots). These compromises may be seen on Figure 17. That at 48.7 knots is obviously insignificant and that at 38 knots is considered insignificant for reasons already presented in the discussion of Figure 17.

The moments for the three flap schedules of Figure 13, hinged to present minimum moments, are presented on Figure 18. Note that the optimum cavitation flap schedule has slightly increased the maximum moment of the unflapped foil, a result of the large weight and normal acceleration spread relative to the flap displacement spread (see the last term of Eq. (45).

It is to be noted that the optimum moment H max is 50% larger than the $1/4\ K\ {}_{\Theta}\frac{W}{S}{}_{m}$ which intuitive consideration would lead us to hope for, The H max is reduced by reducing the section C_{Mac} which requires a reduction in camber and/or the adoption of a camber line offering a more favorable C_{Mac}.

Centering the moments in the zero axis has substantially reduced the maximum hinge moments but 'they are still probably too large to insure a slop-free system at crossover, It is not likely that any special purpose application will ever present itself offering sufficiently restricted weight and normal acceleration ranges for the confident specification of the minimum moment geometry.

MINIMUM NEGATIVE HINGE MOMENT

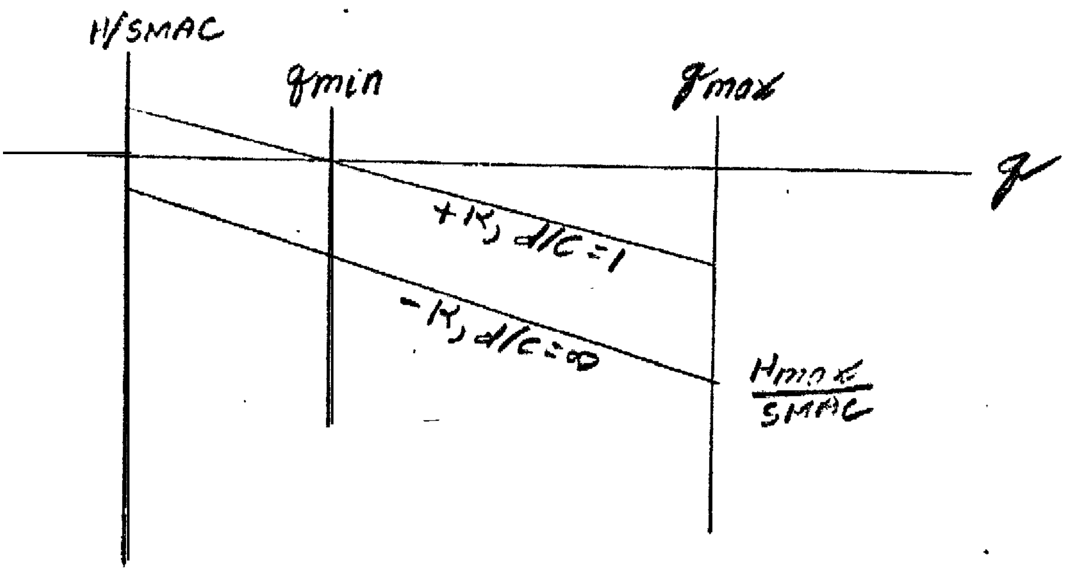

For this case Eq. (10) provides a hinge postion for which the moment vanshes at.

(50)

$$\frac{H}{SMAC} = 0 = \left(\frac{H}{SMAC}\right)_{q_{min},\ +K,\ d/C=1}$$

$$= C_{H_{C_L}}(1+K)\left(\frac{W}{S}\right)_m + \beta - \Delta\left(\frac{W}{S}\right)_S q_{min} + \frac{C_{L\alpha_{IC}}}{C_{L\alpha_\infty}} C'_{H_{\alpha_{C_L=0}}} q_{min}$$

$$C_{H_{C_L}}(1+K)\left(\frac{W}{S}\right)_m = -\beta + \Delta\left(\frac{W}{S}\right)_S q_{min} - \frac{C_{L\alpha_{IC}}}{C_{L\alpha_\infty}} C'_{H_{\alpha_{C_L=0}}} q_{min}$$

The maximum moment employs this hinge in a second application of Eq. (10) :

(51)

$$-\frac{|H_{max}|}{S\,MAC} = \left(\frac{H}{S\,MAC}\right)_{q_{max},\,-K,\,d/c=\infty}$$

$$= \frac{1-K}{1+K}\left\{-\beta + \Delta\left(\frac{W}{S}\right)_{S} q_{min} - \frac{C_{L\alpha_{1C}}}{C_{L\alpha_{\infty}}} C'_{H\alpha_{C_L=0}} q_{min}\right\}$$
$$+ \beta - \Delta\left(\frac{W}{S}\right)_{S} q_{max} + C'_{H\alpha_{C_L=0}} q_{max}$$

$$= \left(1-\frac{1-K}{1+K}\right)\beta + \left[\frac{1-K}{1+K}\left(\frac{W}{S}\right)_{S} q_{min} - \left(\frac{W}{S}\right)_{S} q_{max}\right]\Delta$$
$$+ \left(q_{max} - \frac{1-K}{1+K}\frac{C_{L\alpha_{1C}}}{C_{L\alpha_{\infty}}} q_{min}\right) C'_{H\alpha_{C_L=0}}$$

$$\frac{|H_{max}|}{S\,MAC} = \left(\frac{1-K}{1+K}-1\right)\beta - \left[\frac{1-K}{1+K}\left(\frac{W}{S}\right)_{S} q_{min} - \left(\frac{W}{S}\right)_{S} q_{max}\right]\Delta$$
$$- \left(q_{max} - \frac{1-K}{1+K}\frac{C_{L\alpha_{1C}}}{C_{L\alpha_{\infty}}} q_{min}\right) C'_{H\alpha_{C_L=0}}$$

$$= -\frac{2K}{1+K}\beta - \left[\frac{1-K}{1+K}\left(\frac{W}{S}\right)_{S} q_{min} - \left(\frac{W}{S}\right)_{S} q_{max}\right]\Delta - \left(q_{max} - \frac{1-K}{1+K}\frac{C_{L\alpha_{1C}}}{C_{L\alpha_{\infty}}} q_{min}\right) C'_{H\alpha_{C_L=0}}$$

$$= \frac{1}{1+K}\left\{-2K\beta - \left[(1-K)\left(\frac{W}{S}\right)_{S} q_{min} - (1+K)\left(\frac{W}{S}\right)_{S} q_{max}\right]\Delta - \left[(1+K)q_{max} - (1-K)\frac{C_{L\alpha_{1C}}}{C_{L\alpha_{\infty}}} q_{min}\right] C'_{H\alpha_{C_L=0}}\right.$$

$$= \frac{1}{1+K}\left\{-2K\beta - \left(q_{max} - \frac{C_{L\alpha_{1C}}}{C_{L\alpha_{\infty}}} q_{min}\right) C'_{H\alpha_{C_L=0}} - K\left(q_{max} + \frac{C_{L\alpha_{1C}}}{C_{L\alpha_{\infty}}} q_{min}\right) C'_{H\alpha_{C_L=0}}\right.$$
$$\left. - \left[\left(\frac{W}{S}\right)_{S} q_{min} - \left(\frac{W}{S}\right)_{S} q_{max}\right]\Delta + K\left[\left(\frac{W}{S}\right)_{S} q_{min} + \left(\frac{W}{S}\right)_{S} q_{max}\right]\Delta\right\}$$

$$= -\frac{2K}{1+K}\beta - \frac{C'_{H\alpha_{C_L=0}}}{1+K}\left[\left(q_{max} - \frac{C_{L\alpha_{1C}}}{C_{L\alpha_{\infty}}} q_{min}\right) + K\left(q_{max} + \frac{C_{L\alpha_{1C}}}{C_{L\alpha_{\infty}}} q_{min}\right)\right]$$
$$- \frac{\Delta}{1+K}\left\{\left[\left(\frac{W}{S}\right)_{S} q_{min} - \left(\frac{W}{S}\right)_{S} q_{max}\right] - K\left[\left(\frac{W}{S}\right)_{S} q_{min} + \left(\frac{W}{S}\right)_{S} q_{max}\right]\right\}$$

$$= \frac{|H_{max}|_{unflapped}}{1+K} - \frac{\Delta}{1+K}\left\{\left[\left(\frac{W}{S}\right)_{S} q_{min} - \left(\frac{W}{S}\right)_{S} q_{max}\right] - K\left[\left(\frac{W}{S}\right)_{S} q_{min} + \left(\frac{W}{S}\right)_{S} q_{max}\right]\right\}$$

(51) (Continued)

Eq. (51) is identical in form with Eq. (45) and, in fact, can be written:

$$\left(\frac{|H_{max}|}{SMAC}\right)_{min.\ neg.\ mom.} = \frac{2}{1+K}\left(\frac{|H_{max}|}{SMAC}\right)_{min.\ mom.} \tag{52}$$

Therefore all of the comment with regard to optimization and flap schedules of the minimum moment case apply to the minimum negative moment c&e. The only difference is that one extreme speed presents a zero hinge moment in this case, with potential crossover for careless flap management, and the other extreme speed presents the maximum, or design, hinge moment. For the previous, minimum moment, case both extreme speeds presented the maximum moment.

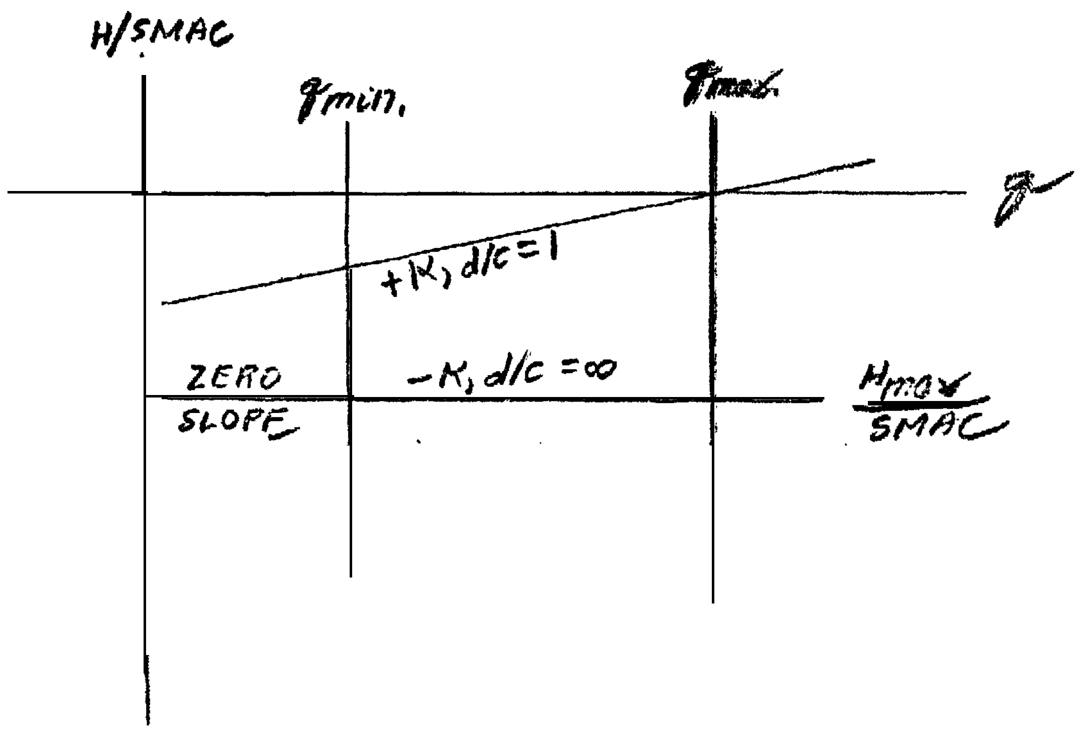

(52) (Continued)

For the "optimum" moment case, having a zero infinite depth moment slope, the hinge must be set by evaluating Eq. (47) as:

(53)

$$\left(\frac{H'}{SMAC}\right)_{q_{max},\,+K,\,d/c=1} = 0$$

$$C'_{H_{C_L}}(1+K)\left(\frac{W}{S}\right)_m + \beta - \Delta\left(\frac{W}{S}\right)_S q_{max} + C'_{H_{\alpha_{C_L=0}}} q_{max} - \left(1-\frac{C_{L_{\alpha_{1c}}}}{C_{L_{\alpha_\infty}}}\right) C'_{H_{\alpha_{C_L=0}}} q_{max} = 0$$

$$C'_{H_{C_L}}(1+K)\left(\frac{W}{S}\right)_m = -\beta + \Delta\left(\frac{W}{S}\right)_S q_{max} - \frac{C_{L_{\alpha_{1c}}}}{C_{L_{\alpha_\infty}}} C'_{H_{\alpha_{C_L=0}}} q_{max}$$

The maximum moment is provided by employing this hinge position in Eq. (47) evaluated as:

(54)

$$-\frac{|H'_{max}|}{SMAC} = \left(\frac{H'}{SMAC}\right)_{q_{max},\,-K,\,d/c=\infty}$$

$$= \frac{1-K}{1+K}\left\{-\beta + \Delta\left(\frac{W}{S}\right)_S q_{max} - \frac{C_{L_{\alpha_{1c}}}}{C_{L_{\alpha_\infty}}} C'_{H_{\alpha_{C_L=0}}} q_{max}\right\}$$

$$+\beta - \Delta\left(\frac{W}{S}\right)_S q_{max} + C'_{H_{\alpha_{C_L=0}}} q_{max}$$

$$= \left(1-\frac{1-K}{1+K}\right)\beta + \left(\frac{1-K}{1+K}-1\right)\Delta\left(\frac{W}{S}\right)_S q_{max} + \left(1-\frac{1-K}{1+K}\,\frac{C_{L_{\alpha_{1c}}}}{C_{L_{\alpha_\infty}}}\right) C'_{H_{\alpha_{C_L=0}}} q_{max}$$

$$\frac{|H'_{max}|}{SMAC} = -\frac{2K}{1+K}\,\beta + \frac{2K}{1+K}\,\Delta\left(\frac{W}{S}\right)_S q_{max} - \left(1-\frac{1-K}{1+K}\,\frac{C_{L_{\alpha_{1c}}}}{C_{L_{\alpha_\infty}}}\right) C'_{H_{\alpha_{C_L=0}}} q_{max}$$

$$= \frac{2}{1+K}\left\{K\left[-\beta + \Delta\left(\frac{W}{S}\right)_S q_{max}\right] - \frac{1+K}{2}\left(1-\frac{1-K}{1+K}\,\frac{C_{L_{\alpha_{1c}}}}{C_{L_{\alpha_\infty}}}\right) C'_{H_{\alpha_{C_L=0}}} q_{max}\right\}$$

(54) (Continued)

The third term will transform into:

(55)

$$-\frac{1+K}{2}\left(1-\frac{1-K}{1+K}\right)C'_{H\alpha_{C_L=0}}\,q_{max} = \left[-\frac{1}{2}(1+K)+\frac{1}{2}(1-K)\frac{C_{L\alpha_{1C}}}{C_{L\alpha_\infty}}\right]C'_{H\alpha_{C_L=0}}\,q_{max}$$

$$= \left[-\frac{K}{2}\left(1+\frac{C_{L\alpha_{1C}}}{C_{L\alpha_\infty}}\right)-\frac{1}{2}\left(1-\frac{C_{L\alpha_{1C}}}{C_{L\alpha_\infty}}\right)\right]C'_{H\alpha_{C_L=0}}\,q_{max}$$

Then Eq. (54) may be written:

(56)

$$\frac{|H'_{max}|}{SMAC} = \frac{2}{1+K}\left\{K\left[-\beta+\Delta\left(\frac{W}{S}\right)_{S\,q_{max}}-\frac{1}{2}\left(1+\frac{C_{L\alpha_{1C}}}{C_{L\alpha_\infty}}\right)C'_{H\alpha_{C_L=0}}\,q_{max}\right]\right.$$

$$\left.-\frac{1}{2}\left(1-\frac{C_{L\alpha_{1C}}}{C_{L\alpha_\infty}}\right)C'_{H\alpha_{C_L=0}}\,q_{max}\right\}$$

Then by reference to Eq. (49)

(57) $$\left(\frac{|H'_{max}|}{SMAC}\right)_{min.\,neg.\,mom.} = \frac{2}{1+K}\left(\frac{|H'_{max}|}{SMAC}\right)_{min.\,mom.}$$

which is identical with Eq. (52) so the optimum negative moment case is simply a special case of the minimum negative moment general case.

(U) (Continued)

The moments for the three flap schedules of Figure 13, hinged to present negative moments for all flight conditions, are presented on Figure 19. The unflapped result of Figure 19 differs slightly from that of Figure 6 of Reference 1 because the hinge has been moved slightly in this note to produce a zero minimum hinge moment.

MINIMUM POSITIVE HINGE MOMENT

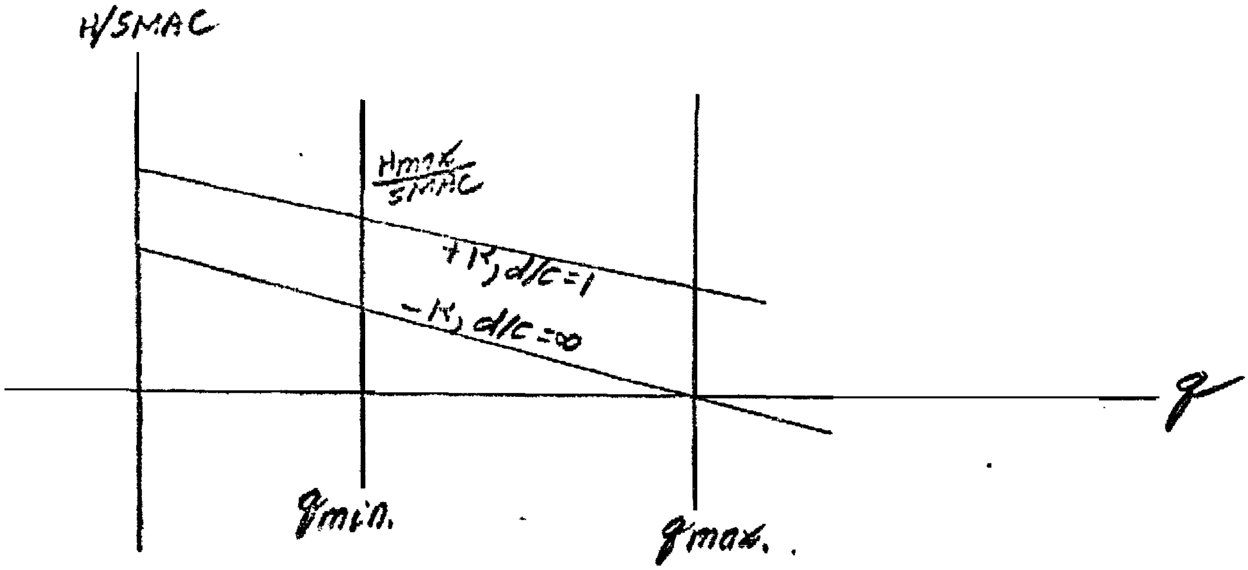

For this case Eq. (10) provides a hinge position for which the moment vanishes at:

$$(58)\quad \frac{H}{S\,MAC} = 0 = \left(\frac{H}{S\,MAC}\right)_{q_{max},\,-K,\,d/c=\infty}$$

$$= C_{H_{C_L}}(1-K)\left(\frac{W}{S}\right)_m + \beta - \Delta\left(\frac{W}{S}\right)_s q_{max} + C'_{H_{\alpha_{C_L=0}}}\, q_{max}$$

$$C_{H_{C_L}}(1-K)\left(\frac{W}{S}\right)_m = -\beta + \Delta\left(\frac{W}{S}\right)_s q_{max} - C'_{H_{\alpha_{C_L=0}}}\, q_{max}$$

The maximum moment employs this hinge in a second application of Eq. (10):

(59)

$$\frac{|H_{max}|}{S\,MAC} = \left(\frac{H}{S\,MAC}\right)_{q_{min},\,+K,\,d/C=1}$$

$$= \frac{1+K}{1-K}\left\{-\beta + \Delta\left(\frac{W}{S}\right)\delta\, q_{max} - C'_{H\alpha_{C_L=0}}\, q_{max}\right\}$$

$$+\beta - \Delta\left(\frac{W}{S}\right)\delta\, q_{min} + \frac{C_{L\alpha_{IC}}}{C_{L\alpha_\infty}}\, C'_{H\alpha_{C_L=0}}\, q_{min}\,.$$

$$= \left(1 - \frac{1+K}{1-K}\right)\beta - \Delta\left[\left(\frac{W}{S}\right)\delta\, q_{min} - \frac{1+K}{1-K}\left(\frac{W}{S}\right)\delta\, q_{max}\right]$$

$$- C'_{H\alpha_{C_L=0}}\left(\frac{1+K}{1-K}\, q_{max} - \frac{C_{L\alpha_{IC}}}{C_{L\alpha_\infty}}\, q_{min}\right)$$

$$= -\frac{2K}{1-K}\,\beta - \frac{1+K}{1-K}\,\Delta\left[\frac{1-K}{1+K}\left(\frac{W}{S}\right)\delta\, q_{min} - \left(\frac{W}{S}\right)\delta\, q_{max}\right]$$

$$- \frac{1+K}{1-K}\, C'_{H\alpha_{C_L=0}}\left(q_{max} - \frac{1-K}{1+K}\,\frac{C_{L\alpha_{IC}}}{C_{L\alpha_\infty}}\, q_{min}\right)$$

This equation is identical in form with one appearing in the development of Eq. (51) and may be written:

(60)

$$\left(\frac{|H_{max}|}{SMAC}\right)_{min.\,pos.\,mom.} = \frac{2}{1-K}\left(\frac{|H_{max}|}{SMAC}\right)_{min.\,mom.}$$

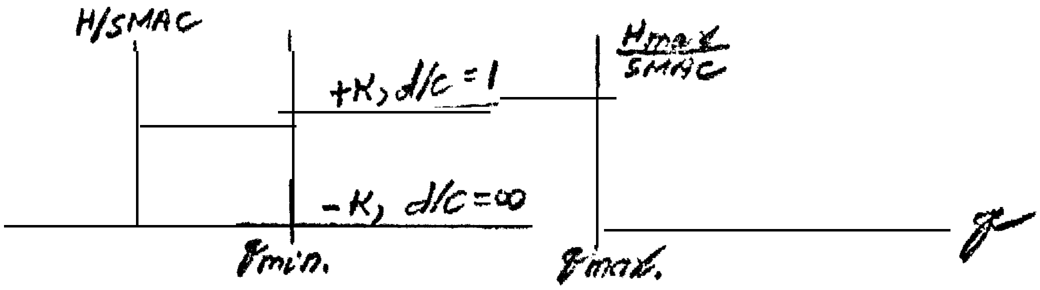

For the optimum moment case, having a zero infinite depth moment slope, the hinge must be set by evaluating Eq. (47) as :

(61)

$$\left(\frac{H'}{SMAC}\right)_{q_{max},\,-K,\,d/c=\infty} = 0$$

$$C_{H_{C_L}}(1-K)\left(\frac{W}{S}\right)_m + \beta - \Delta\left(\frac{W}{S}\right)_{S\,q_{max}} + C'_{H\alpha_{C_L=0}}\,q_{max} = 0$$

$$C'_{H_{C_L}}(1-K)\left(\frac{W}{S}\right)_m = -\beta + \Delta\left(\frac{W}{S}\right)_{S\,q_{max}} - C'_{H\alpha_{C_L=0}}\,q_{max}.$$

The maximum moment is provided by employing this hinge position in Eq. (47) evaluated as:

(62)

$$\frac{|H'_{max}|}{SMAC} = \left(\frac{H'}{SMAC}\right)_{q_{max},\,+K,\; d/K=1}$$

$$= \frac{1+K}{1-K}\left\{-\beta + \Delta\left(\frac{W}{S}\right)_{\delta}q_{max} - C''_{H\alpha_{C_L=0}}\,q_{max}\right\} + \beta - \Delta\left(\frac{W}{S}\right)_{\delta}q_{max} + \frac{C_{L\alpha_{fe}}}{C_{L\alpha_\infty}}\,C'_{H\alpha_{C_L=0}}\,q_{max}$$

$$= \left(1-\frac{1+K}{1-K}\right)\beta - \left(1-\frac{1+K}{1-K}\right)\Delta\left(\frac{W}{S}\right)_{\delta}q_{max} - \left(\frac{1+K}{1-K} - \frac{C_{L\alpha_{fe}}}{C_{L\alpha_\infty}}\right)C'_{H\alpha_{C_L=0}}\,q_{max}$$

$$= -\frac{2K}{1-K}\,\beta + \frac{2K}{1-K}\,\Delta\left(\frac{W}{S}\right)_{\delta}q_{max} - \left(\frac{1+K}{1-K} - \frac{C_{L\alpha_{fe}}}{C_{L\alpha_\infty}}\right)C'_{H\alpha_{C_L=0}}\,q_{max}$$

$$= \frac{2}{1-K}\left\{K\left[-\beta + \Delta\left(\frac{W}{S}\right)_{\delta}q_{max}\right] - \frac{1+K}{2}\left(1 - \frac{1-K}{1+K}\,\frac{C_{L\alpha_{fe}}}{C_{L\alpha_\infty}}\right)C'_{H\alpha_{C_L=0}}\,q_{max}\right\}$$

and by reference to Eq. (54) this may be written:

$$(63)\qquad \left(\frac{|H'_{max}|}{SMAC}\right)_{min.\,pos.\,mom.} = \frac{2}{1-K}\left(\frac{|H'_{max}|}{SMAC}\right)_{min.\,mom.}$$

which is identical with Eq. (60).

The moments for the three flap schedules of Figure 13, hinged to present positive moments for all flight conditions, are presented on Figure 20.

FLAP CAVITATION AND MOMENT CONTROL SUMMARY

The hinge location equations are summarized in Table V and the corresponding maximum hinge moment equations are summarized in Table VI. Expression of the numerical results of this note in terms of H/SMAC insures that the results are characteristic of any size craft. The AG(EH) camber , and these numerical results, are characteristic of any craft of design top speed less than 50-60 knots,

Referring to the optimum maximum moment equation of Table VI it is evident that the zero hinge moment incidence lift control foil does exist, but only if the following explicit restrictions on the operating conditions can be observed:

1. No variation in craft weight or C,G, (zero fuel consumption) (for K = 0), and
2. Platforming operation ($\Delta n = 0$ for $K = 0$), and
3. Operation at a constant depth (to make the final term vanish),

<u>and</u> if the following implicit conditions are satisified,

4. Aerodynamic center prediction is perfect, and
5. Residual pitching moment prediction is perfect, and
6. Flap hinge moment derivative, Δ , prediction is perfect

Violation of each of these six conditions is associated with an increment of maximum hinge moment and conversely, approaching each of those six conditions reduces the maximum hinge moment.

The numerical results for the AG(EH) are summarized in Table VII and lead to the following conclusions. These numerical results are strongly influenced by K but the AG(EH) is typical for this factor,

It is not likely that any design objective will be sufficiently restricted to allow use of the minimum MOMENT LOCATION AND POSITIVE moments are about twice as high as negative moments, therefore the negative moment hinge position will probably be employed on all incidence Bift systems.

Flaps can reduce the limit hinge moment by some 40%. Flaps can also increase the hinge moment, of course,. but only through careless scheduling. One decided current advantage of flaps is that they can be employed to correct for design errors; i.e., to eliminate crossover or reduce excessive moments caused by faulty hinging.

Flaps can be employed to ~~slope~~ shape the cavitation bucket but this is a sophisticated technique requiring knowledge of the effective cavitation boundaries which is totally lacking now,

As a still more sophisticated use of flaps to shape the cavitation bucket, it appears that the speed range of the conventional section could' be extended to something of the order of 80 knots, cavitation free, by flaps. The transit foil employs a conventional section in this speed range but with significant cavitation.

THE "FLYI' ' FOIL

The "flying" foil is defined here to be an incidence lift control foil which is freely pivoted about the incidence axis and which carries an incidence control, trailing edge flap,

In coefficient form Eq. (10) reads:

(64)

$$\frac{H}{SMAC} = C_{Hc_L}\frac{W}{S} + \beta - \Delta\left(\frac{W}{S}\right)_\delta + \frac{C_{L\alpha}}{C_{L\alpha\infty}} C'_{H\alpha_{C_L=0}}\, g$$

$$C_H = \frac{H}{SMAC}\Big/ g = C_{Hc_L} C_L + \frac{\beta}{g} - \Delta(C_L)_\delta + \frac{C_{L\alpha}}{C_{L\alpha\infty}} C'_{H\alpha_{C_L=0}}$$

having the deverative:

(65) $$\frac{dC_H}{dC_L} = C_{Hc_L}$$

The flying foil, then, requires a negative C_{Hc_L} ; i.e., the incidence' hinge is ahead of the aerodyromic center,

The flying foil trims at an angle defined by

(66)

$$C_H = 0 = C_{H_{C_L}} C_L + \frac{\beta}{\rho} - \Delta (C_L)_\delta + \frac{C_{L\alpha}}{C_{L\alpha_0}} C'_{H_{\alpha_0 C_L = 0}}$$

$$C_L = \frac{1}{C_{H_{C_L}}} \left[-\frac{\beta}{\rho} + \Delta (C_L)_\delta - \frac{C_{L\alpha}}{C_{L\alpha_0}} C'_{H_{\alpha_0 C_L = 0}} \right]$$

having the derivative with respect to flap angle, $(C_L)_\delta$, of

(67) $$\frac{dC_L}{d(C_L)_\delta} = \frac{\Delta}{C_{H_{C_L}}}$$

which is also negative. Thus the situation presented is .

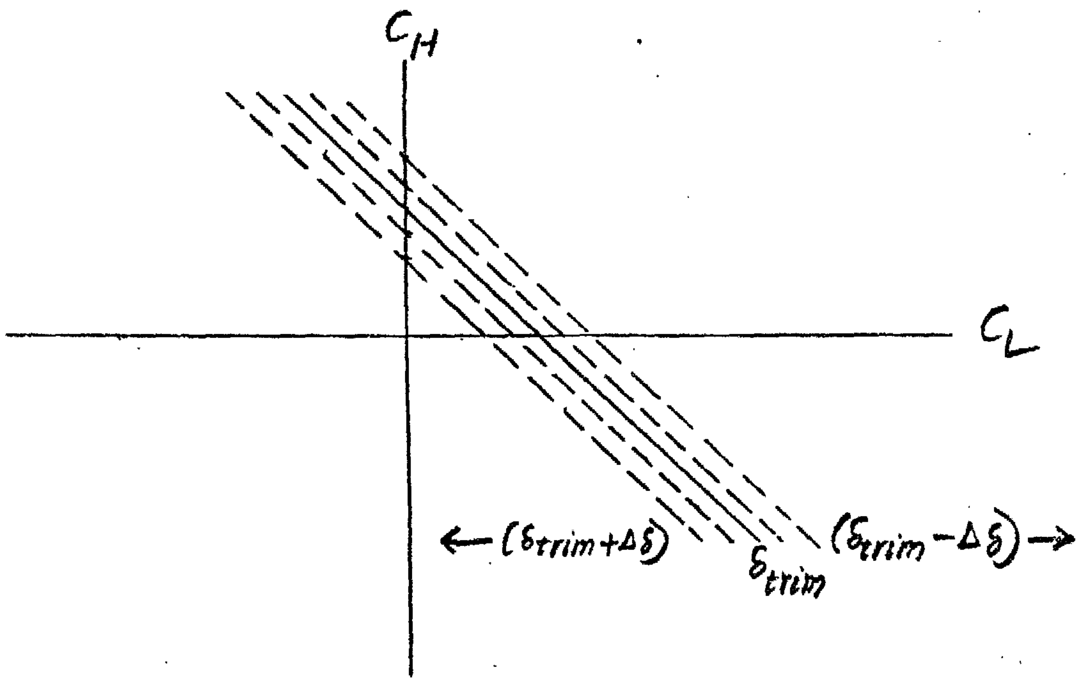

The desirable value for C_{Hc_L} is a dynamic problem which would have to be examined on SLOCOP but that value has a cavitation significance which can be examined here.

Eq. (66) may be written:

(68a)

$$\frac{W}{S} = C_L q = \frac{1}{C_{H_{C_L}}}\left[-\beta + \Delta\left(\frac{W}{S}\right)_\delta - \frac{C_{L\alpha}}{C_{L\alpha\infty}} C'_{H\infty_{C_L=0}}\, q\right]$$

$$\Delta\left(\frac{W}{S}\right)_\delta = C_{H_{C_L}} \frac{W}{S} + \beta + \frac{C_{L\alpha}}{C_{L\alpha\infty}} C'_{H\infty_{C_L=0}}\, q$$

$$\left(\frac{W}{S}\right)_\delta = \frac{1}{\Delta}\left[C_{H_{C_L}} \frac{W}{S} + \beta + \frac{C_{L\alpha}}{C_{L\alpha\infty}} C'_{H\infty_{C_L=0}} \cdot q\right]$$

For the AG(EH) fwd foils at infinite depth this evaluated to:

(68b)

$$\left(\frac{W}{S}\right)_\delta = \frac{1}{\Delta}\left(C_{H_{C_L}} \frac{W}{S} + \beta\right) - \frac{.0686}{.1852}\, q$$

$$= \frac{1}{\Delta}\left(C_{H_{C_L}} \frac{W}{S} + \beta\right) - .37\, q$$

At 50 knots this requires a $\left(\frac{W}{S}\right)_\delta$ of some -2600 psf at 50 knots just for the q term; the first two terms are also negative. This is sufficient demonstration of the infeasibility of the trailing edge flap as a control device for the fiying foil.

It must be noted that the discussion. above is limited to consideration of the trailing edge flap controlled flying, foil. There is an arrangement of the flying foil that is entirely feasible hydrodynamically though it has not yet been explored mechanically:

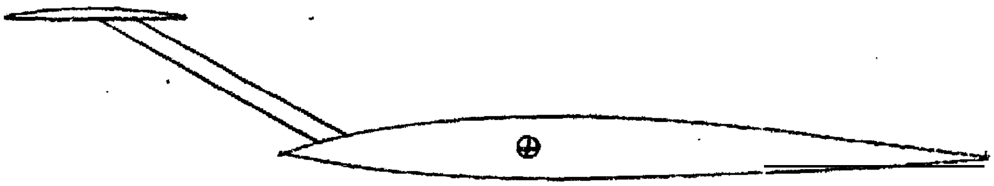

The flying foil is deserving of serious consideration because it relieves the autopilot of the problem of cancelling the orbital angle of attack and because it might incorporate some depth sensitivity. The arrangement was not included in the scope of the AG(EH) lift study because the arrangement presents formidable dynamic analytical problems. The SLOCOP program now makes it possible to evaluate this arrangement and its detailed consideration is recommended.

REFERENCES

1. Hydrodynamic Note AG-14, "AG(EH) Incidence Hinge Moments," in preparation.

2. Hydrodynamic Note AG-16, "AG(EH) Flapped Foil Incidence Hinge Moments, " in preparation.

3. Hydrodynamic Note AG-13, "Analysis of AG(EH) Prototype Fwd. Foil Lift and Moment Data," 2/15/73.

4. "Interim Report On Optimization of Forward Foil Lift Control For AG(EH) Hydrofoil Craft Vol. I: Hydrodynamics," GAC Rpt. No. HCG-72-19(I), 12/72.

5. H. J. Allen, "Calculation Of The Chordwise Load Distribution Over Airfoil Sections With Plain, Split, Or Serially Hinged Trailing-Edge Flaps," NACA Report No 634, 1938.

6. Abbott, von Doenhoff, & Stivers," Summary of Airfoil Data," NACA Rpt. 824, 1945.

SYMBOLS

NOTES: 1. ALL DIMENSIONS IN FT./#/SEC./RAD. UNLESS OTHERWISE NOTED
2. PARENTHESIS READ "DUE TO"; e.g. $(C_L)_\delta$ = C_L DUE TO FLAP DEFLECTION, $C_{L_\delta}\delta$.
3. EXCEPT AS NOTED BELOW, PRIMES INDICATE VALUES MEASURED IN PLANE PERPENDICULAR TO QUARTER-CHO
4. "MIN. HINGE MOMENT" IS MOMENT FOR $(dh/d\alpha)_{min} = 0$.

	a.c.	AERODYNAMIC CENTER, SUBSCRIPT INDICATES WHETHER FOR PITCH OR INCIDENCE LIFT BUT THE TWO ARE PRACTICALLY THE SAME FOR THE AG(EH). FRACTION OF MAC.
	B	BUOYANCY
	b.c.	BUOYANT CENTER. FRACTION OF MAC.
	C	CHORD, USUALLY MAC.
	C_H	INCIDENCE HINGE MOMENT COEFFICIENT, $H/qSMAC$.
	C_{H_0}	RESIDUAL HINGE MOME COEFFICIENT, C_H FOR $i=\theta=\delta=0$,
	$C_{H_{C_L}}$	$dC_H/dC_L = \frac{H}{c} - a.c.$ IN THIS NOTE $C_{H_{C_L}} = C_{H_{C_{L_i}}} = C_{H_{C_{L\alpha}}}$
	$C'_{H_{C_L}}$	$C_{H_{C_L}}$ FOR MINIMUM HINGE MOMENT.
	$C_{H_{C_{L_i}}}$	$dC_H/d(C_L)_i = \frac{H}{c} - a.c._{i}' = C_{H_{C_{L\alpha}}} = C_{H_{C_L}}$ IN THIS NOTE.
	$C_{H_{C_{L\alpha}}}$	$dC_H/d(C_L)_\alpha = \frac{H}{c} - a.c._\alpha = C_{H_{C_{L_i}}} = C_{H_{C_L}}$ IN THIS NOTE.
	$C_{H_{C_{L\delta}}}$	$dC_H/d(C_L)_\delta = C_{H_{C_{L_i}}} - \Delta$
	C_{H_i}	$dC_H/di = C_{L_i}' C_{H_{C_{L_i}}}$
	C_{H_α}	$dC_H/d\alpha$ OR $dC_H/d\theta = C_{L\alpha} C_{H_{C_{L\alpha}}}$
	C_{H_δ}	$dC_H/d\delta = C_{L_\delta} C_{H_{C_{L\delta}}}$
	$C'_{H_{C_L=0}}$	ZERO LIFT HINGE MOMENT COEFFICIENT FOR $\delta=0$. ONLY DEFINED WHEN $a.c._i' = a.c._\alpha$
	$C'_{H_{\infty C_L=0}}$	$C'_{H_{C_L=0}}$ AT INFINITE DEPTH (AERODYNAMIC)
$C_{L_{ref}}$ SEE END OF TABLE	C_L	LIFT COEFFICIENT, L/qS
	C_{L_0}	RESIDUAL LIFT COEFFICIENT
	C_{L_i}'	INCIDENCE LIFT CURVE SLOPE, $dC_L/di = \frac{C_{L_i}'}{C_{L\alpha}} C_{L\alpha}$
	$C_{L\alpha}$	PITCH LIFT CURVE SLOPE, $dC_L/d\alpha$
	$C_{L_i}/C_{L\alpha}$	A CONFIGURATION CHARACTERISTIC WHICH APPEARS TO BE INDEPENDENT OF DEPTH.
	C_{L_δ}	FLAP LIFT CURVE SLOPE, $dC_L/d\delta = \frac{d\alpha}{d\delta}\frac{C_{L_i}'}{C_{L\alpha}} C_{L\alpha}$
	C_l	SECTION LIFT COEFFICIENT
	C_l/C_L	MEASURE OF THE SPANWISE LIFT DISTRIBUTION
	C_{l_i}	DESIGN LIFT COEFFICIENT (CAMBER)
	$C_{l_{i\,eff}}$	EFFECTIVE DESIGN LIFT COEFFICIENT, C_l AT $\alpha=0$. $(\alpha_i=0)$ 83% OF C_{l_i} IS EMPLOYED IN THIS NOTE FOR THE 16-008 THICKNESS DISTRIBUTION.

SYMBOLS (CONT.)

c_{la}	ADDITIONAL (TYPE) LIFT DISTRIBUTION (ON CHORD) DUE TO FLAP.
c_{lb}	BASIC (TYPE) LIFT DISTRIBUTION (ON CHORD) DUE TO FLAP.
c_{mac}	SECTION MOMENT COEFFICIENT ABOUT a.c. FOR 16-SERIES SECTION a.c. APPEARS TO BE C/4 WITH $c_{mac} = \frac{1}{4} c_{l_{i}}$ EFF. ($a = 1.0$ CHORD LINE).
C.P.	CENTER OF PRESSURE. FRACTION OF MAC.
d	DEPTH, IDENTICAL WITH h.
$d\alpha/d\delta$	FLAP EFFECTIVENESS.
G^*	ALLEN'S CENTROID FOR FLAP BASIC LOAD DISTRIBUTION REFERENCED TO C/4 AND EXPRESSED AS FRACTION OF CHORD. * INDICATES ABSOLUTE VALUE TO AVOID ASSIGNING SIGN TO A DISTANCE.
g	ACCELERATION OF GRAVITY.
H	INCIDENCE HINGE MOMENT POSITIVE NOSE UP.
H'	MINIMUM HINGE MOMENT, $(dH/dq)_{d=0} = 0$.
H/C	INCIDENCE HINGE POSITION, FRACTION OF MAC.
H_B	BUOYANT HINGE MOMENT B MAC $(\frac{H}{C} - b.c.)$
h	DEPTH, IDENTICAL WITH d.
i	INCIDENCE ANGLE.
K	$[(\frac{W}{S})_{max} - (\frac{W}{S})_{min}] / 2 (\frac{W}{S})_{m}$. SIMILAR TO Δn BUT INCLUDING ACCOUNTABILITY FOR RANGE IN FLIGHT WEIGHT & C.G.
L	LIFT, POSITIVE UP.
MAC	MEAN AERODYNAMIC CHORD
Δn	NORMAL ACCELERATION MARGIN FOR NEGOTIATING SEAS. NOMINAL VALUE OF $\pm 1/4\ g$ ASSUMED HERE.
P_A	ATMOSPHERIC PRESSURE. THIS NOTE EMPLOYS $P_A - P_V = 2094$ psf.
P_V	VAPOR PRESSURE. SEE P_A.
q	DYNAMIC PRESSURE, $2.84 V_K^2$ psf.
S	FOIL AREA OR LOCAL PRESSURE COEFFICIENT. SEE EQS. (12) & (20)
T_4, T_{10}	THEODORSEN COEFFICIENTS. T_{10}/π IS THEORETICAL $d\alpha/d\delta$.
V	SPEED
V_C	CAVITATION SPEED
V_{C0}	CAVITATION SPEED FOR ZERO DEPTH (A MATHEMATICAL CONCEPT.
V_K	SPEED IN KNOTS.

SYMBOLS (CONT.)

$\frac{v}{V}$	LOCAL VELOCITY RATIO (ON CHORD) DUE TO THICKNESS DISTRIBUTION.
$\frac{\Delta v}{V}$	LOCAL VELOCITY RATIO INCREMENT DUE TO CAMBER (DISTRIBUTION ON CHORD FOR $C_{l_{i\,eff}}$.
$\left(\frac{\Delta v}{V}\right)_F$	LOCAL VELOCITY RATIO INCREMENT DUE TO FLAP BASIC (TYPE) LOAD, PER UNIT C_{l_b}
$\frac{\Delta v_a}{V}$	LOCAL VELOCITY RATIO INCREMENT OF ADDITIONAL LOAD TYPE, DUE TO ANGLE OF ATTACK AND/OR FLAP DEFLECTION, PER UNIT C_l INCREMENT.
$\left(\frac{W}{S}\right)_{REF}$ SEE END OF TABLE; $\frac{W}{S}$	TOTAL FOIL LOADING, $(W/S)_B+(W/S)_\alpha+(W/S)_i+(W/S)_\delta$; $=C_L q+(W/S)_B$
$(W/S)_B$	BUOYANT FOIL LOADING, B/S
$(W/S)_i$	INCIDENCE FOIL LOADING, $C_{L_i} i\, q$
$(W/S)_\alpha$	PITCH FOIL LOADING, $C_{L_\alpha}\theta\, q$
$(W/S)_\delta$	FLAP FOIL LOADING, $C_{L_\delta}\delta\, q$
$(W/S)_m$	MEAN FOIL LOADING, $[(W/S)_{max}+(W/S)_{min}]/2$ WHERE MAX. & MIN. FOIL LOADINGS ACCOUNT FOR FLIGHT WT. & BALANCE RANGE AND FOR NOMINAL NORMAL ACCELERATION REQUIREMENTS.
α	ANGLE OF ATTACK, TOTAL OF GEOMETRIC AND DYNAMIC COMPONENTS. NOT EMPLOYED IN THIS NOTE.
β	A BUOYANT MOMENT PARAMETER, $(a.c.-b.c.)(W/S)_B$
Δ	A FLAP CHORDWISE LIFT DISTRIBUTION PARAMETER, $=\frac{1}{4}\left(1+\frac{T_2/\pi}{T_{11}/\pi}\right)$ IN THIS NOTE. (DOUBTFUL CONFIDENCE LEVEL)
δ	FLAP DEFLECTION, POSITIVE NOSE UP
ζ	A FLAP CHORDWISE LIFT DISTRIBUTION PARAMETER, $=C_{l_b}/(C_L)_F=\Delta/6^{*}$ IN THIS NOTE. (DOUBTFUL CONFIDENCE LEVEL).
θ	CRAFT PITCH ANGLE. POSITIVE BOW UP.
ξ_i	A SPANWISE LOAD DISTRIBUTION PARAMETER, $\frac{(c_l/C_L)_i}{(c_l/C_L)_\delta}-1$
ξ_α	A SPANWISE LOAD DISTRIBUTION PARAMETER, $\frac{(c_l/C_L)_\alpha}{(c_l/C_L)_\delta}-1$
ρ	DENSITY, 1.9905 lb. sec.^{2}/ft.^{4} (slugs/ft.^{3})
σ	CAVITATION NUMBER, $(P_0-P_v+\rho g h)/q$

SYMBOLS (CONT.)

ψ	A CHORDWISE VELOCITY DISTRIBUTION PARAMETER, $= \frac{v}{V} \pm \frac{\Delta v}{V} \mp \frac{\Delta v_a}{V} C_{l_{i\,eff}}$ $\left(\begin{matrix}\pm \text{ UPPER SURFACE} \\ \text{LOWER SURFACE}\end{matrix}\right)$
ω	A FLAP LOAD DISTRIBUTION PARAMETER, $\delta\left[\left(\frac{\Delta v}{V}\right)_F - \frac{\Delta v_1}{V}\right]$

SUBSCRIPTS

B	DUE TO BUOYANCY
F	DUE TO FLAP DEFLECTION
H	HYDRODYNAMIC (EXCLUDING BUOYANCY)
i	DUE TO INCIDENCE
max	MAXIMUM
min	MINIMUM
nom	NOMINAL
q_{max}	AT MAXIMUM FLIGHT SPEED
q_{min}	AT MINIMUM FLIGHT SPEED
$q=0$	AT ZERO SPEED (A MATHMATICAL CONCEPT)
α	DUE TO PITCH LIFT (ANY CHANGE IN ANGLE OF ATTACK FOR FOIL AND POD)
δ	DUE TO FLAP DEFLECTION
O	RESIDUAL, AT $\alpha = i = \delta = 0$
1C	AT 1 MAC DEPTH
∞	~~AT INFINITE DEPTH (AERODYNAMIC)~~

$$C_{L_{ref}} = (C_L)_i + C_{L_0}$$

$$\left(\frac{W}{S}\right)_{ref} = \left(\frac{W}{S}\right)_i + \left(\frac{W}{S}\right)_0$$

$$= \left[(C_L)_i + C_{L_0}\right] q$$

TABLE I
CAVITATION PARAMETERS
AG(EH) FWD. FOIL MODEL

STATION, %	1.25	2.5	5	50	60	70	80
v/V	1.025	1.051	1.060	1.088	1.092	1.088	1.067
$\frac{v}{V} \pm \frac{\Delta v}{V}$	1.098 .952	1.124 .978	1.133 .987	1.161 1.015	1.165 1.019	1.161 1.015	1.140 .994
$\Delta v_a/V$	1.346	.970	.686	.160	.131	.103	.076
$C_{l_{i\,eff}} \frac{\Delta v_a}{V}$	.394	.284	.201	.047	.038	.030	.022
ψ	.704 1.346	.840 1.262	.932 1.188	1.114 1.062	1.127 1.057	1.131 1.045	1.118 1.016

16-(.353)08 SECTION
8.5 ft. & 9.33 ft. DEPTHS

$q = 2.84\, V_K^2$

$q' = .668\, q$

$\sigma' = 2588/q'$ & $2641/q'$

$\left(\frac{W}{S}\right)_B = 90$

$\left(\frac{W}{S}\right)_\alpha = C_{L_\alpha}\, \alpha\, q = .048\, q$ FOR 1° @ IMAC

$C_{l_{i\,eff}} = .83\, C_{l_i} = .293$

$\Delta v/V = .25\, C_{l_{i\,eff}} = .073$

$\psi = \frac{v}{V} \pm \frac{\Delta v}{V} \mp C_{l_{i\,eff}} \frac{\Delta v_a}{V}$

UPPER NUMBER OR SIGN IS UPPER SURFACE

$\left(\frac{c_l}{C_L}\right)_S = \left(\frac{c_l}{C_L}\right)_i = \begin{matrix} 1.310 \\ .710 \end{matrix}$

$\xi_\alpha = \begin{matrix} -.109 \\ +.240 \end{matrix}$

TABLE II
CAVITATION PARAMETERS
AG(EH) FWD. FOIL PROTOTYPE

STATION, %	1.25	2.5	5	50	60	70	80
v/V	1.025	1.051	1.060	1.088	1.092	1.078	1.067
$\frac{v}{V} \pm \frac{\Delta v}{V}$	1.106 .944	1.132 .970	1.141 .979	1.169 1.007	1.173 1.011	1.169 1.007	1.148 .936
$\Delta v_a/V$	1.346	.970	.686	.160	.131	.103	.076
$Cl_{i_{eff}} \frac{\Delta v_a}{V}$	.436	.314	.222	.052	.042	.033	.025
γ	.670 1.380	.818 1.284	.919 1.201	1.117 1.059	1.131 1.053	1.136 1.040	1.123 1.011
$(\Delta v/V)_F$	.015	.027	.040	.218	.283	.400	1.100
ω $(\delta=.545)$ $(\delta=.466)$	.725 .620	.514 .439	.352 .301	-.032 -.027	-.083 -.071	-.162 -.138	-.559 -.477

16-(.390)08 SECTION
1 MAC (9.33 ft.) DEPTH
20% CHORD FLAP
$q = 2.84\, V_K^2$
$q' = .668\, q$
$\sigma' = 2641/q'$

$Cl_{i_{eff.}} = .83\, Cl_i = .324$
$\Delta v/V = .25\, Cl_{i_{eff}} = .081$
$\gamma = \frac{v}{V} \pm \frac{\Delta v}{V} \mp Cl_{i_{eff}} \frac{\Delta v_a}{V}$

$\omega = \delta \left[\frac{\Delta v_a}{V} - \left(\frac{\Delta v}{V}\right)_F \right]$

UPPER NUMBER OR SIGN IS UPPER SURFACE

$\left(\frac{c_l}{c_L}\right)_\delta = \left(\frac{c_l}{c_L}\right)_i = \begin{matrix} 1.310 \\ .710 \end{matrix}$

$\delta_\alpha = \begin{matrix} -.109 \\ +.240 \end{matrix}$

TABLE III

OPTIMUM CAVITATION BUCKET

EFFECT OF δ

SECTION	16-(.353)08		16-(.390)08					
FLAP C	20%		20%					
CHORD STA.	1.25%	80%	1.25%	80%	1.25%	80%	1.25%	80%
$\Delta v_a/V$	1.[illegible]	.076	1.346	.076	1.346	.076	1.346	.076
$C_{l_{i\,eff}}$	.[illegible]3		.324					
$C_{l_{i\,eff}}\,\Delta v_a/V$	.324	.022	.436	.025	.436	.025	.436	.025
$v/V+\Delta v/V$	1.098	1.140	1.106	1.148	1.106	1.148	1.106	1.148
ψ	.704	1.118	.670	1.123	.670	1.123	.670	1.123
T_4/π							-.1424	
T_{10}/π							.5498	
$T_4/\pi / T_{10}/\pi$							-.259	
$1+\frac{T_4/\pi}{T_{10}/\pi}$							.741	
Δ							.1852	
G^*							.397	
δ	.545 (SEE NOTE)						.466	
$(\Delta v/V)_F$	.015	1.100	.015	1.100	.015	1.100	.015	1.100
$(\Delta v/V)_F/(\Delta v_a/V)$	.01115	14.48	.01115	14.48	.01115	14.48	.01115	14.48
$1-\frac{(\Delta v/V)_F}{\Delta v_a/V}$	.98885	-13.48	.98885	-13.48	.98885	-13.48	.98885	-13.48
K	-.539	7.35	-.539	7.35	-.539	7.35	-.460	6.28
$(C_d/C_L)_\delta$	1.310					-		
$P_A-P_V+\rho gh$	2588		2588		2641		2641	
$C_{L_\alpha}\alpha$	0		0		.0479		.0479	
$(W/S)_B$	0		0		90		90	

NOTES: 1. ALL VELOCITY DISTRIBUTIONS ARE FOR UPPER SURFACE.
2. .545 IS VALUE GIVEN δ IN INTERIM REPORT FOR 20%C FLAP.

SEE TABLES I & II FOR $C_{l_{i\,eff}}$.

$$\psi = \frac{v}{V} + \frac{\Delta v}{V} - C_{l_{i\,eff}}\frac{\Delta v_a}{V}$$

T_4 & T_{10} FROM TABLE 3.1, REF. 4.

G^* FROM TABLE IV, REF. 5 FOR $\delta = 5°, 10°, 15°$.

$\delta = \Delta/G^*$

$(\Delta v/V)_F$ FROM FIG. 4.

$P_A-P_V+\rho gh$ FOR 8.5 & 9.33 ft. DEPTHS

$C_{L_\alpha}\alpha$ FOR 1° α @ 9.33 ft.

$$K = -\delta\left[1 - \frac{(\Delta v/V)_F}{\Delta v_a/V}\right]$$

$(C_d/C_L)_\delta = (C_d/$ [illegible] $)$; OF FIG. 1.1 REF 4

TABLE IV

OPTIMUM CAVITATION BUCKET

EFFECT OF SECTION AND FLAP CHORD

SECTION	16-(.390)08				16-008			
FLAP C	20%		50%		20%		50%	
CHORD STA.	1.25%	80%	1.25%	50%	1.25%	80%	1.25%	50%
$\Delta v_a/V$	1.346	.076	1.346	.160	1.346	.076	1.346	.160
$Cl_{i_{eff}}$	.324				0			
$Cl_{i_{eff}} \Delta v_a/V$	.436	.025	.436	.052	0	0	0	0
$v/V + \Delta v/V$	1.106	1.148	1.106	1.169	1.025	1.067	1.025	1.088
Ψ	.670	1.123	.670	1.117	1.025	1.067	1.025	1.088
T_4/π	-.1424		-.5		-.1424		-.5	
T_{10}/π	.5498		.8183		.5498		.8183	
$T_4/\pi / T_{10}/\pi$	-.259		-.612		-.259		-.612	
$1 + \frac{T_4/\pi}{T_{10}/\pi}$	.741		.388		.741		.388	
Δ	.1852		.0970		.1852		.0970	
G^*	.397		.242		.397		.242	
ζ	.466		.401		.466		.401	
$(\Delta v/V)_F$	.015	1.100	.035	.788	.015	1.100	.035	.788
$(\Delta v/V)_F/(\Delta v_a/V)$	.01115	14.48	.0260	4.925	.01115	14.48	.0260	4.925
$1-\frac{(\Delta v/V)_F}{\Delta v_a/V}$	.98885	-13.48	.974	-3.925	.98885	-13.48	.974	-3.925
K	-.460	6.28	-.391	1.575	-.460	6.28	-.391	1.575
$(C_\ell/C_L)_S$	1.310							
$P_A - P_V + \rho g h$	2641							
$C_{L_\alpha}\alpha$	.0479							
$(W/S)_B$	90							

NOTES: 1. ALL VELOCITY DISTRIBUTIONS ARE FOR UPPER SURFACE.

SEE TABLE II FOR $Cl_{i_{eff}}$

$\Psi = \frac{v}{V} + \frac{\Delta v}{V} - Cl_{i_{eff}} \frac{\Delta v_a}{V}$

T_4 & T_{10} FROM TABLE 3.1, REF. 4.

G^* FROM TABLE IV, REF. 5 FOR $\delta = 5°, 10°, 15°$.

$\zeta = \Delta/G^*$

$(\Delta v/V)_F$ FROM FIG. 4.

$K = -\zeta\left[1 - \frac{(\Delta v/V)_F}{\Delta v_a/V}\right]$

$(C_\ell/C_L)_S = (C_\ell/C_L)_1$ OF FIG. 6.1, REF. 4.

$P_A - P_V + \rho g h$ FOR 9.33 FT. DEPTH

$C_{L_\alpha}\alpha$ FOR 1° α @ 9.33 FT.

TABLE V
OPTIMUM HINGE LOCATIONS
(FOR MINIMUM $|H_{max}|$)

	MINIMUM POSITIVE MOMENT	MINIMUM MOMENT	MINIMUM NEGATIVE MOMENT
LAPPED	$C_{Hc_L}(1-K)\left(\frac{W}{S}\right)_m =$ $-\beta - C'_{H\alpha_{c_L=0}}\, q_{max}$	$C_{Hc_L}\left(\frac{W}{S}\right)_m =$ $-\beta$ $-C'_{H\alpha_{c_L=0}}\, q_{max} \times \frac{1}{2}\left(1+\frac{C_{L\alpha_{ic}}}{C_{L\alpha_\infty}}\frac{q_{min}}{q_{max}}\right)$	$C_{Hc_L}(1+K)\left(\frac{W}{S}\right)_m =$ $-\beta$ $-C'_{H\alpha_{c_L=0}}\, q_{min}\, \frac{C_{L\alpha_{ic}}}{C_{L\alpha_\infty}}$
.APPED :RAL CASE, INCLUDING MUM CAVITATION CASE. $\frac{H}{q} < 0$	$+\Delta\left(\frac{W}{S}\right)_\delta q_{max}$	$+\Delta \times \frac{1}{2}\left[\left(\frac{W}{S}\right)_\delta q_{min} + \left(\frac{W}{S}\right)_\delta q_{max}\right]$	$+\Delta\left(\frac{W}{S}\right)_\delta q_{min}$
LAPPED IMUM MOMENT CASE $\left(\frac{dH}{dq}\right)_{dl/c=\infty} = 0$		$C'_{Hc_L}\left(\frac{W}{S}\right)_m =$ $-\beta$ $-C'_{H\alpha_{c_L=0}}\, q_{max} \times \frac{1}{2}\left(1+\frac{C_{L\alpha_{ic}}}{C_{L\alpha_\infty}}\right)$ $+\Delta\left(\frac{W}{S}\right)_\delta q_{max}$	$C'_{Hc_L}(1+K)\left(\frac{W}{S}\right)_m =$ $-\beta$ $-C'_{H\alpha_{c_L=0}}\, q_{max}\, \frac{C_{L\alpha_{ic}}}{C_{L\alpha_\infty}}$ $+\Delta\left(\frac{W}{S}\right)_\delta q_{max}.$

NOTES: 1. $\frac{H}{c} = C_{Hc_L} + a.c.$
2. TO SUIT OPERATING LIMITATIONS, SUBSTITUTE ANY LIFT CURVE SLOPE (INCLUDING ∞) FOR $C_{L\alpha_{ic}}$.

TABLE VI
MAXIMUM HINGE MOMENT, $\left|\frac{H_{max}}{SMAC}\right|$
FOR HINGE LOCATIONS OF TABLE V

	MINIMUM POSITIVE MOMENT	MINIMUM MOMENT	MINIMUM NEGATIVE MOMENT
IFLAPPED		$\frac{\lvert H_{max}\rvert}{SMAC} = -K\beta - \frac{1}{2}K\left(q_{max} + \frac{C_{L\alpha_{IC}}}{C_{L\alpha_0}} q_{min}\right) C'_{H\alpha_{C_L=0}} - \frac{1}{2}\left(q_{max} - \frac{C_{L\alpha_{IC}}}{C_{L\alpha_0}} q_{min}\right) C'_{H\alpha_{C_L=0}}$	
FLAPPED NERAL CASE, INCLUDING TIMUM CAVITATION CASE $\frac{dH}{dq} < 0$	$\frac{2}{1-K}\left(\frac{\lvert H_{max}\rvert}{SMAC}\right)_{MIN.\ MOM.}$	$+\frac{1}{2}K\left[\left(\frac{W}{S}\right)_\delta q_{min} + \left(\frac{W}{S}\right)_\delta q_{max}\right]\Delta - \frac{1}{2}\left[\left(\frac{W}{S}\right)_\delta q_{min} - \left(\frac{W}{S}\right)_\delta q_{max}\right]\Delta$	$\frac{2}{1+K}\left(\frac{\lvert H_{max}\rvert}{SMAC}\right)_{MIN.\ MOM.}$
FLAPPED TIMUM MOMENT CASE $\left(\frac{dH}{dq}\right)_{d/c=\infty} = 0$		$\frac{\lvert H'_{max}\rvert}{SMAC} = K\left[-\beta + \Delta\left(\frac{W}{S}\right)_\delta q_{max} - C'_{H\alpha_{C_L=0}} q_{max} \times \frac{1}{2}\left(1 + \frac{C_{L\alpha_{IC}}}{C_{L\alpha_0}}\right)\right] - C'_{H\alpha_{C_L=0}} q_{max} \times \frac{1}{2}\left(1 - \frac{C_{L\alpha_{IC}}}{C_{L\alpha_0}}\right)$	

TABLE VII
AG(EH) OPTIMUM HINGE MOMENTS, $\frac{|H_{max}|}{S_{MAC}}$

	MINIMUM POSITIVE MOMENT	MINIMUM MOMENT	MINIMUM NEGATIVE MOMENT
LAPPED	810 (+96%)	273.5 (-33.9%)	413 (0)
OPTIMUM AVITATION	849 (+105%)	286.6 (-30.6%)	433 (+4.7%)
OPTIMUM MOMENT	496 (+20%)	167.5 (-59.5%)	253 (-38.7%)

NOTE: $\Delta n = 1/4$ $\Delta(W/S) = 1435-1220$ $K = .325$

FIG. 1

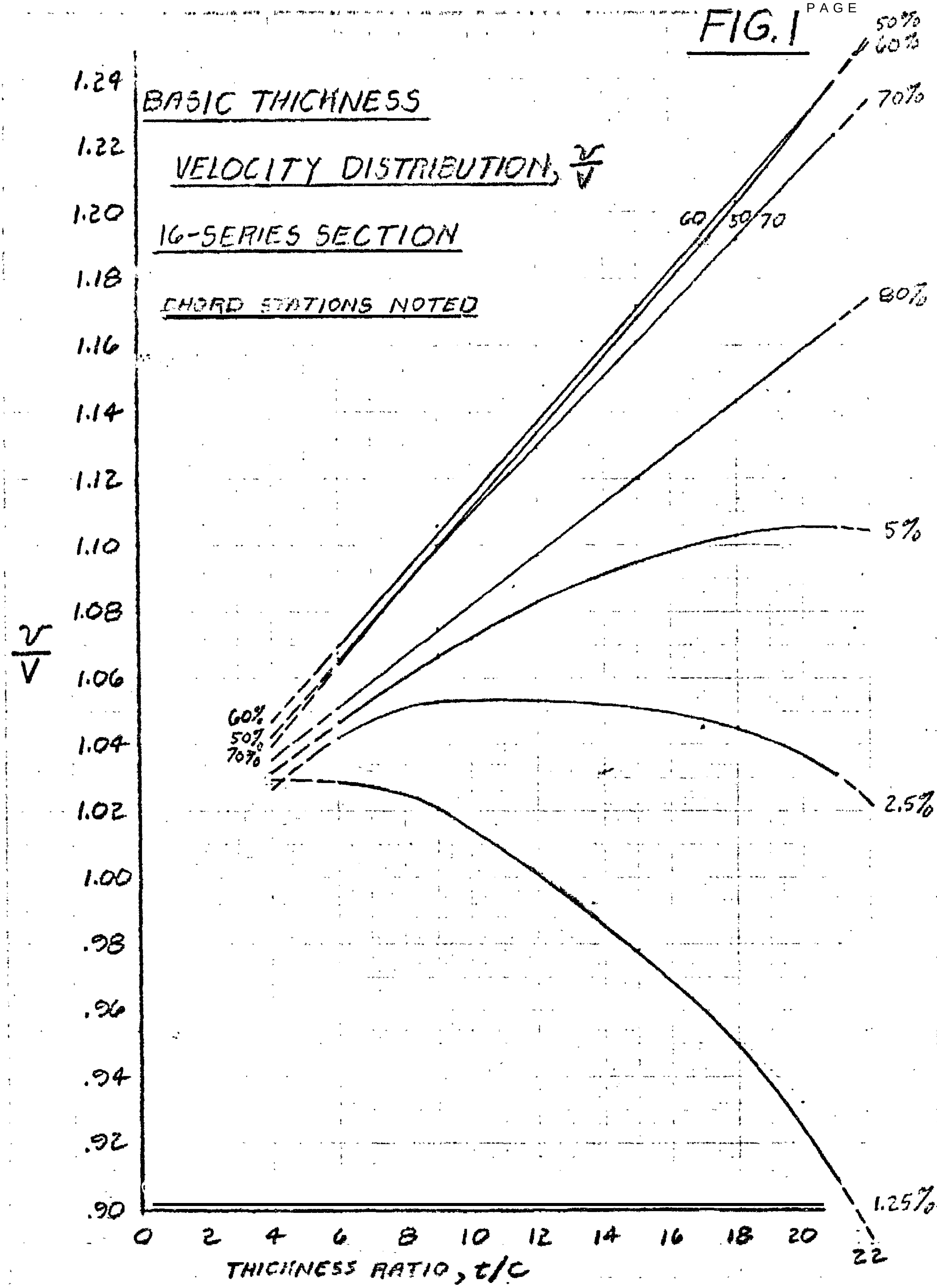

HRW 4/17/73

FIG. 2

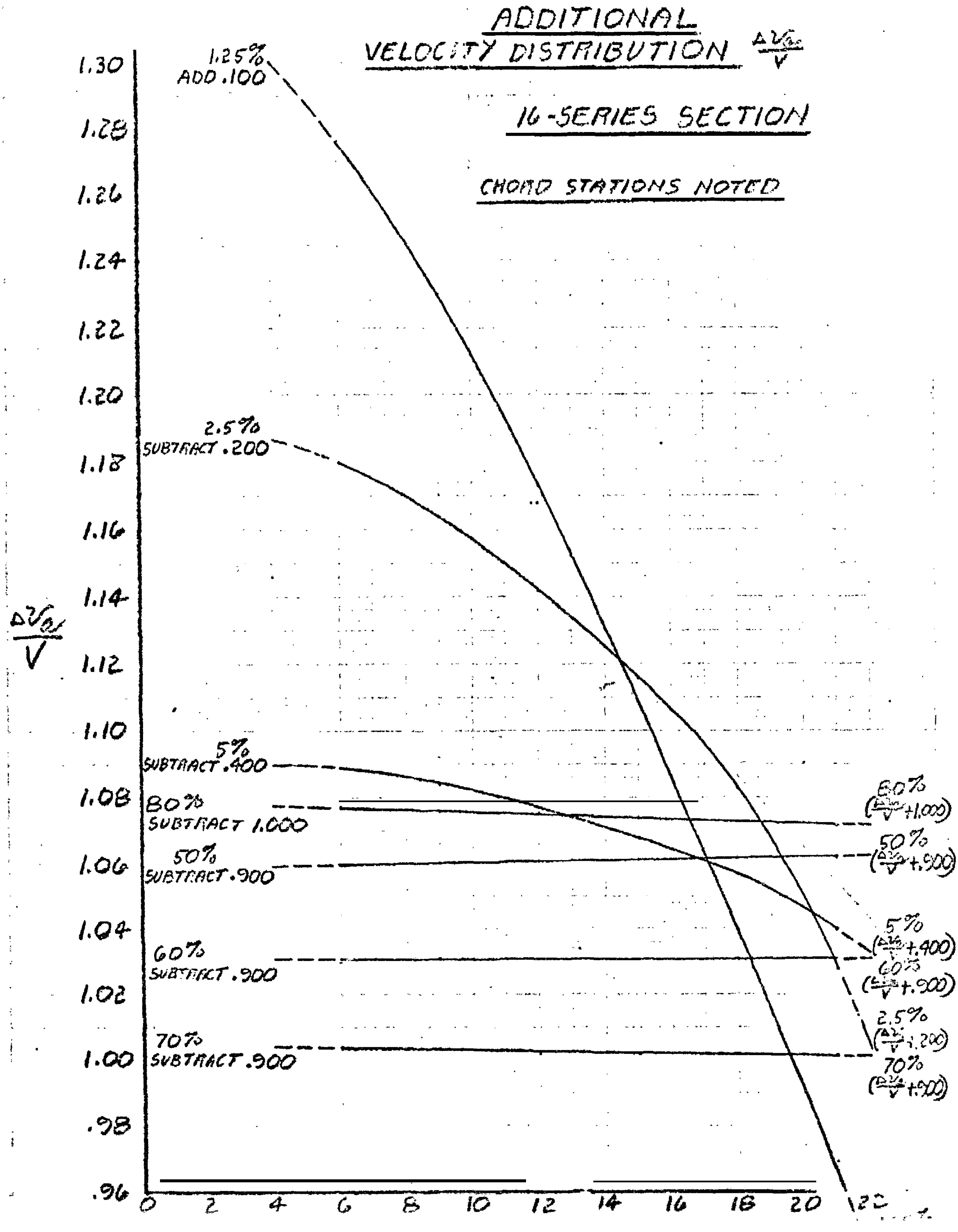
ADDITIONAL
VELOCITY DISTRIBUTION $\frac{\Delta V_{a}}{V}$
16-SERIES SECTION
CHORD STATIONS NOTED
1.25%
ADD .100
2.5%
SUBTRACT .200
5%
SUBTRACT .400
80%
SUBTRACT 1.000
50%
SUBTRACT .900
60%
SUBTRACT .900
70%
SUBTRACT .900
80% ($\frac{\Delta V_a}{V}$+1.000)
50% ($\frac{\Delta V_a}{V}$+.900)
5% ($\frac{\Delta V_a}{V}$+.400)
60% ($\frac{\Delta V_a}{V}$+.900)
2.5% ($\frac{\Delta V_a}{V}$+.200)
70% ($\frac{\Delta V_a}{V}$+.900)
$\frac{\Delta V_{a}}{V}$
1.30
1.28
1.26
1.24
1.22
1.20
1.18
1.16
1.14
1.12
1.10
1.08
1.06
1.04
1.02
1.00
.98
.96
0
2
4
6
8
10
12
14
16
18
20
22

CAVITATION SPEED vs. DEPTH

SALT WATER

$P_A - P_V = 2044$ psf

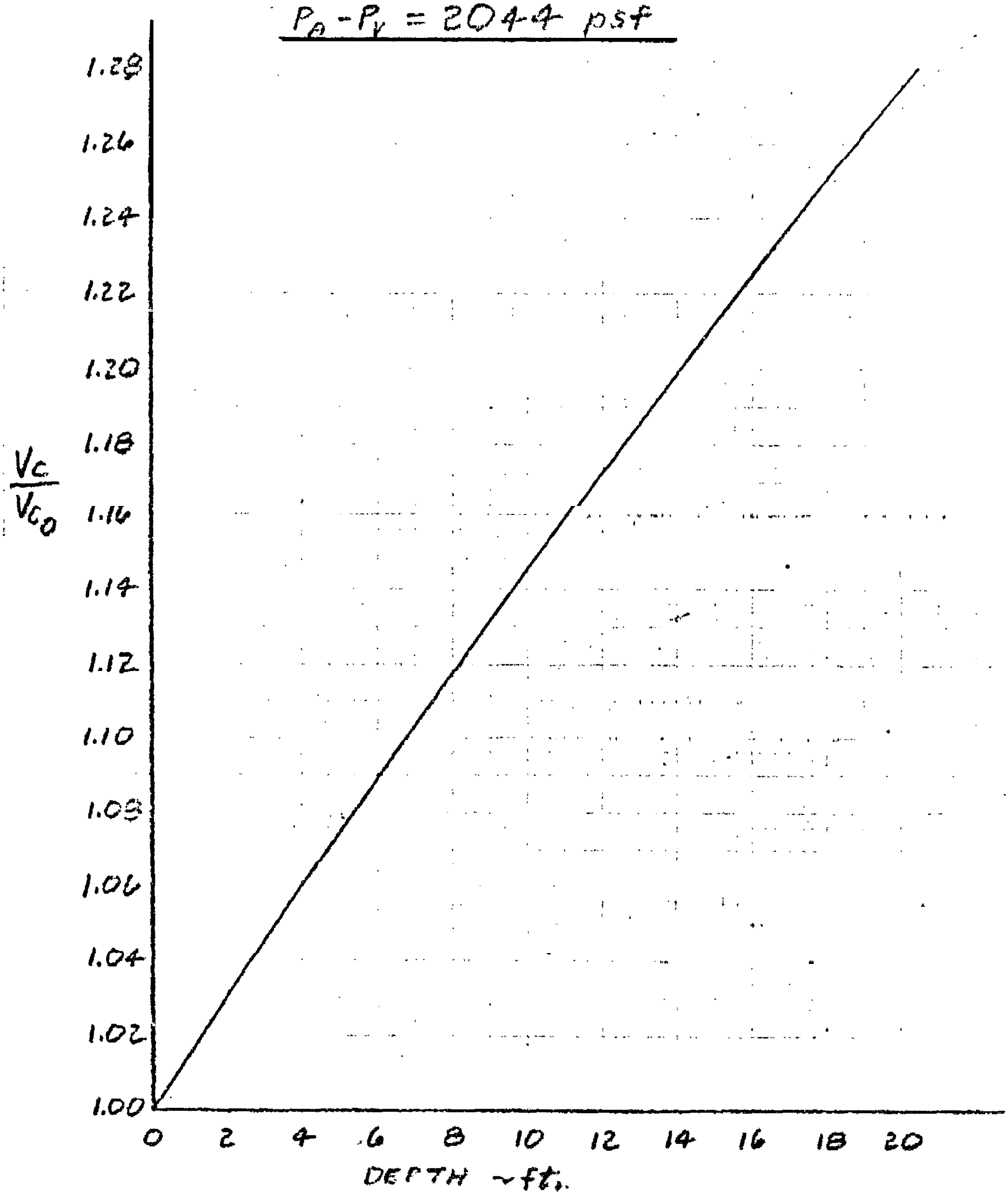

FLAP BASIC LOAD DISTRIBUTION

δ LESS THAN 20°

FROM TABLE III OF REF. 5.

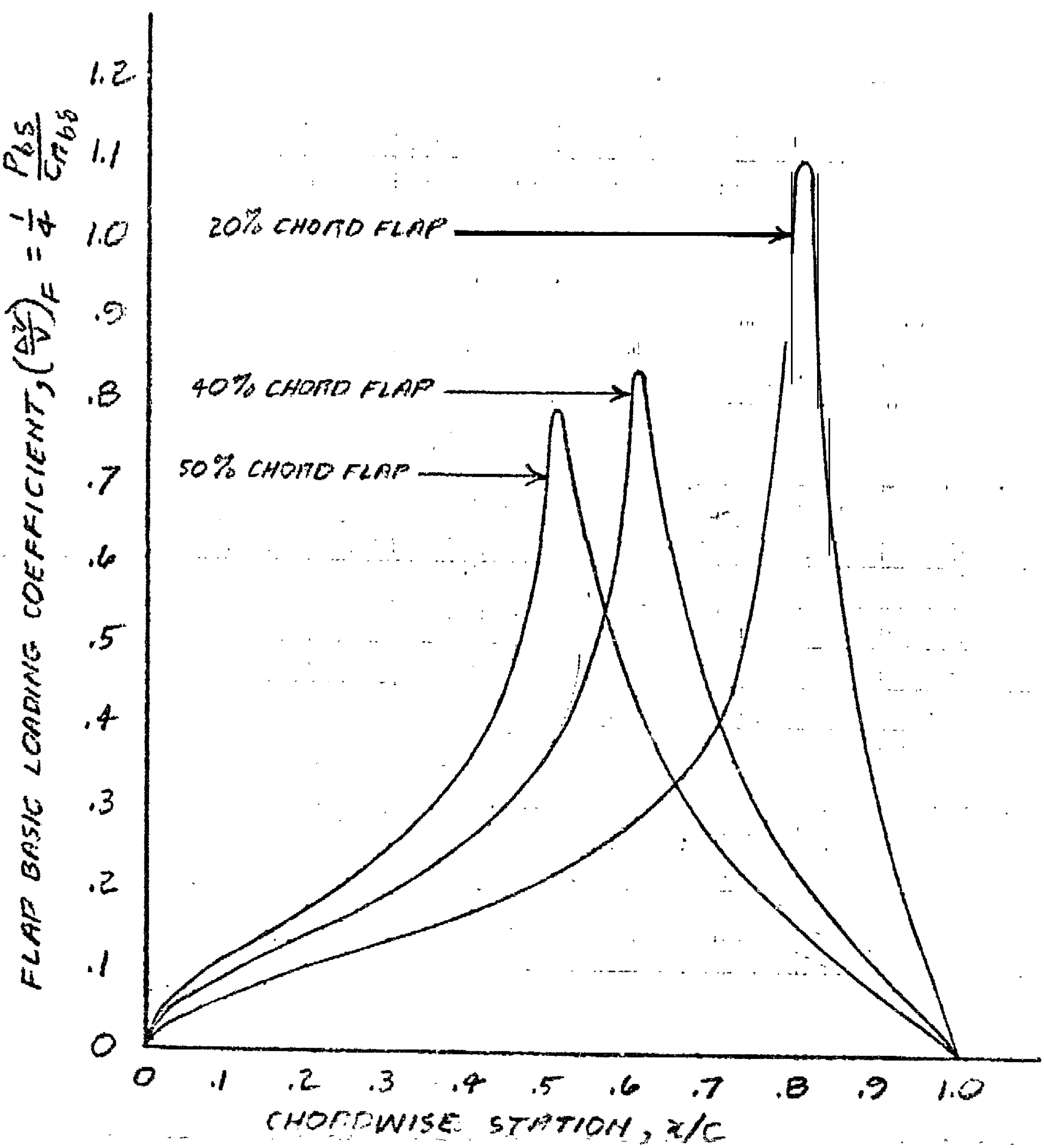

FIG. 5

CAVITATION BUCKET

EFFECT OF BUOYANCY AND DEPTH

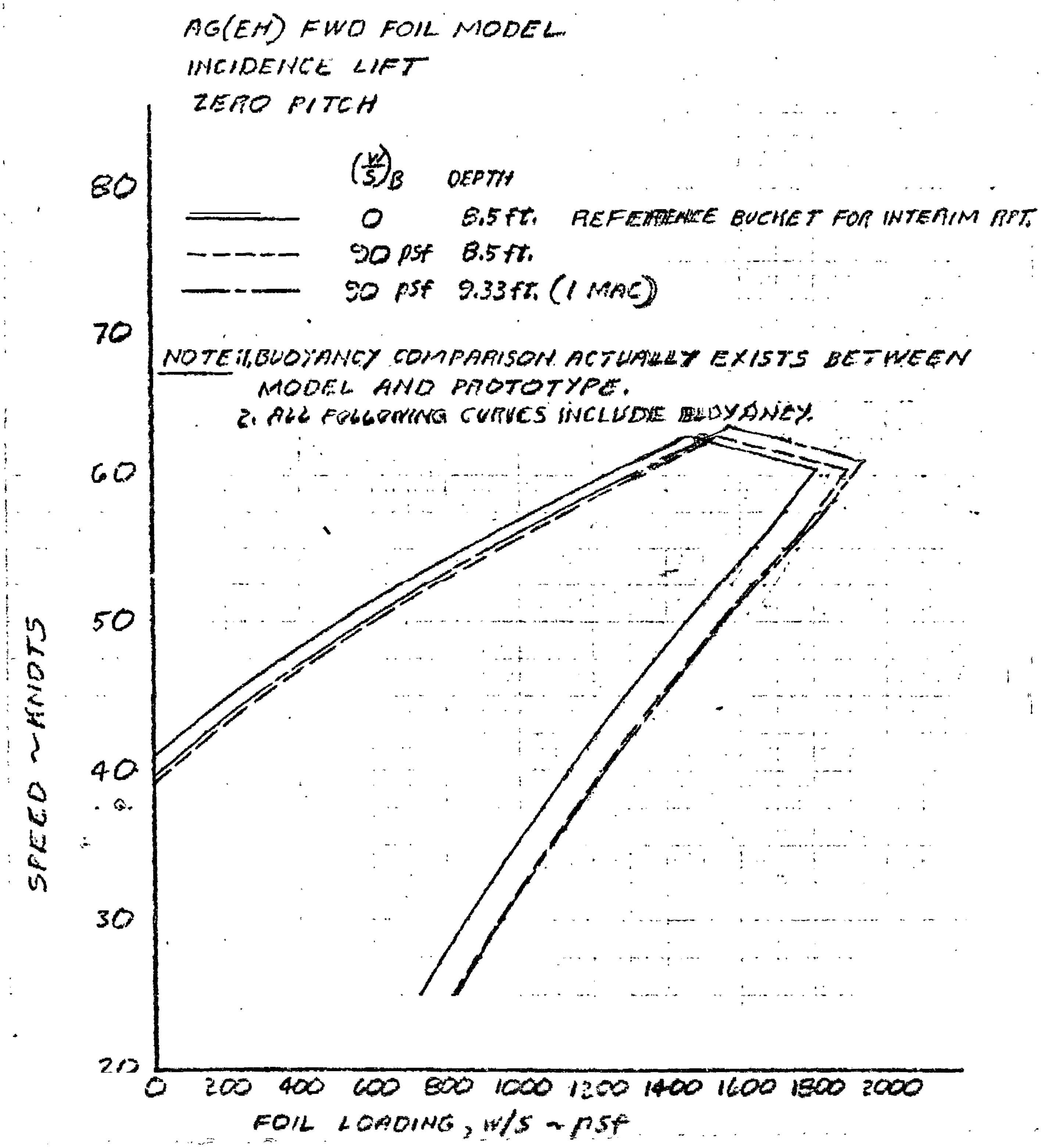

CAVITATION BUCKET

EFFECT OF PITCH AND CAMBER

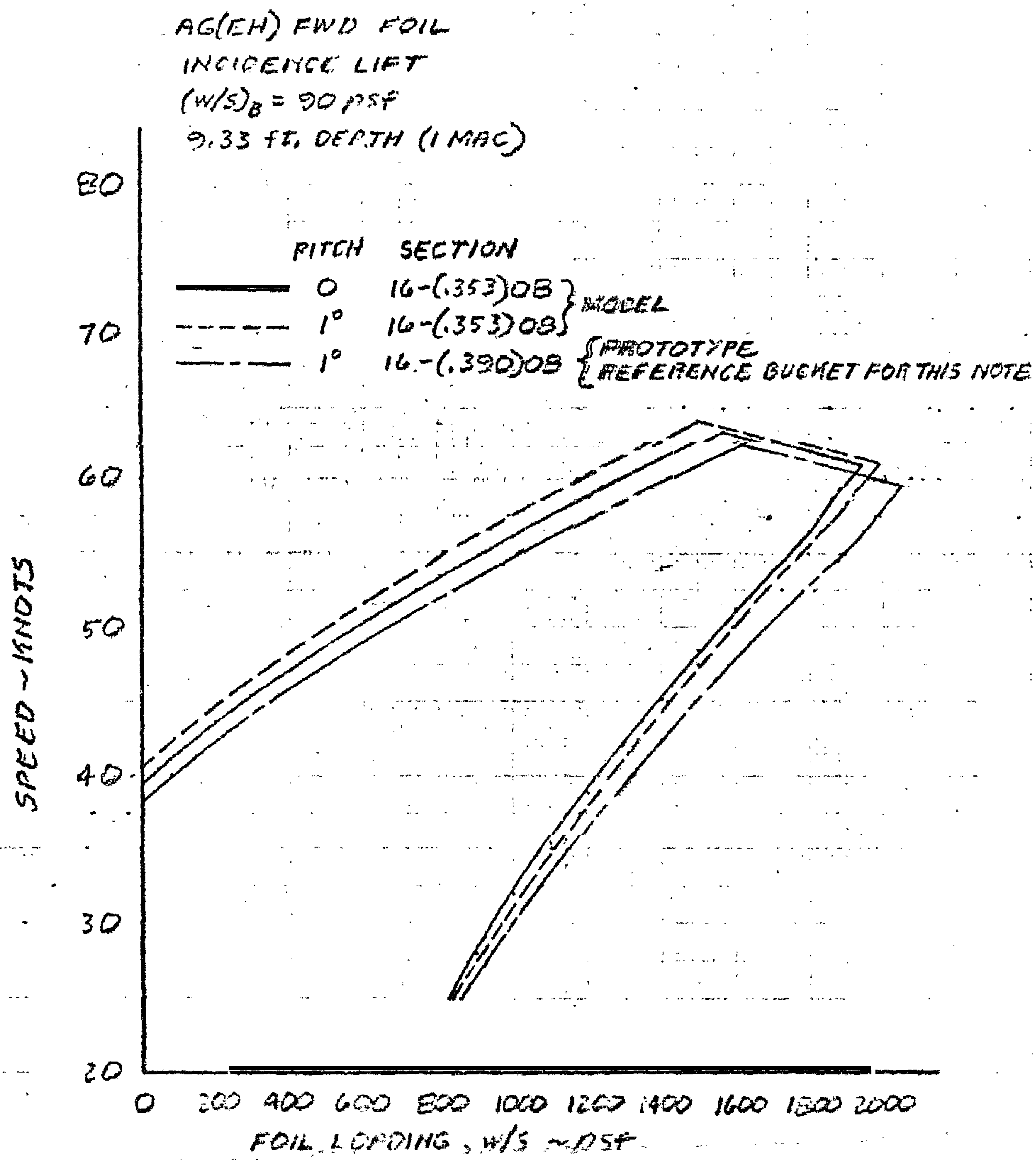

OPTIMUM UPPER SURFACE CAVITATION BOUNDARIES

EFFECT OF OPERATING CONDITIONS AND S

	SECTION	S	DEPTH ft.	PITCH deg.	(l/b)B
1	16-(.353)03	.545	8.5	0	0
2	16-(.390)03				
3			9.33	1	90
4		.466			

AG(EH) FWD. FOIL
INCIDENCE LIFT CONTROL
20% FLAP CHORD RATIO
NOTE: CURVE #1 IS INTERIM REPORT REFERENCE.

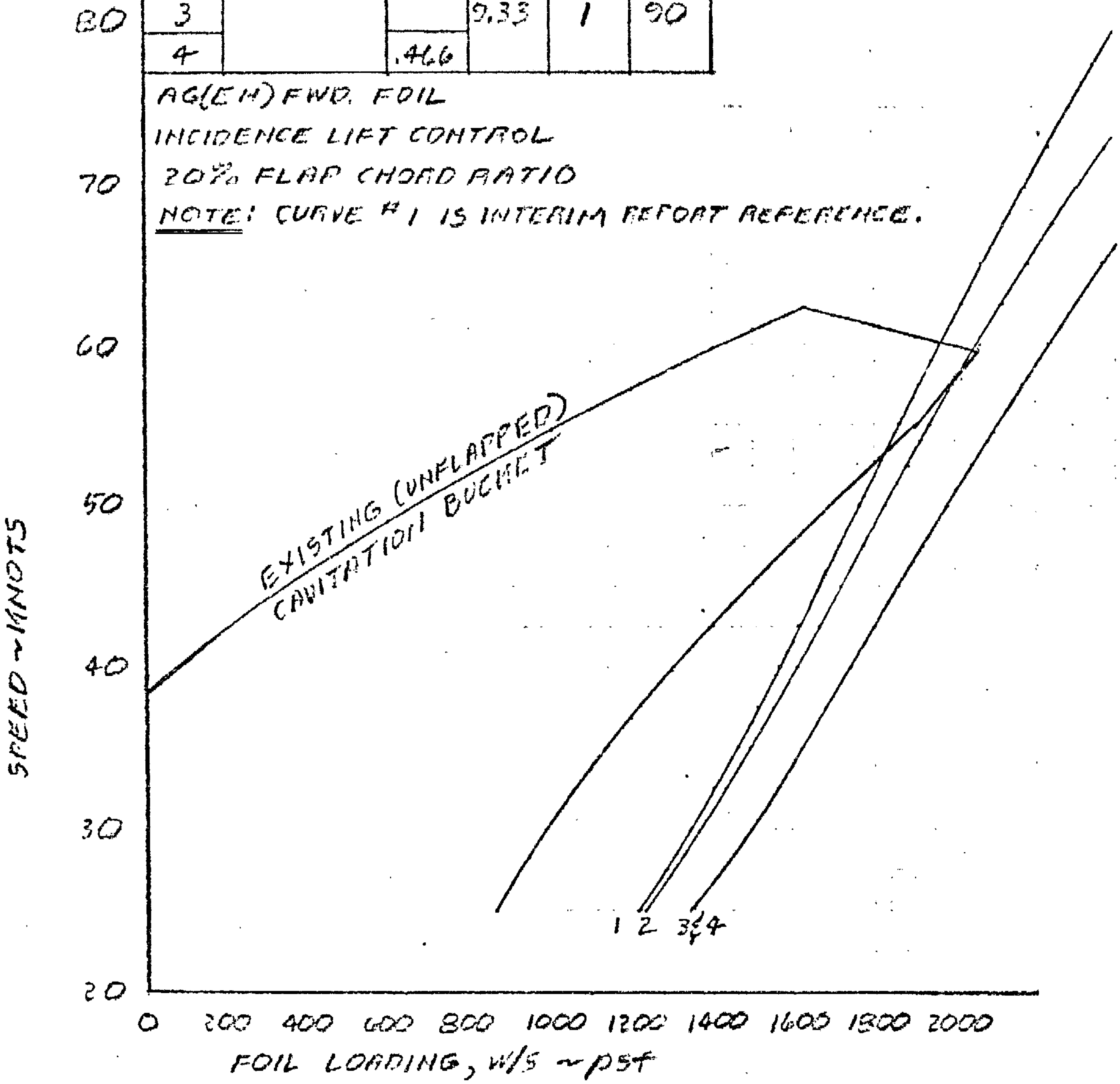

HAW 4/24/73

FIG. 8

OPTIMUM FLAP SCHEDULES

EFFECT OF OPERATING CONDITIONS AND ξ

	SECTION	ξ	DEPTH ft.	PITCH deg.	$\left(\frac{W}{S}\right)_B$
1	16-(.353)08	.545	8.5	0	0
2	16-(.390)08				
3			9.33	1	90
4		.466			

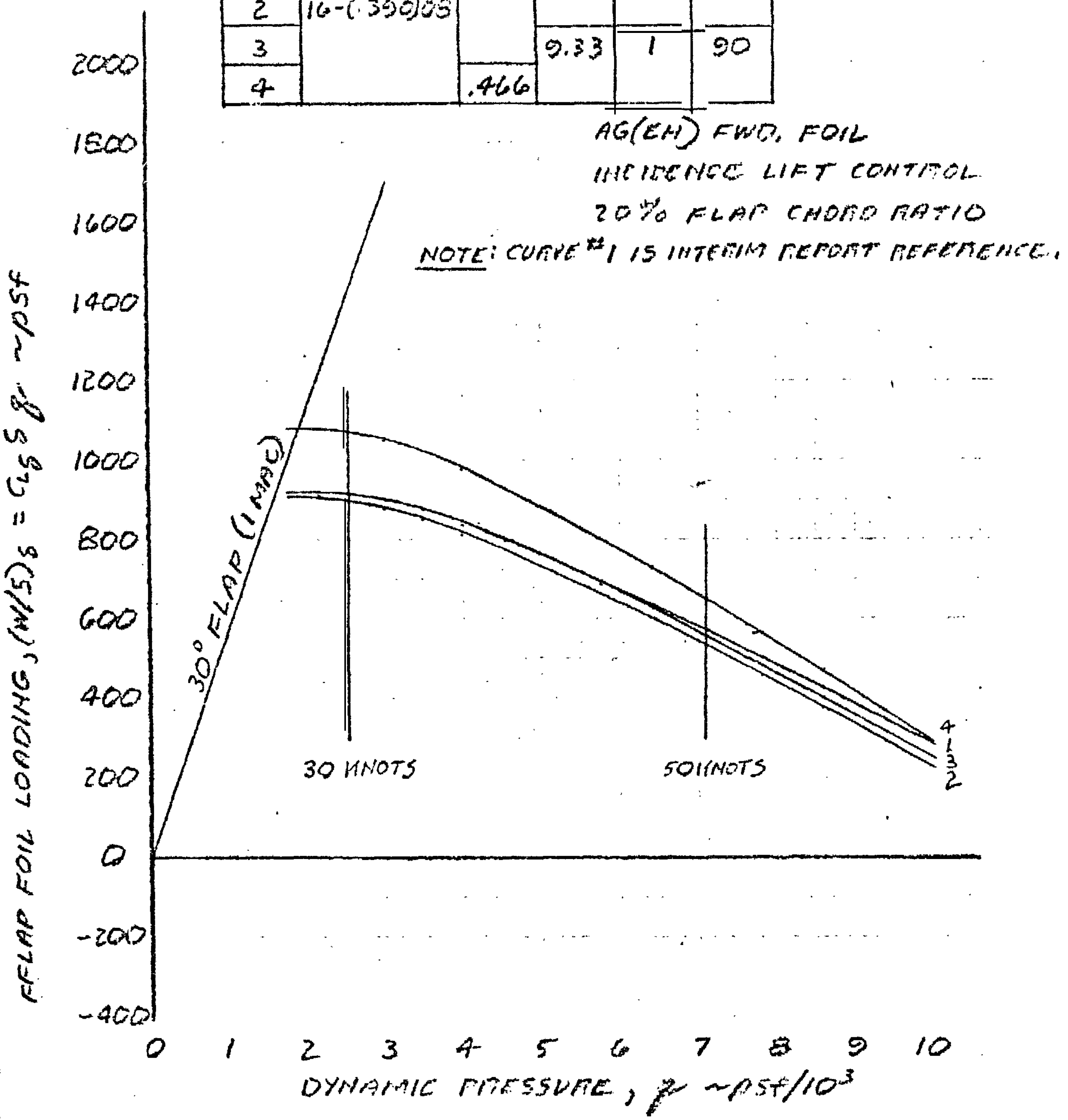

INCIDENCE ANGLE AT OPTIMUM CAVITATION BOUNDARY

EFFECT OF OPERATING CONDITIONS AND ξ

	SECTION	ξ	DEPTH ft.	PITCH deg.	$\left(\frac{W}{S}\right)_0$
1	16-(.353)08	.545	8.5	0	0
2	16-(.390)08				
3			9.33	1	90
4		.466			

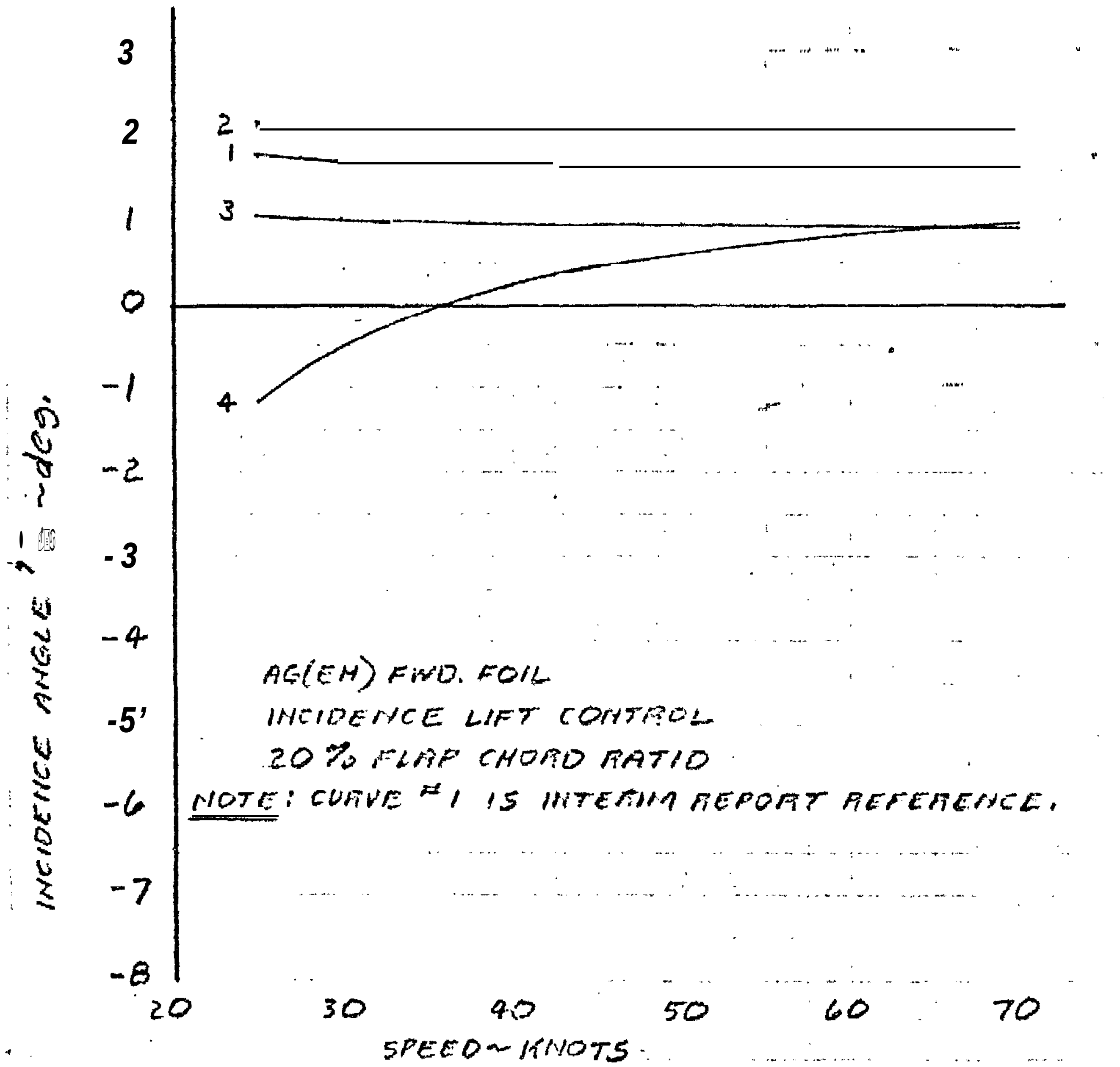

HRW 4/20/73

OPTIMUM UPPER SURFACE CAVITATION BOUNDARIES

EFFECT OF CAMBER AND FLAP CHORD

AG(EH) PROTOTYPE FWD. FOIL
INCIDENCE LIFT CONTROL
δ AS IN TABLE III
1° PITCH
(W/S = 90 9.33 FT. DEPTH
NOTE: CURVE #1 IS REFERENCE FOR THIS REPORT.

	SECTION	FLAP CHORD %
1	16-(330)09	20
2		50
3	16-009	20
4		50

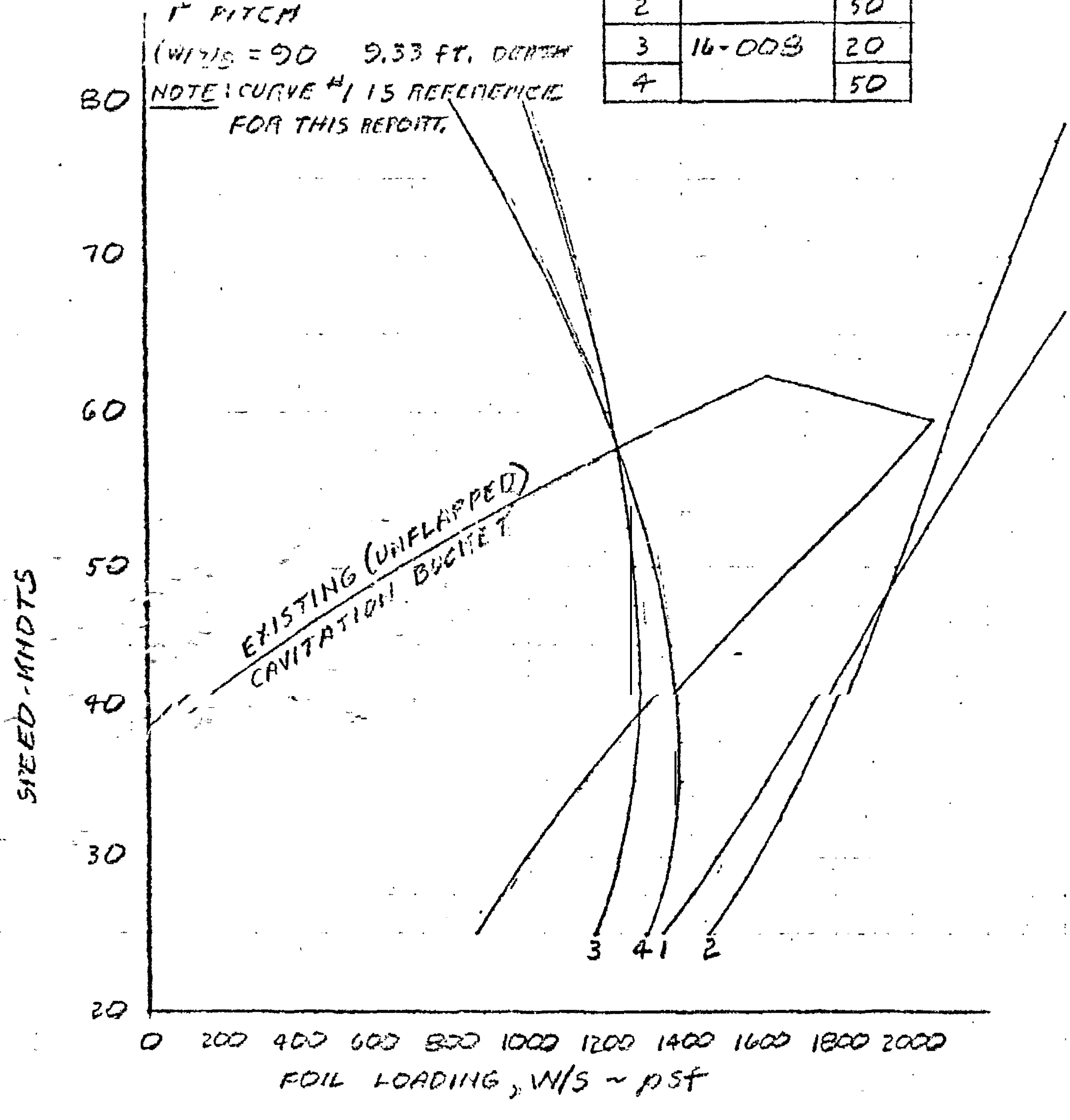

HRW 4/24/73

OPTIMUM FLAP SCHEDULES

EFFECT OF CAMBER AND FLAP CHORD

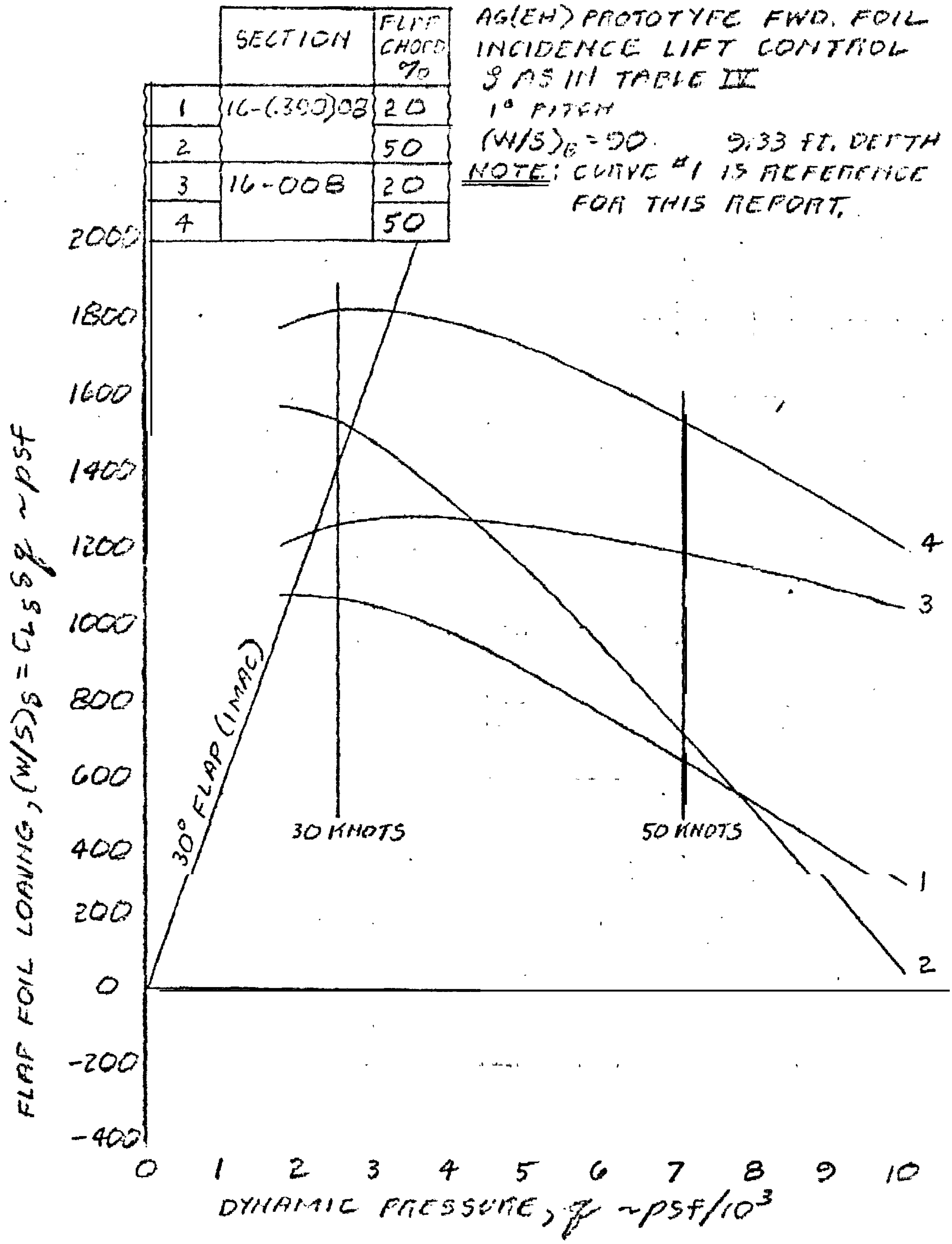

HRW 4/24/73

INCIDENCE ANGLE AT OPTIMUM CAVITATION BOUNDARY

EFFECT OF CAMBER AND FLAP CHORD

	SECTION	FLAP CHORD %
1	16-(.390)08	20
2		50
3	16-008	20
4		50

AG(EH) PROTOTYPE FWD. FOIL
INCIDENCE LIFT CONTROL
δ AS IN TABLE IV.
1° PITCH
$(W/S)_B = 90$
9.33 FT. DEPTH
NOTE: CURVE #1 IS REFERENCE FOR THIS REPORT.

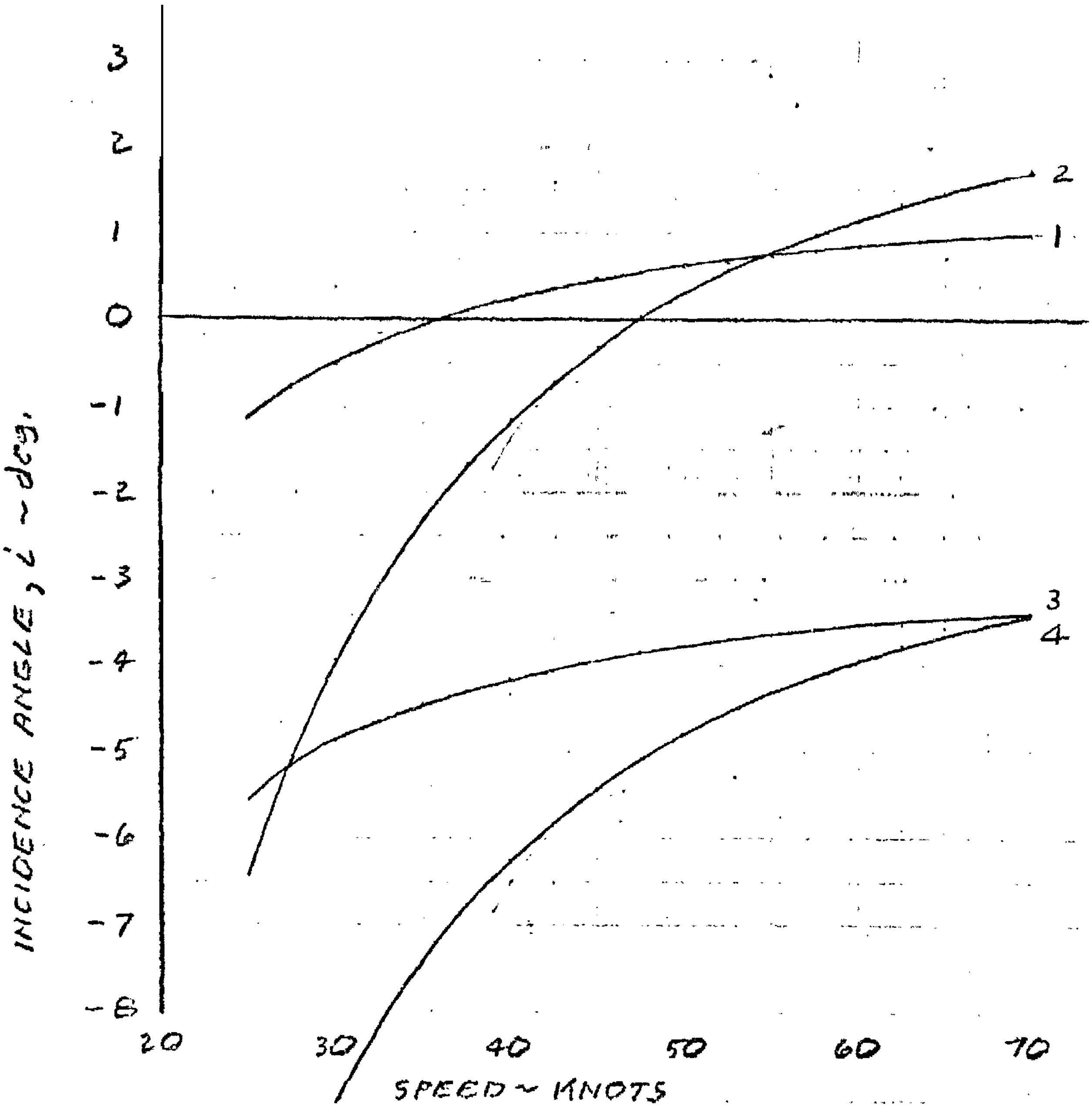

HRW 4/24/73

REFERENCE FLAP SCHEDULES

AG(EH) PROTOTYPE FWD. FOIL
INCIDENCE LIFT CONTROL
20% CHORD FLAP

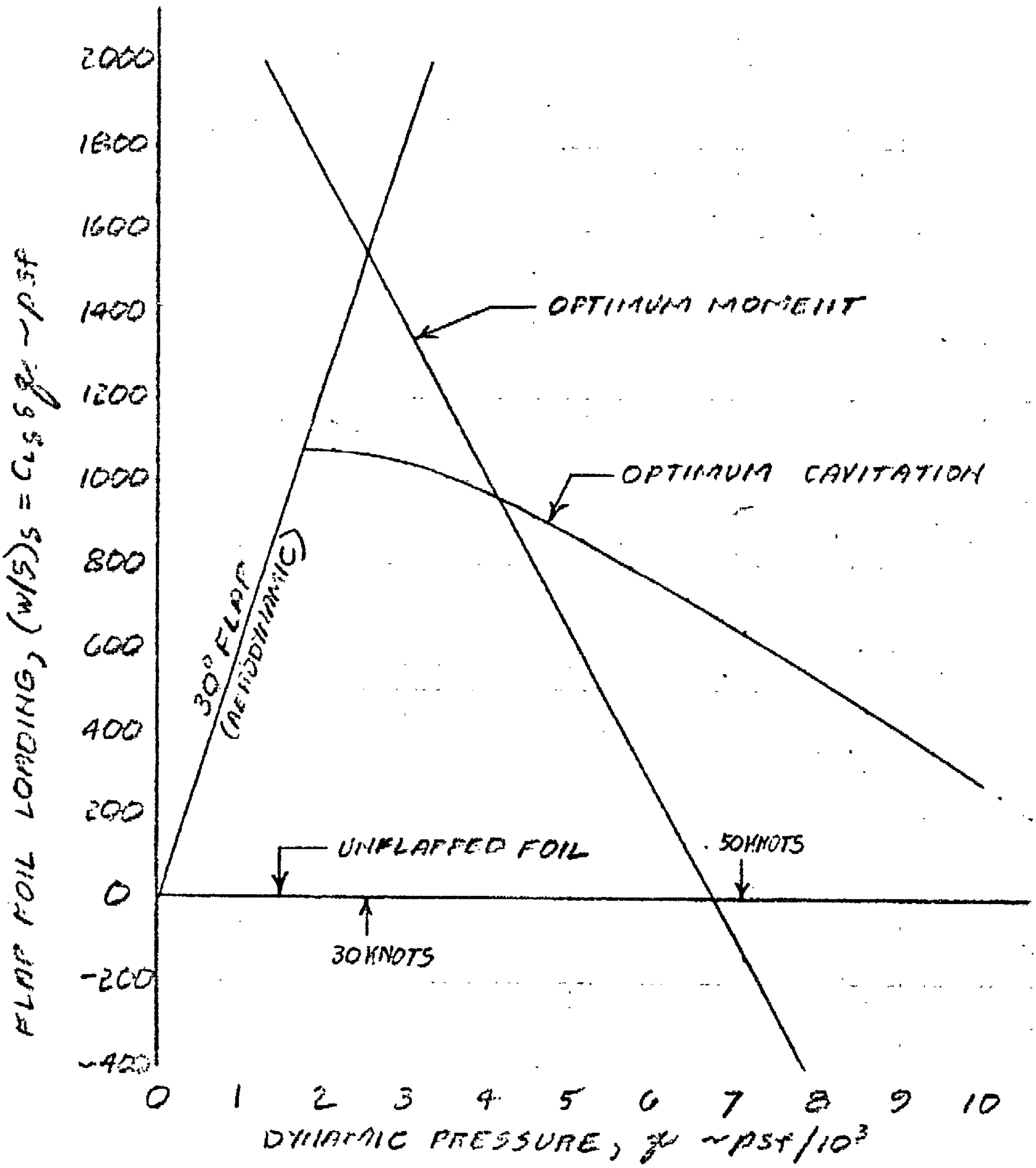

HFW 4/20/73

PAGE FIG. 14

CAVITATION BUCKET CONSTRUCTION

UNFLAPPED FOIL

AG(EH) PROTOTYPE FWD. FOIL
INCIDENCE LIFT CONTROL
9.33 ft. (1 MAC) DEPTH
1° PITCH
$(W/S)_B$ = 90 psf

NOTE: CHORD STATIONS INDICATED IN % AND ARE UPPER SURFACE UNLESS PREFIXED L.

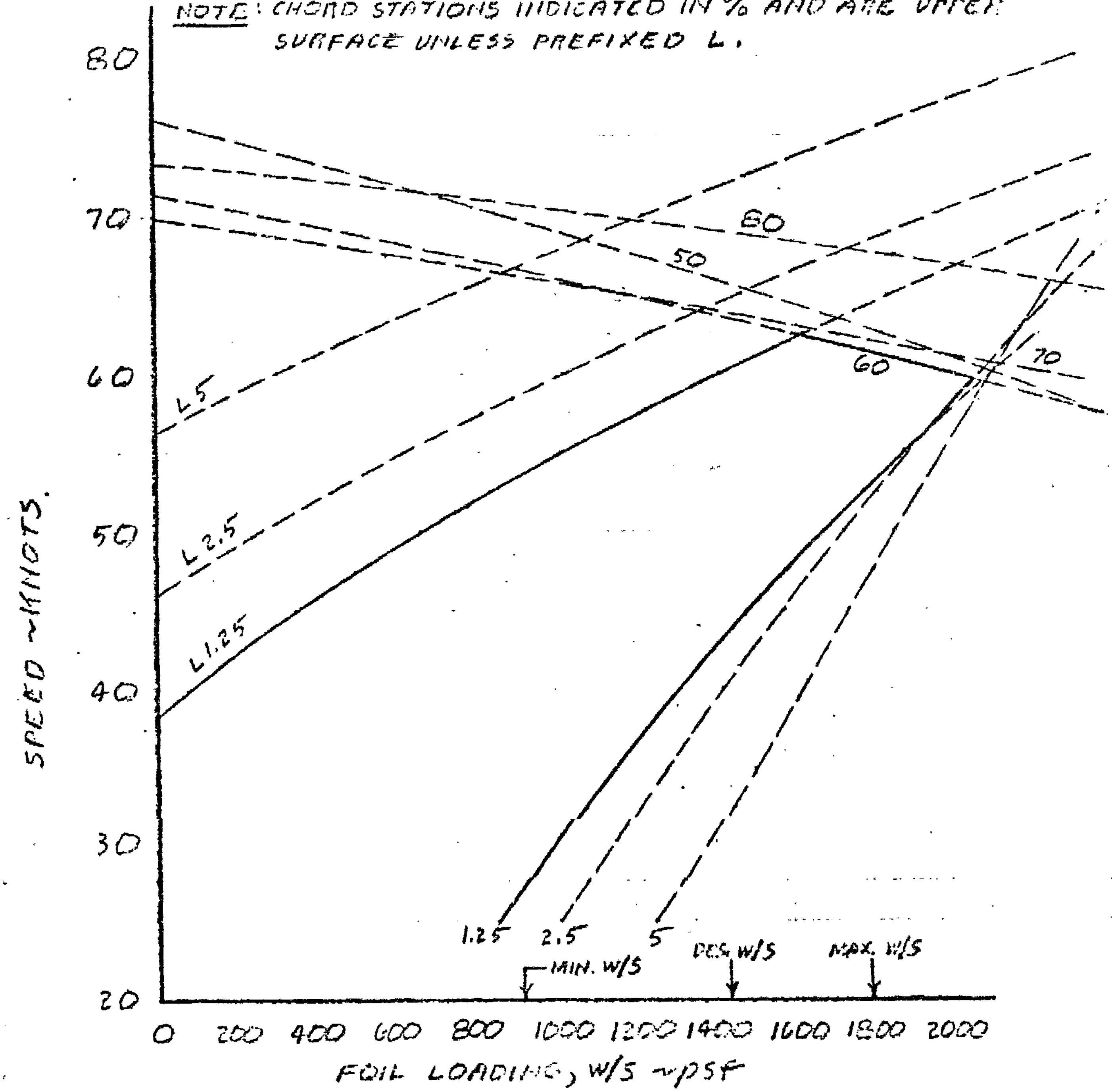

HRW 4/24/73

CAVITATION BUCKET CONSTRUCTION

OPTIMUM CAVITATION FLAP SCHEDULE

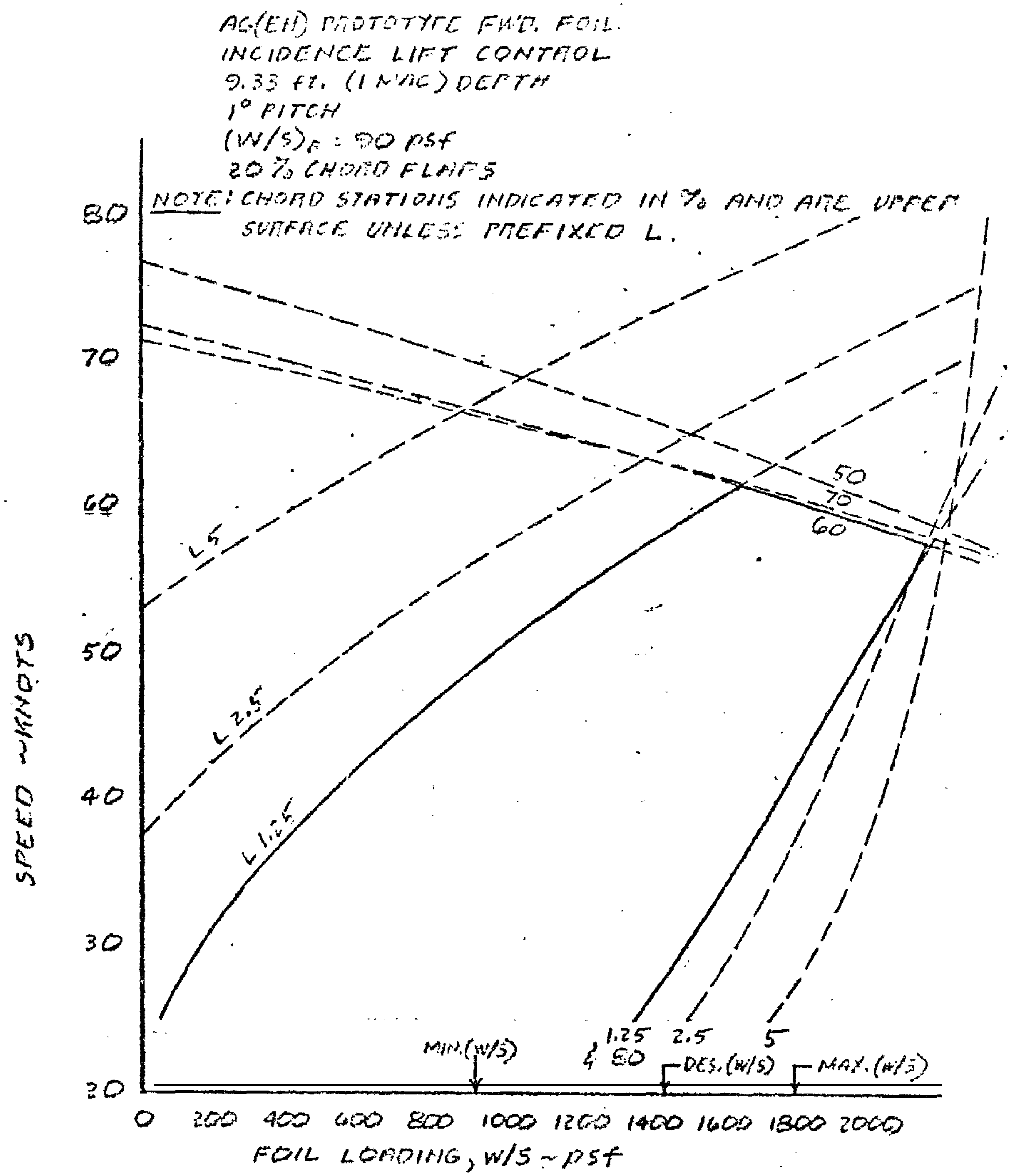

HRW 4/25/75

CAVITATION BUCKET CONSTRUCTION

OPTIMUM MOMENT FLAP SCHEDULE

AG(EH) PROTOTYPE FWD. FOIL
INCIDENCE LIFT CONTROL
9.33 ft. (1 MAC) DEPTH
1° PITCH
$(W/S)_B = 50$ psf
20% CHORD FLAPS

NOTE: CHORD STATIONS INDICATED IN % AND ARE UPPER SURFACE UNLESS PREFIXED L.

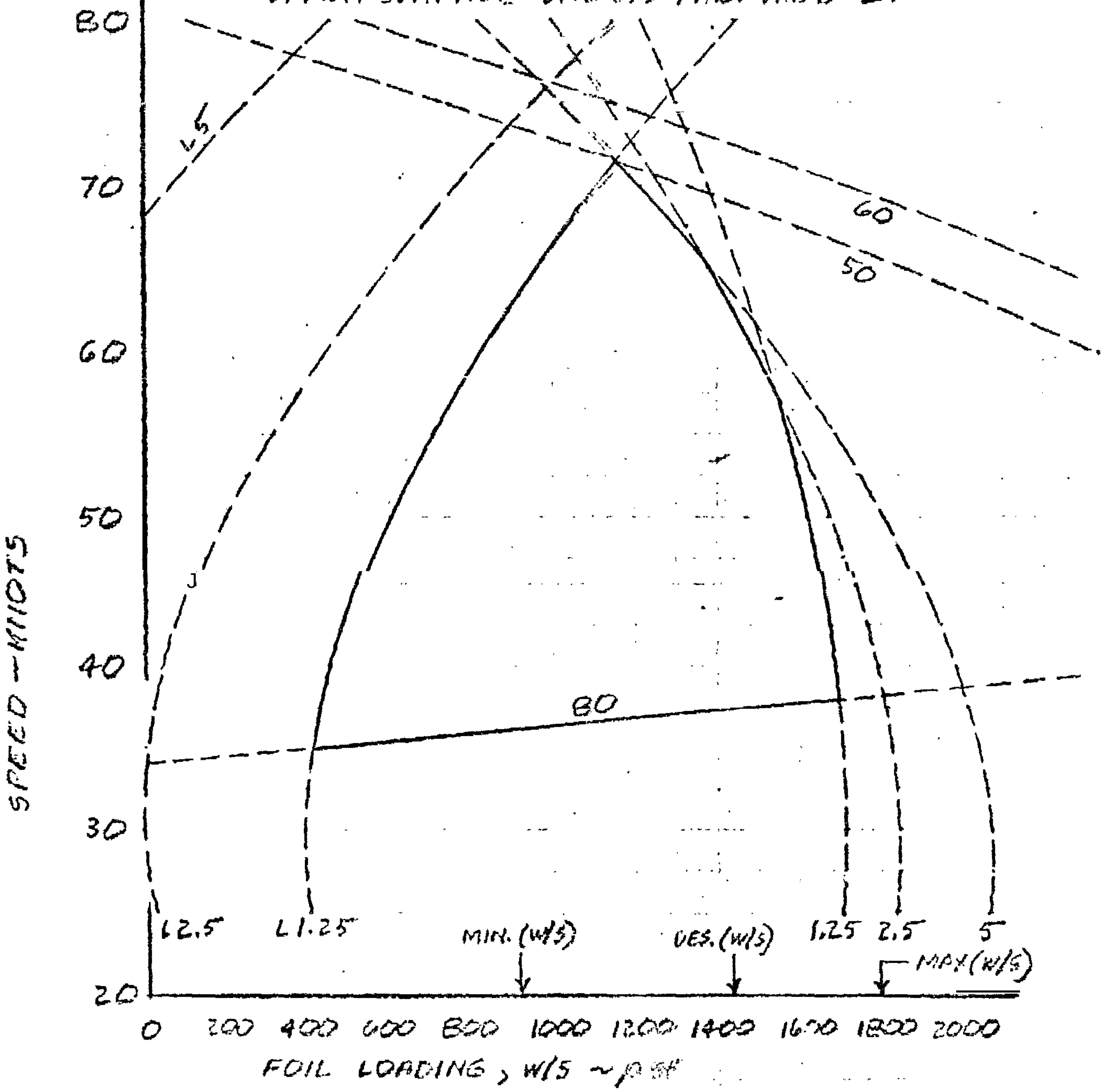

HRW 4/25/73

REFERENCE CAVITATION BUCKETS

AG(EH) PROTOTYPE FWD FOIL
INCIDENCE LIFT CONTROL
9.33 ft. (1 MAC) DEPTH
1° PITCH
$(W/S)_B$ = 90 psf
20% FLAP

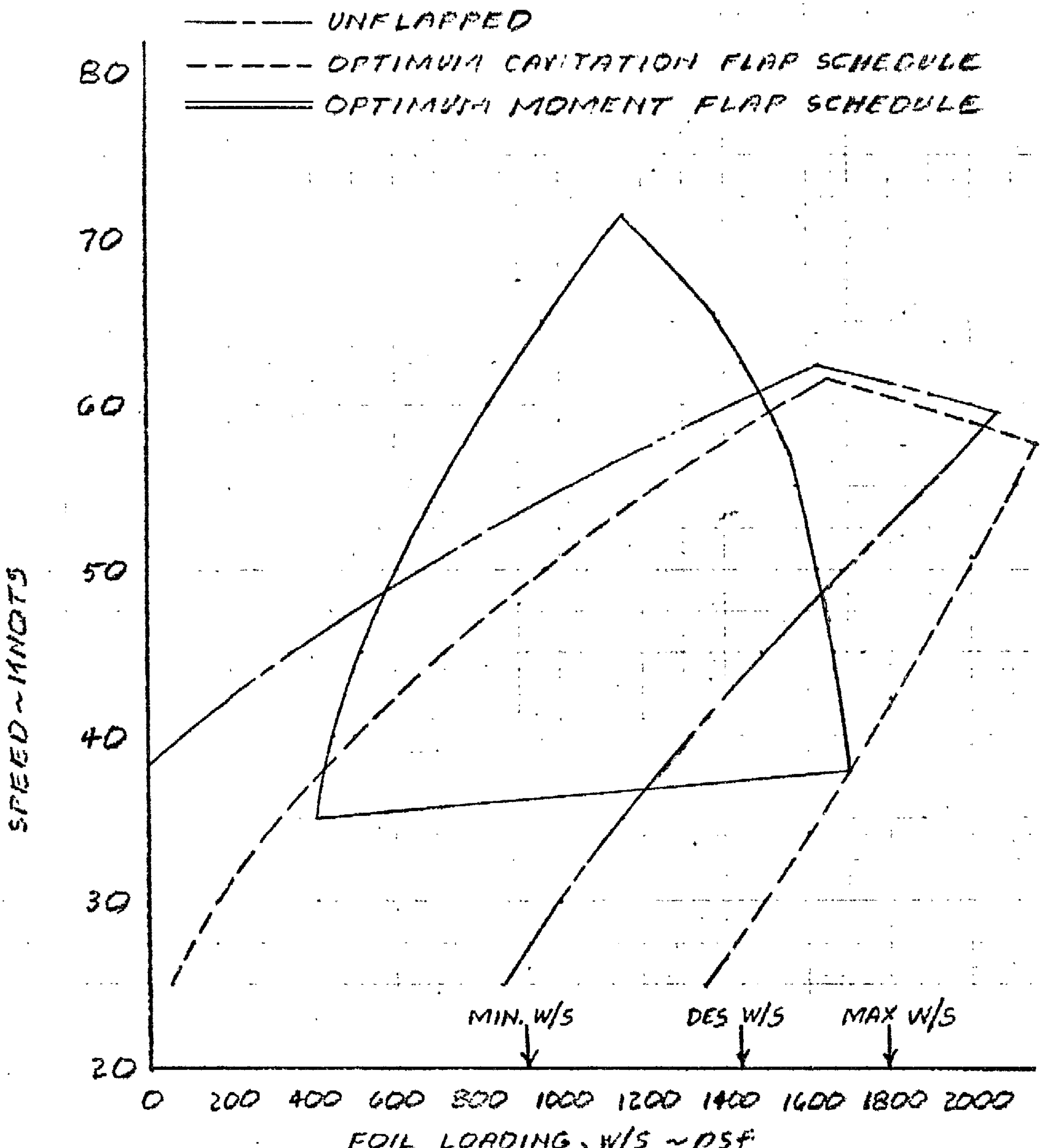

HAW 4/25/73

MINIMUM HINGE MOMENTS

AG(EH) FWD. FOILS

	FLAP SCHED.	$\frac{H}{c}$	$C_{H_{C_L}}$	$\frac{\lvert H_{max}\rvert}{S_{MAC}}$	$\lvert H_{max}\rvert$ IN-# $\times 10^{-6}$
———————	UNFLAPPED	.5655	.2505	273.5	6.89
- - - - - - -	OPT. CAV.	.6832	.2622	286.6	7.23
——— - ———	OPT. MOM.	.654	.3399	167.5	4.22

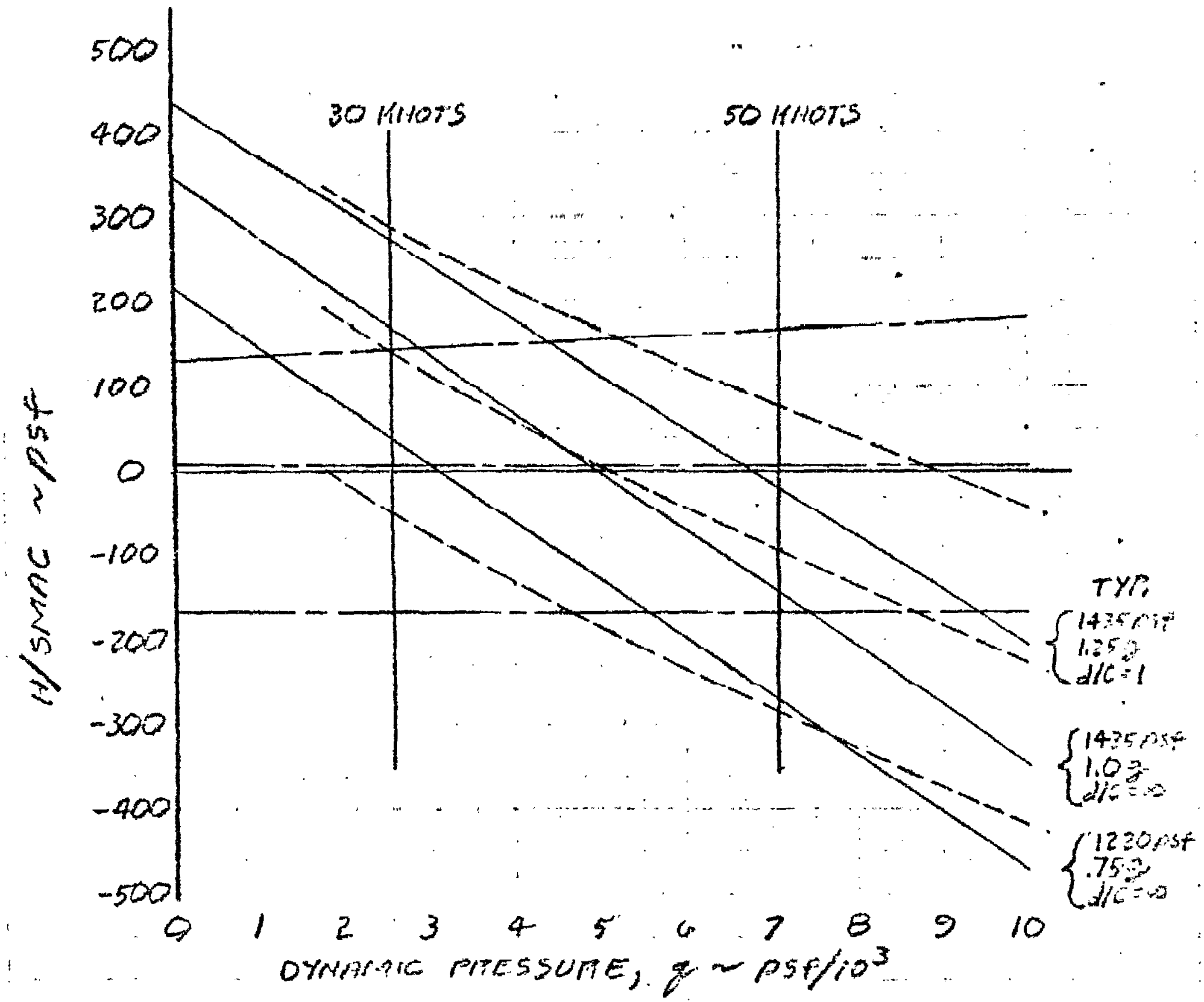

HRW 4/26/73

MINIMUM NEGATIVE HINGE MOMENTS

AG(EH) FWD. FOILS

	FLAP SCHED.	$\frac{H}{C}$	$C_{H_{C_L}}$	$\frac{\lvert H_{MAX}\rvert}{SMAC}$	$\lvert H_{MAX}\rvert$ in # $\times 10^{-6}$
————	UNFLAPPED	.4135	.0995	413	10.4
- - - - - -	OPT. CAV.	.524	.209	433	10.9
—— ——	"OPT." MOM.	.5604	.2454	253	6.35

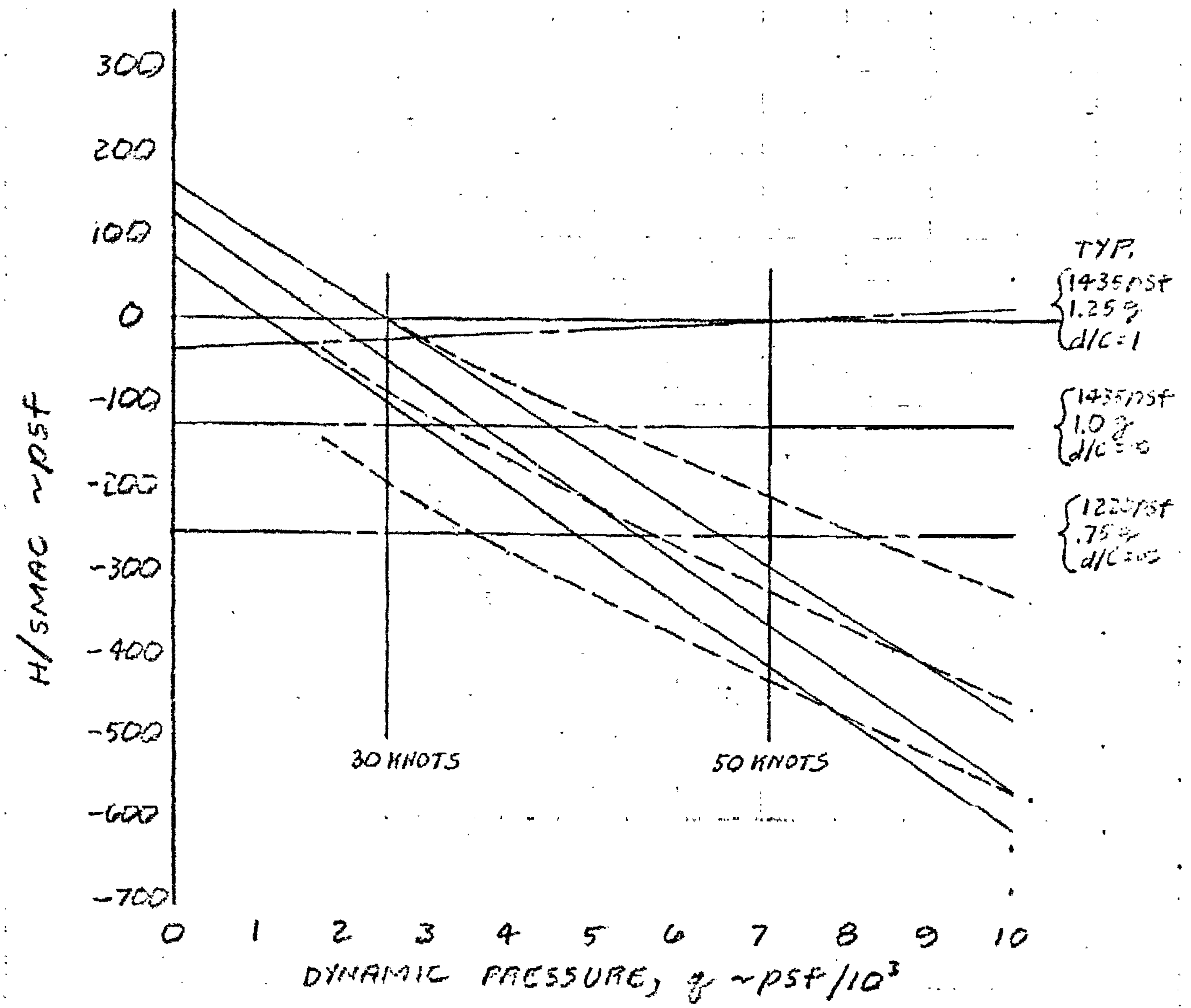

HRW 4/26/73

MINIMUM POSITIVE HINGE MOMENTS

AG(EH) FWD. FOILS

	FLAP SCHEDULE	$\frac{H}{C}$	$C_{H_{C_L}}$	$\frac{\lvert H_{max}\rvert}{S\,MAC}$	$\lvert H_{max}\rvert$ "# $\times 10^{-6}$
————	UNFLAPPED	.864	.549	810	20.4
- - - - - -	OPT. CAV.	[illegible]	.681	849	21.35
—— - ——	OPT. MOM.	.837	.522	496	12.5

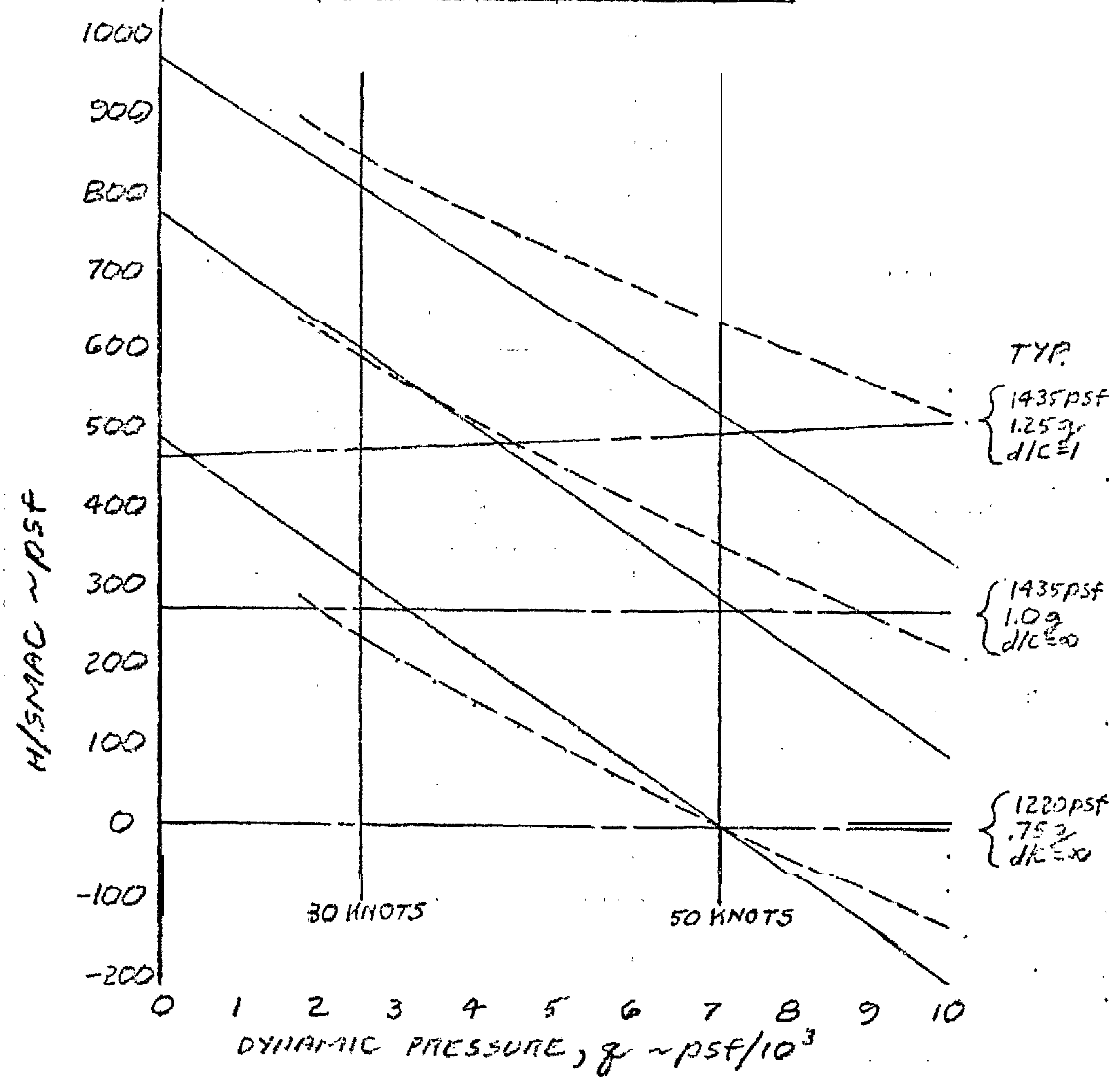

HRW 4/27/73